Single and Dual Growth Factor Delivery from Poly-Ɛ-caprolactone Scaffolds for Pre-Fabricated Bone Flap Engineering

by

Janki Jayesh Patel

A dissertation submitted in partial fulfillment
of the requirements for the degree of
Doctor of Philosophy
(Biomedical Engineering)
in the University of Michigan
2015

Doctoral Committee:

Professor Scott J. Hollister, Chair
Associate Professor Sean P. Edwards
Professor Paul H. Krebsbach
Professor Jan P. Stegemann

--- α ---

To my parents and sister whose love and guidance have made me the person I am today. I could not have done this without you.

ACKNOWLEDGEMENTS

I pursued a Ph.D. in Biomedical Engineering to feed my passion for science and to explore the boundaries of research to make an impact in the field of tissue engineering. I was told that all I need to do is complete my Masters coursework, pass my qualifying exam, and complete my dissertation. That was the approach I had in mind when starting graduate school at the University of Michigan. It seemed pretty straight-forward. I thought I would simply complete the steps one by one, and I would see the light at the end of the tunnel. False. Little did I know that graduate school was filled with limitations, alternative methods, and troubleshooting. What should happen in theory does not always correlate to what happens in reality. To get to the end there were set-backs, optimizing, encouragement and sometimes just plain luck. I was challenged to think creatively and to critically solve issues when faced with frustrations with protein assays and data analysis. My involvement with dance teams in the evenings helped to round out my experience and gave me the opportunity to make some long-lasting friendships. Through the ups and downs that I faced at the University of Michigan as a Ph.D. student, I have created some unforgettable memories. I could not have completed this dissertation without the support, well-wishes, and advice that my colleagues, friends, and family have provided me with. Firstly, I'd like to thank Dr. Scott Hollister, my research advisor, for always being there to lend a guiding hand and to help me outline my project. He gave me the creative freedom to independently outline goals and was always there to share advice. Thank you

for believing in my potential and always encouraging me to stay positive. Other academic mentors were my committee members: Drs. Paul Krebsbach, Sean Edwards, and Jan Stegemann. Thank you for sharing your knowledge and providing your support throughout the years. Your enthusiasm for science, medicine, and technology is contagious.

I'd like to thank the Biomedical Engineering Department and especially Maria Steele for being so prompt when handling all of the logistics. Maria was always there to give me a last minute copy of my transcript, tell me which form to fill out, and tell me exactly who to contact for a reimbursement.

Research is rarely completed individually, and I received a lot of support from the members of the Scaffold and Tissue Engineering Group. Thank you to: Annie Mitsak, Auresa Thomas, Marta Dias, Colleen Flanagan, Xiuyuan Yang, Eiji Saito, and Sophia Pilipchuk. You were there to motivate me during the late nights spent in lab or when I needed to discuss project details. I would like to mention a special thank you to Annie Mitsak who took the time to mentor me when I first joined the lab and helped me to avoid a lot of the pitfalls that first years fall into. Thanks to Colleen Flanagan who was always there to calm me down when I made a mistake, to help edit my papers, or just to talk about science fiction T.V. shows on long road-trips to Illinois. Also, thank you to all of the undergraduate and graduate students that assisted me in my research projects- Crystal Chen, Kari Green, Manasa Amancherla, Sean Miller, Kevin Merchak, Manny Hill, Rui Fan, Joshua Duel, and Jane Modes. The long hours you spent doing cell culture, mechanical testing, protein assays, and histology have helped me tremendously, and I greatly appreciate it. Also, I'd like to thank the Dr. Rhima Coleman's Laboratory, and the

MicroCT and Histology Cores at the Dental School because without your assistance, my research would incomplete.

Although I spent most of my time on research, I also invested some time in extracurricular activities. I met some wonderful people through my involvement with the Michigan TAAL dance team and the Biomedical Engineering Graduate Student Council. Thank you, Ishani, for your positive encouragement and helping me to use dance as a positive outlet for the frustrations I faced in lab. I will remember the hours spent listening to music, choreographing, and creating formations. To Paras and Melanie, thank you for your mentorship and helping me to navigate the complex Ph.D. maze from your own experiences.

I would like to thank all of my friends for their unconditional support, words of encouragement, and unwavering patience. I am so lucky to have all of you in my life, and I consider you a family away from home. Thank you to my Georgia Tech and high school friends: Kalpi, Ricky, Neil, Bijal, Janu, Sonali, Tasha, and Nikki. Those hour-long skype dates, phone calls, and long emails have provided words of encouragement, strengthened my confidence, and lifted my spirits. You have been an amazing support system for me. To my Michigan friends- especially Matt, John, Sriram, Nidhi, Sydney, and Niharika- thank you for all of the unforgettable memories which include exploring Ann Arbor, impromptu pool parties, movie nights, grapes, and orange leaf outings.

Finally, I would like to express my gratitude to my family for their unwavering support and love and for always pushing me to do my best. Thank you to my parents for encouraging me to relax and take a step back when I felt overwhelmed or stressed. Mom, I loved the lunches we had together at the University of Michigan Hospital, and Dad,

thanks for always being there to count on when I needed to move apartments or when my car was in trouble. I loved coming home to recharge with some delicious home-cooked food. To Radhika, through the years you've always been a role model for me, and I strive to follow in your footsteps. Thanks for always being there to lend a guiding hand and for teaching me the do's and don'ts of graduate school. You always knew the right words to tell me to make me feel better after I was rejected by science. Lastly, thank you to Harish for being my number one fan and chanting every time I had positive experimental results. Thank you for believing in me even when I thought everything was going wrong and falling apart. Your love and support have meant everything to me.

TABLE OF CONTENTS

LIST OF FIGURES

LIST OF TABLES

ABSTRACT

Approximately 2.2 million bone graft procedures are performed worldwide annually. Autografts are widely utilized to reconstruct large craniofacial bone defects; however, they result in donor site morbidity and defect geometry mismatch. Pre-fabricating a bone flap overcomes these drawbacks and involves integrating a patient specific scaffold with biologics, implanting it in the latissimus dorsi for a period of time and then transplanting it to the defect site as a partially remodeled construct. Poly-Ɛ-caprolactone (PCL) is a biocompatible polymer that has mechanical properties suitable for bone tissue engineering; however, it must be integrated with biologics to stimulate bone formation. The purpose of this work was to investigate single and dual growth factor binding to PCL scaffolds in a clinically applicable environment and analyze the bone regenerated in an ectopic site for pre-fabrication applications.

Bone morphogenetic protein-2 (BMP2) was adsorbed or conjugated onto a PCL scaffold in a clinically applicable setting (1hour exposure at room temperature). Adsorbed BMP2 had in a small burst release and was bioactive as indicated by C2C12 alkaline phosphatase expression. Interestingly, conjugated BMP2 had a sustained release but was not bioactive. When implanted subcutaneously, adsorbed BMP2 had increased bone volume (BV), elastic modulus, and ingrowth when compared to conjugation. Next, a collagen sponge was fabricated inside of a BMP2-adsorbed PCL scaffold to deliver vascular endothelial growth factor (VEGF). Also, a modular PCL scaffold was developed

in which the inner and outer modular portions were adsorbed with BMP2 and VEGF, respectively. In both systems, the VEGF was bioactive as indicated by increased endothelial cell proliferation. Dual delivery of BMP2 and VEGF significantly increased BV from 4 to 8weeks in an ectopic location, whereas, BMP2 alone did not. Finally, erythropoietin (EPO) and BMP2 were delivered from the outer and inner portions of the modular scaffold, respectively. The adsorbed EPO was bioactive as indicated by increased endothelial cell proliferation. At 4 weeks, dual EPO and BMP2 delivery had increased BV and ingrowth when compared to BMP2 alone.

In conclusion, adsorbing BMP2 onto PCL may be optimal for clinical use. Delivering VEGF with BMP2 increases the bone regeneration rate from 4 to 8 weeks and delivering EPO with BMP2 increases the BV at 4 weeks when compared to BMP2 alone. Multiple biologics delivery is a promising method to increase the regenerated bone for pre-fabricated flaps. Future studies should investigate adsorbing the whole scaffold with both proteins, optimizing protein dosages, and determining the mechanism of synergy between the growth factors.

CHAPTER 1

INTRODUCTION

1.1 Problem Statement

Annually, approximately 2.2 million bone graft procedures are performed worldwide of which 500,000 are performed in the U.S., a $1.39 billion market [1-3]. Bone graft usage will most likely increase due to an aging population. Methods to treat bone defects resulting from trauma, tumor resection, developmental anomalies or facture non-unions include autografts, allografts, synthetics, or natural material scaffolds. Autografts are considered the gold standard; however, they have the drawbacks of donor site morbidity, increased risk for infection, and geometry mismatch. Alternatives such as allografts and natural scaffolds have the limitations of mechanical failure and poor growth factor delivery. Due to inadequate delivery, a large dose is needed which increases the product cost and potential complications as seen with Medtronic's product Infuse™. Bone morphogenetic protein-2 devices can cost as much as $5,000 per product, whereas demineralized bone matrix and ceramics cost about $700-$1,000 per implant [4]. There is a need to tissue engineer a patient-specific bone graft that is autologous in nature to reduce the drawbacks associated with autografts and alternative bone grafts.

1.2 Repairing Bone Defects

Fracture non-unions, tumor resections, trauma, and developmental anomalies can result in large bone defects that will not heal naturally. In these situations a bone graft is needed to fill the void and assist in the regeneration process. The worldwide market value for bone grafts and substitutes is expected to rise from $2.1 billion in 2013 to approximately $2.7 billion by 2020. The United States holds the largest market share with 65.6%, and the revenue is expected to rise from $1.39 billion to $1.78 billion [3]. Bone and bone graft substitutes used to repair defects include autografts, allografts, and synthetic/natural material grafts [5].

1.2.1 *Autografts & Allografts*

The gold standard for reconstructing large bone defects is an autograft typically taken from the patient's fibula, iliac crest, or scapula. These osteoconductive, osteoinductive, and osteogenic autografts can either be used as a graft or as a flap (a graft with an attached vascular pedicle). The vascular pedicle in the bone flap is connected to a local vessel at the defect site to provide blood flow. Autografts have proven to integrate well at the defect site and support further remodeling; however, each of the harvest sites varies in bone quality. The fibula offers the longest bone with a good pedicle, but it is frequently not available due to atherosclerosis or congenital vascular anomalies. The iliac crest offers limited soft tissue, a short pedicle, and significant morbidity. Autografts from the scapula are the most limited in terms of bone quality and pedicle length. With these limitations, it is difficult to provide the best quality of life, functional return and aesthetic recovery for the patient. In addition to these limitations, autografts are associated with

major drawbacks that include high donor site morbidity, increased risk for infection, and poorly matched defect geometry.

One alternative to an autograft is an allograft, which is a bone graft that is taken from another person (usually a cadaver) and implanted into the defect site. These cancellous or cortical bone grafts maintain biologic (osteoconductive) properties and mechanical integrity. First, the donor is screened and then the graft is collected, processed, disinfected, and tested to ensure it is safe for use. Allografts are provided in fresh, fresh-frozen, or freeze-dried forms. There is limited time to test fresh grafts for diseases, and there have been four cases of human immunodeficiency virus (HIV) infection associated with using fresh-frozen allografts [6]. Fresh-frozen grafts are regulated by the Food and Drug Administration (FDA), and the processing method preserves biomechanical properties. Freeze-dried grafts can be stored for a longer period of time; however, processing negatively impacts the graft effectiveness in terms of mechanical integrity and osteoconductive abilities. In addition to the risk of disease transfer and eliciting an immune response, the process of screening a donor, harvesting, packaging, and processing can be expensive. For these reasons, allografts are a substandard alternative to autografts [6]. Both autografts and allografts result in poorly matched defect geometry, making them suboptimal solutions for reconstructing complex geometries in the craniofacial region.

1.2.2 *Bone Graft Substitutes*

Bone graft substitutes can address a few of the drawbacks associated with allografts and autografts. Some commercially available substitutes are made of calcium phosphate (CaP), calcium sulfate (CaS), hydroxyapatite (HA), or tricalcium phosphate

(TCP). These materials can be used individually or in combination to increase the osteoinductive or osteoconductive properties.

The scaffold resorption rates and mechanical properties vary greatly depending on the material, geometry, and porosity. CaP products have a very high compressive strength once hardened and can be injected. CaS has a low compressive strength so it is not used for load bearing applications and is used as a bone void filler. HA is derived from marine coral exoskeletons that are converted to hydroxyapatite. The porous structure resembles cancellous bone porosity. TCP has a modulus that is in the lower range of cancellous bone. It is available in block, wedge, or granule forms [7]. Sometimes β-TCP (a more porous version of TCP) is used to create more porous scaffolds [8]. Commercial bone void fillers include Biomet's BonePlast® (CaS/HA), Exactech's OpteMx™ (HA/TCP), Medtronic's MasterGraft® Granules (HA/ β-TCP), Wright Medical Technology's PRO-DENSE® (CaS/CaP), Synthes Norian SRS® (CaP), and Orthovita's Vitoss® (β-TCP) [9].

Other commercially available bone graft substitutes are derived from naturally occurring materials such as demineralized bone matrix (DBM) and collagen type I. DBM is an osteoconductive material produced from processed allograft bone. It is composed of noncollagenous proteins, growth factors (GFs), and collagen [1]. DBM is available in the form of powder, granules, or it can be mixed into a gelatin or hydrogel (a glycoprotein) to make putty. Approved products include Biomet's InterGro® (DBM/lecithin), Exactech's Optecure® (DBM/hydrogel) and Optefil® (DBM/gelatin), Life Net Health's Optium DBM® (DBM/glycerol), Medtronic's Osteofil® (DBM/gelatin), Smith and Nephew's VIAGRAF (DBM/glycerol), and Osteotech's GRAFTON Plus® (DBM). Although successful in some applications, due to the sterilization methods utilized the bone

morphogenetic protein-2 (BMP2) availability may decrease. There also exists batch to batch variation in protein content.

Other natural materials (e.g. collagen, alginate, hyaluronic acid) are utilized as scaffold materials for mineralized tissue. Collagen based matrices are generally highly purified type 1 bovine dermal fibrillar collagen. Natural materials are structurally complex and more difficult to manipulate into specific geometries when compared to synthetic polymers. They lack the mechanical properties needed to withstand the forces that exist in the bone environment, and they would not be useful in a large bone defect in which a large bone volume is needed [10,11]. For these reasons, natural bone graft materials are generally used as bone void fillers. To strengthen load bearing properties, collagen can be combined with a ceramic such as Integra's Mozaik™ (β-TCP/Collagen) or Medtronic's MasterGraft Strip® (hyaluronic acid/ β-TCP/Collagen) [9].

Currently, two biologic/material combination devices are approved by the FDA for clinical use. One is BMP2 loaded into a collagen matrix (Infuse™, Medtronic Sofamor Danek, Inc) used to for spinal fusion, open tibial fractures, sinus augmentation, and dental procedures. The other is bone morphogenetic protein-7 (BMP7) (OP-1TM, Stryker Biotech) [9] used for long bone defects and non-union treatment [12]. These products are costly due to high BMP doses (2-12mg) which greatly exceed the physical concentrations (18.8-22pg/mL) present in defect areas by several orders of magnitude [12].

Synthetic polymers can be fabricated to match a patient's complex facial geometry and can be integrated with biologics to induce bone growth when implanted *in vivo*. Synthetic scaffolds have controllable properties such as degradation rate, pore

structure, and mechanical stability. Poly-L-lactic acid (PLLA), poly-glycolic acid (PGA), poly-D,L-lactic coglycolic acid (PLGA), and poly-Ɛ-caprolactone (PCL) are commonly used in bone plugs, and screws. The ester linkages on their backbone degrade via hydrolysis into non-toxic metabolites, and their degradation rates are controlled by altering their crystallinity and lactide/glycolide ratio [13]. A mineral coating such as TCP can be added to alter the surface chemistry or to promote GF binding/release [14]. HA or CaP can also be mixed into the synthetic polymer to increase osteoconductivity [15].

Although successful in some tissue engineering applications, non-osteoinductive synthetic materials are not ideal for reconstructing large craniofacial bone defects when used in isolation. These polymer grafts could be readily available and easily produced; however, they do not integrate as well as autografts when placed directly into a large defect site [16]. Generally, surrounding blood vessels cannot penetrate the graft sufficiently to provide nutrients to the graft's core. This may be because nutrient diffusion is optimally effective within 150-200μm from a blood supply source and irradiated wound sites are not conducive to developing a rich vasculature [17,18].

To increase osteoinductive properties, stem cells can be added to the synthetic scaffold to promote graft integration and bone remodeling. The most common stem cell sources are adult stem cells which can come from the bone marrow as mesenchymal stem cells (MSCs) or more frequently from easy-to-harvest adipose tissue (adipose derived stem cells) [16]. Bone growth on a cell-seeded graft is better than its acellular counterpart, which indicates that stem cells have a positive impact on graft maturation; however, challenges associated with adding cells include obtaining enough stem cells from the patient and then rapidly and uniformly seeding a large scaffold [19-21].

Although cell therapy has been widely studied, translation of this process into clinical practice has been hindered due to the lack of FDA-approved off-the-shelf devices that incorporate patient cells [22].

1.2.3 *Tissue Engineering a Bone Graft*

An ideal large synthetic graft should have osteoinductive/conductive properties as well as native autograft mechanical properties. The matured flap should have a vascular pedicle that can be connected to a blood vessel at the defect site to provide nutrient supply throughout the flap. To tissue engineer a scaffold with these properties, first, a patient-specific biomaterial scaffold design is combined with a biologic at a site remote from the defect site. Next, after a maturation period the construct is transplanted as a bone flap to the defect site. The maturation phase can be completed *in vitro* or *in vivo*.

In vitro fabrication requires the scaffold to be seeded with the patient's stem cells and then placed in an external bioreactor. Integration has been comparable to that of an autograft [16]; however, this method is a very complicated and variable one due to the need for uniform cell seeding and for maintaining an optimal nutrient perfusion throughout the construct. Furthermore, the internal interconnecting microarchitecture not only needs to be sufficiently porous to promote cell ingrowth and nutrient diffusion (150-200μm from the blood supply) [17,18], but also strong enough to withstand the forces exerted in the region [15]. As mentioned previously, a cell-based construct will need to overcome many regulatory hurdles prior to entering the clinic. An alternative to creating the flap *in vitro* is to fabricate the bone flap *in vivo* by using the patient's body as a bioreactor to partially remodel the construct prior to transplanting it to the defect site.

1.3 Pre-Fabricating a Bone Flap

Pre-fabricating a flap i*n vivo* involves implanting a customized synthetic scaffold with associated biologics in the latissimus dorsi for a maturation period, and then transplanting it to the defect site as a complex bone tissue flap with an attached vascular pedicle. The latissimus dorsi was chosen due to its high vascularity and easy access during surgery. Studies in this field have been conducted in Europe and Asia, but not in the United States to the best of our knowledge. There are few reports of this procedure in animal models [23-28] and even less in humans [29-31].

In a study conducted by Warnke et al [28], an external titanium mesh cage in the shape of a human mandible was filled with BioOss blocks, soaked in 3.5mg BMP7, and implanted in a minipig for six weeks. The engineered bone had similar mechanical properties to that of natural bone. In 2004, the same research group conducted a clinical trial using a customized titanium mesh cage filled with bone mineral blocks soaked in 7mg BMP7 and added the patient's bone marrow [30]. Despite initial positive results, 9 months post implantation the construct fractured due to overloading, became infected, and contained necrotic areas [31]. Terheyden et al. created collagen cylinders filled with BioOss soaked in 0-1000µg BMP7 and implanted the cylinders in a minipig. Results found 1mg BMP7 was needed to produce sufficient bone [27]. Finally, Heliotis et al. used a hydroxyapatite scaffold with 3.5mg osteopontin-1 (BMP7) in a clinical trial. No patient stem cells or bone marrow were added. Five months post transplantation to the defect, the graft was infected with methicillin-resistant staphylococcus aureus (MRSA) and failed [29].

The constructs used in previous pre-fabricated flap studies had relatively crude geometries. Furthermore, using titanium as the scaffolding material can cause titanium mesh exposure and fatigue issues. An ideal flap would contain a scaffold with mechanical properties similar to that of bone which degrades gradually as the bone tissue regenerates. The material should be biocompatible and easily integrated with GFs in the clinic. Tissue engineering a vascularized bone flap *in vivo* is a promising alternative to using an autograft to reconstruct a large craniofacial defect.

1.3.1 *Multiple Biologics Delivery*

BMP2 has been extensively investigated for bone tissue engineering applications due to its potent osteogenic properties. Depending on the binding and delivery method utilized, BMP2 can regenerate bone on both synthetic and natural scaffolds. Additionally, there is a positive relationship between osteogenic and angiogenic factors in native bone healing. Angiogenic protein vascular endothelial growth factor (VEGF) has been delivered with BMP2 utilizing various complex dual delivery devices; however, the results are conflicting regarding the impact on the regenerated bone volume in an ectopic location [11,32-34]. The effect of dual delivering hematopoietic protein erythropoietin (EPO) and BMP2 has been superficially investigated due to the two proteins' synergistic relationship [35,36], but further studies are needed to determine the effect of locally delivering both proteins on ectopic bone regeneration. With respect to pre-fabricated flaps, considering the clinical applicability when binding the GFs to a scaffold and delivering multiple biologics have not been investigated to the best of our knowledge.

The ultimate goal of bone tissue engineering for large bony defects is to fabricate a vascularized bone flap *in vivo* that regenerates enough bone and a vascular pedicle for

successful reconstruction. PCL is an appropriate material for bone tissue engineering applications due to its slow degradation rate that will support load while bone is regenerating, its compatibility with selective laser sintering to fabricate complex geometries, and its ability to deliver osteogenic growth factor BMP2. Electrostatic adsorption completed in a clinically applicable environment may be more advantageous over covalent conjugation via sulfo-SMCC for binding BMP2 to PCL because it regenerates more bone. Delivering angiogenic protein VEGF along with BMP2 could be a potential method to increase the bone regeneration rate due to increased vasculature and nutrient delivery. Finally, since EPO has a synergistic relationship with BMP2, dual delivery may increase the regenerated bone volume. Increased bone volume is important for pre-fabricated flap applications because the flap would mature faster and could be transplanted at an earlier time point. This dissertation investigates osteogenic factor binding to PCL scaffolds in a clinically applicable environment and determines the effect of dual GF delivery on bone regenerated in an ectopic location to further optimize the pre-fabrication process.

1.4 Thesis Aims

This thesis addresses the limitations of the current pre-fabrication process and advances it by integrating patient-specific design, 3D printing, multiple biologics delivery, and considering a clinical setting. AIM I refines and compares BMP2 adsorption and conjugation binding methods to PCL scaffolds in a clinically applicable setting (<1 hour protein to material exposure at room temperature) and analyzes the resulting bone regenerated *in vivo*. BMP2 binding and release kinetics are also characterized. Scaffolds with adsorbed or conjugated BMP2 are implanted

subcutaneously in mice for 8 weeks to determine the resulting bone formation. AIM II determines the effect of delivering VEGF along with BMP2 on ectopic bone regeneration. BMP2 is delivered from a PCL scaffold as described in AIM I, and VEGF is delivered from a collagen sponge fabricated inside of the PCL scaffold. Dual delivery scaffolds are implanted in mice for 4 & 8 weeks to determine the bone growth. In AIM III a novel modular scaffold is created to modify dual growth factor binding to be clinically applicable. BMP2 and VEGF are adsorbed onto the inner and outer portions of a modular scaffold, respectively, for 1 hour. The two scaffolds are then manually assembled and implanted *in vivo* for 4 & 8 weeks. The results are compared to BMP2 delivery alone. Finally, in AIM IV we determine the binding and release kinetics of BMP2 and EPO from the inner and outer portions of the modular scaffold, respectively, that is described in AIM III. We then assess the effect of dual BMP2 and EPO delivery on ectopic bone regeneration in comparison to BMP2 delivery alone. The objectives of each aim are summarized as follows:

AIM I*:* Compare conjugation and adsorption methods of binding BMP2 to PCL in a clinically applicable setting (<1 hour protein exposure to PCL) and analyze the resulting regenerated bone in an ectopic site.

*We **hypothesize** that adsorption will be more optimal than conjugation for clinical usage due to protocol simplicity, retained bioactivity, and increased bone regenerated in vivo.*

AIM II: Develop a novel dual BMP2 and VEGF delivery system comprised of PCL and a collagen sponge to increase the bone regeneration rate.

AIM III: Create a modular PCL dual growth factor delivery scaffold such that BMP2 and VEGF are bound in a clinically applicable setting (<1 hour protein to PCL exposure) to the inner and outer modules, and assess the bone regenerated in an ectopic site.

*We **hypothesize** that delivering VEGF along with BMP2 from a PCL construct will increase the regenerated bone rate from 4 to 8 weeks when compared to BMP2 delivery alone in an ectopic location.*

AIM IV: Characterize binding and release kinetics of BMP2 and EPO from the components of a modular PCL scaffold, and determine if locally delivering both factors increases the bone regenerated at an early time point.

*We **hypothesize** that delivering adsorbed EPO with BMP2 from a modular PCL scaffold will result in more regenerated bone volume at 4 weeks when compared to BMP2 delivery alone in an ectopic location.*

These aims are connected by their goal to further optimize the pre-fabricated flap process. The first aim refines a method of binding BMP2 to PCL while considering a clinical setting. Current methods vary greatly for binding BMP2 to scaffolds, and they fail to consider an operating room (OR) environment. Studies have used various methods for delivering BMP2 from biomaterial scaffolds including sulfosuccinimidyl-4-(N-maleimidomethyl) cyclohexane-1-carboxylate (sulfo-SMCC), heparin, trauts, adsorption, or microparticle incorporation [37-45]. Temperatures and exposure times at which protein binding studies have been tested range from 4^{o}C-37^{o}C and 1-24 hours [14,39,46,47]. However, temperatures that are different than the OR environment and

long protein to scaffold exposure times make it very difficult to use such binding methods in a clinical setting. *We **hypothesize** that adsorption will be more optimal than conjugation for clinical usage due to protocol simplicity, retained bioactivity, and increased bone regenerated in vivo.*

To create a bone flap for a large defect, there must be enough bone volume as well as sufficient vasculature to provide nutrients and remove waste for the regenerating bone. Delivering angiogenic growth factor VEGF along with BMP2 from complex carriers has resulted in conflicting information that either shows an increase or no change in the regenerated bone volume [11,32-34,48]. In AIMS II and III, we apply the BMP2 and VEGF dual delivery concept to the pre-fabrication model. The two delivery systems investigated are a BMP2-adsorbed PCL scaffold with an internal collagen sponge to deliver VEGF and a modular PCL scaffold with BMP2 and VEGF adsorbed onto the inner and outer portions of a modular scaffold, respectively, and manually assembled. *We **hypothesize** that delivering VEGF along with BMP2 from a PCL construct will increase the regenerated bone rate from 4 to 8 weeks when compared to BMP2 delivery alone in an ectopic location.*

Finally, the time required for the flap to mature once implanted is crucial for oncology patients awaiting adjuvant therapy. Hematopoietic protein EPO is FDA approved and has resulted in increased orthotopic bone growth when delivered in combination with BMP2 [36]. There are few studies that deliver both factors locally [36] and none of which we know that investigate dual delivery on PCL or designed scaffolds in general. In AIM IV, we apply dual EPO and BMP2 delivery to the prefabrication process. *We **hypothesize** that delivering adsorbed EPO with BMP2 from a modular PCL*

scaffold will result in more regenerated bone volume at 4 weeks when compared to BMP2 delivery alone in an ectopic location. The results of these studies will increase scientific knowledge for researchers looking to pre-fabricate a customized complex bone tissue flap to reconstruct craniofacial bone defects.

1.5 Dissertation Contents

Chapters 2 and 3 of this dissertation review the background of topics used in the experimental work included in Chapters 4-7. Chapter 2 provides more information on the natural bone regeneration stages and describes the roles that BMP2, VEGF, and EPO play in native bone healing. After understanding how these proteins are naturally expressed, we can mimic their expression to produce a tissue engineered construct. Chapter 3 elaborates on fabrication methods for synthetic scaffolds used to deliver GFs. Single and dual growth factor delivery vehicles are described as well as their effect on bone regeneration. Chapter 4 is the first experimental chapter that discusses protein binding and release of adsorbed and conjugated BMP2 to PCL scaffolds. BMP2-modified scaffolds were implanted subcutaneously in mice and explanted samples were assessed for bone regeneration using micro computed tomography (microCT), mechanical testing, and histology analyses methods. Chapter 5 builds on Chapter 4's results by fabricating a collagen sponge inside of the BMP2-adsorbed PCL scaffold to co-deliver VEGF. Similar methods of assessing bone formation used in Chapter 4 are employed in Chapter 5, except that two *in vivo* time points (4 & 8 weeks) are studied instead of one. In Chapter 6, a novel modular PCL construct is developed to deliver both GFs. The scaffold is composed of inner and outer modular components that are individually exposed to growth factors in a clinically applicable setting, manually assembled, and implanted

subcutaneously in a murine model. Two VEGF dosages were tested, and the regenerated bone was analyzed as previously described in Chapter 4. Chapter 7 investigates delivering EPO along with BMP2 from the modular scaffold. Binding and release kinetics were characterized and the regenerated bone in an ectopic location was analyzed as previously mentioned. Finally, Chapter 8 will discuss a summary of the results and will propose suggestions for future studies.

1.6 References

[1] Jahangir A, Nunley R, Mehta S, Sharan A. Bone-graft substitutes in orthopaedic surgery. American Academy of Orthopaedic Surgeons 2008(January 2008).

[2] Giannoudis PV, Dinopoulos H, Tsiridis E. Bone substitutes: an update. Injury 2005 Nov;36 Suppl 3:S20-7.

[3] Bone Grafts and Substitutes Market Bending Towards Steady Growth by 2020, says GlobalData. 2014; Available at: http://healthcare.globaldata.com/media-center/press-releases/medical-devices/bone-grafts-and-substitutes-market-bending-towards-steady-growth-by-2020-says-globaldata.

[4] Fast Facts for Purchasers: The Growing Bone-Graft Substitute Marke**t**. 2013; Available at: http://www.hfma.org/Content.aspx?id=19318.

[5] Roberts TT, Rosenbaum AJ. Bone grafts, bone substitutes and orthobiologics: the bridge between basic science and clinical advancements in fracture healing. Organogenesis 2012 Oct-Dec;8(4):114-124.

[6] Center for Disease Control and Prevention. Frequently Asked Questions - Bone Allografts. 2013; Available at: http://www.cdc.gov/oralhealth/infectioncontrol/faq/allografts.htm.

[7] Krieg J, Hak D. Bone Grafting and Bone Graft Substitutes. 2010.

[8] Kundu B, Lemos A, Soundrapandian C, Sen PS, Datta S, Ferreira JM, et al. Development of porous HAp and beta-TCP scaffolds by starch consolidation with foaming method and drug-chitosan bilayered scaffold based drug delivery system. J Mater Sci Mater Med 2010 Nov;21(11):2955-2969.

[9] Summary of typical bone-graft substitutes that are commercially available - 2010. Available at:

http://www.aatb.org/aatb/files/ccLibraryFiles/Filename/000000000323/BoneGraftSubstituteTable2010.pdf.

[10] Bae JH, Song HR, Kim HJ, Lim HC, Park JH, Liu Y, et al. Discontinuous release of bone morphogenetic protein-2 loaded within interconnected pores of honeycomb-like polycaprolactone scaffold promotes bone healing in a large bone defect of rabbit ulna. Tissue Eng Part A 2011 Oct;17(19-20):2389-2397.

[11] Kanczler JM, Ginty PJ, White L, Clarke NM, Howdle SM, Shakesheff KM, et al. The effect of the delivery of vascular endothelial growth factor and bone morphogenic protein-2 to osteoprogenitor cell populations on bone formation. Biomaterials 2010 Feb;31(6):1242-1250.

[12] Santo VE, Gomes ME, Mano JF, Reis RL. Controlled Release Strategies for Bone, Cartilage, and Osteochondral Engineering-Part I: Recapitulation of Native Tissue Healing and Variables for the Design of Delivery Systems. Tissue Eng Part B Rev 2013 Feb 19.

[13] Liu X, Ma PX. Polymeric scaffolds for bone tissue engineering. Ann Biomed Eng 2004 Mar;32(3):477-486.

[14] Autefage H, Briand-Mesange F, Cazalbou S, Drouet C, Fourmy D, Goncalves S, et al. Adsorption and release of BMP-2 on nanocrystalline apatite-coated and uncoated hydroxyapatite/beta-tricalcium phosphate porous ceramics. J Biomed Mater Res B Appl Biomater 2009 Nov;91(2):706-715.

[15] Kanczler JM, Oreffo RO. Osteogenesis and angiogenesis: the potential for engineering bone. Eur Cell Mater 2008 May 2;15:100-114.

[16] Bhumiratana S, Vunjak-Novakovic G. Concise review: personalized human bone grafts for reconstructing head and face. Stem Cells Transl Med 2012 Jan;1(1):64-69.

[17] Sutherland RM, Sordat B, Bamat J, Gabbert H, Bourrat B, Mueller-Klieser W. Oxygenation and differentiation in multicellular spheroids of human colon carcinoma. Cancer Res 1986 Oct;46(10):5320-5329.

[18] Colton CK. Implantable biohybrid artificial organs. Cell Transplant 1995 Jul-Aug;4(4):415-436.

[19] Yamada Y, Ueda M, Naiki T, Takahashi M, Hata K, Nagasaka T. Autogenous injectable bone for regeneration with mesenchymal stem cells and platelet-rich plasma: tissue-engineered bone regeneration. Tissue Eng 2004 May-Jun;10(5-6):955-964.

[20] Boo JS, Yamada Y, Okazaki Y, Hibino Y, Okada K, Hata K, et al. Tissue-engineered bone using mesenchymal stem cells and a biodegradable scaffold. J Craniofac Surg 2002 Mar;13(2):231-9; discussion 240-3.

[21] Mendonca JJ, Juiz-Lopez P. Regenerative facial reconstruction of terminal stage osteoradionecrosis and other advanced craniofacial diseases with adult cultured stem and progenitor cells. Plast Reconstr Surg 2010 Nov;126(5):1699-1709.

[22] Chen FM, Zhang J, Zhang M, An Y, Chen F, Wu ZF. A review on endogenous regenerative technology in periodontal regenerative medicine. Biomaterials 2010 Nov;31(31):7892-7927.

[23] Alam MI, Asahina I, Seto I, Oda M, Enomoto S. Prefabrication of vascularized bone flap induced by recombinant human bone morphogenetic protein 2 (rhBMP-2). Int J Oral Maxillofac Surg 2003 Oct;32(5):508-514.

[24] Becker ST, Bolte H, Krapf O, Seitz H, Douglas T, Sivananthan S, et al. Endocultivation: 3D printed customized porous scaffolds for heterotopic bone induction. Oral Oncol 2009 Nov;45(11):e181-8.

[25] Terheyden H, Jepsen S, Rueger DR. Mandibular reconstruction in miniature pigs with prefabricated vascularized bone grafts using recombinant human osteogenic protein-1: a preliminary study. Int J Oral Maxillofac Surg 1999 Dec;28(6):461-463.

[26] Terheyden H, Knak C, Jepsen S, Palmie S, Rueger DR. Mandibular reconstruction with a prefabricated vascularized bone graft using recombinant human osteogenic protein-1: an experimental study in miniature pigs. Part I: Prefabrication. Int J Oral Maxillofac Surg 2001 Oct;30(5):373-379.

[27] Terheyden H, Menzel C, Wang H, Springer IN, Rueger DR, Acil Y. Prefabrication of vascularized bone grafts using recombinant human osteogenic protein-1--part 3: dosage of rhOP-1, the use of external and internal scaffolds. Int J Oral Maxillofac Surg 2004 Mar;33(2):164-172.

[28] Warnke PH, Springer IN, Acil Y, Julga G, Wiltfang J, Ludwig K, et al. The mechanical integrity of in vivo engineered heterotopic bone. Biomaterials 2006 Mar;27(7):1081-1087.

[29] Heliotis M, Lavery KM, Ripamonti U, Tsiridis E, di Silvio L. Transformation of a prefabricated hydroxyapatite/osteogenic protein-1 implant into a vascularised pedicled bone flap in the human chest. Int J Oral Maxillofac Surg 2006 Mar;35(3):265-269.

[30] Warnke PH, Springer IN, Wiltfang J, Acil Y, Eufinger H, Wehmoller M, et al. Growth and transplantation of a custom vascularised bone graft in a man. Lancet 2004 Aug 28-Sep 3;364(9436):766-770.

[31] Warnke PH, Wiltfang J, Springer I, Acil Y, Bolte H, Kosmahl M, et al. Man as living bioreactor: fate of an exogenously prepared customized tissue-engineered mandible. Biomaterials 2006 Jun;27(17):3163-3167.

[32] Kempen DH, Lu L, Heijink A, Hefferan TE, Creemers LB, Maran A, et al. Effect of local sequential VEGF and BMP-2 delivery on ectopic and orthotopic bone regeneration. Biomaterials 2009 May;30(14):2816-2825.

[33] Geuze RE, Theyse LF, Kempen DH, Hazewinkel HA, Kraak HY, Oner FC, et al. A differential effect of bone morphogenetic protein-2 and vascular endothelial growth factor release timing on osteogenesis at ectopic and orthotopic sites in a large-animal model. Tissue Eng Part A 2012 Oct;18(19-20):2052-2062.

[34] Young S, Patel ZS, Kretlow JD, Murphy MB, Mountziaris PM, Baggett LS, et al. Dose effect of dual delivery of vascular endothelial growth factor and bone morphogenetic protein-2 on bone regeneration in a rat critical-size defect model. Tissue Eng Part A 2009 Sep;15(9):2347-2362.

[35] Sun H, Jung Y, Shiozawa Y, Taichman RS, Krebsbach PH. Erythropoietin modulates the structure of bone morphogenetic protein 2-engineered cranial bone. Tissue Eng Part A 2012 Oct;18(19-20):2095-2105.

[36] Nair AM, Tsai YT, Shah KM, Shen J, Weng H, Zhou J, et al. The effect of erythropoietin on autologous stem cell-mediated bone regeneration. Biomaterials 2013 Oct;34(30):7364-7371.

[37] Han J, Cao RW, Chen B, Ye L, Zhang AY, Zhang J, et al. Electrospinning and biocompatibility evaluation of biodegradable polyurethanes based on L-lysine diisocyanate and L-lysine chain extender. J Biomed Mater Res A 2011 Mar 15;96(4):705-714.

[38] Kim TH, Oh SH, Na SY, Chun SY, Lee JH. Effect of biological/physical stimulation on guided bone regeneration through asymmetrically porous membrane. J Biomed Mater Res A 2012 Jun;100(6):1512-1520.

[39] Zhao Y, Zhang J, Wang X, Chen B, Xiao Z, Shi C, et al. The osteogenic effect of bone morphogenetic protein-2 on the collagen scaffold conjugated with antibodies. J Control Release 2010 Jan 4;141(1):30-37.

[40] Kumagai T, Anada T, Honda Y, Takami M, Kamijyo R, Shimauchi H, et al. Osteoblastic Cell Differentiation on BMP-2 Pre-Adsorbed Octacalcium Phosphate and Hydroxyapatite. Key Engineering Materials 2007;361-363:1025.

[41] Gharibjanian NA, Chua WC, Dhar S, Scholz T, Shibuya TY, Evans GR, et al. Release kinetics of polymer-bound bone morphogenetic protein-2 and its effects on

the osteogenic expression of MC3T3-E1 osteoprecursor cells. Plast Reconstr Surg 2009 Apr;123(4):1169-1177.

[42] Zhang Q, He QF, Zhang TH, Yu XL, Liu Q, Deng FL. Improvement in the delivery system of bone morphogenetic protein-2: a new approach to promote bone formation. Biomed Mater 2012 Aug;7(4):045002-6041/7/4/045002. Epub 2012 May 4.

[43] Bae SE, Choi J, Joung YK, Park K, Han DK. Controlled release of bone morphogenetic protein (BMP)-2 from nanocomplex incorporated on hydroxyapatite-formed titanium surface. J Control Release 2012 Jun 28;160(3):676-684.

[44] Hosseinkhani H, Hosseinkhani M, Khademhosseini A, Kobayashi H. Bone regeneration through controlled release of bone morphogenetic protein-2 from 3-D tissue engineered nano-scaffold. J Control Release 2007 Feb 26;117(3):380-386.

[45] Kirby GTS, White LJ, Rahman CV, Cox HC, Qutachi O, Rose, Felicity R. A. J., et al. PLGA-Based Microparticles for the Sustained Release of BMP-2. Polymers 2011;3:571.

[46] Apatite-Polymer Composite Particles for Controlled Delivery of BMP-2: *In Vitro* Release and Cellular Response. Proceedings of the Singapore-MIT Alliance Symposium; 2005.

[47] Park YJ, Kim KH, Lee JY, Ku Y, Lee SJ, Min BM, et al. Immobilization of bone morphogenetic protein-2 on a nanofibrous chitosan membrane for enhanced guided bone regeneration. Biotechnol Appl Biochem 2006 Jan;43(Pt 1):17-24.

[48] Patel ZS, Young S, Tabata Y, Jansen JA, Wong ME, Mikos AG. Dual delivery of an angiogenic and an osteogenic growth factor for bone regeneration in a critical size defect model. Bone 2008 Nov;43(5):931-940.

CHAPTER 2

BONE DEVELOPMENT, REGENERATION, AND GROWTH FACTORS

2.1 Endochondral vs. Intramembranous Ossification

There are two methods by which bone forms during development: endochondral and intramembranous ossification. Long bones are formed through endochondral ossification, and flat bones, such as those seen in the skull, are created through intramembranous ossification. During the latter method, capillaries invade the mesenchymal zone and mesenchymal stem cells (MSCs) differentiate into osteoblasts (bone forming cells). These osteoblasts deposit osteoid to form bone spicules which develop into the trabeculae. As the trabeculae grow, woven bone forms in a weak disorganized structure. After continuous remodeling, lamellar, or mature, bone forms [1].

During endochondral ossification, long bones initially begin as a cartilage model and then transition to bone tissue. Prior to birth, ossification begins at the primary ossification center which is where the diaphysis (or shaft) of the bone will eventually form. After birth, the secondary ossification sites appear which are where the epiphyses (the two rounded ends of the long bone) form. First, MSCs cluster and form a cartilage model of the bone (Figure 2.1A-C). Then, osteoblasts deposit osteoid around the cartilage and create a bone collar (Figure 2.1D). Osteoblasts secrete osteoid, and minerals like calcium are deposited. Next, the chondrocytes (cartilage cells) inside of the diaphysis proliferate, hypertrophy, and apoptose to create a cavity which allows for blood vessel

infiltration (Figure 2.1E). The vasculature transports osteoblasts to the marrow area and ossification begins which elongates the bone. Finally, trabecular (or cancellous) bone forms in the marrow space, and compact bone forms around the outside (Figure 2.1F) [1].

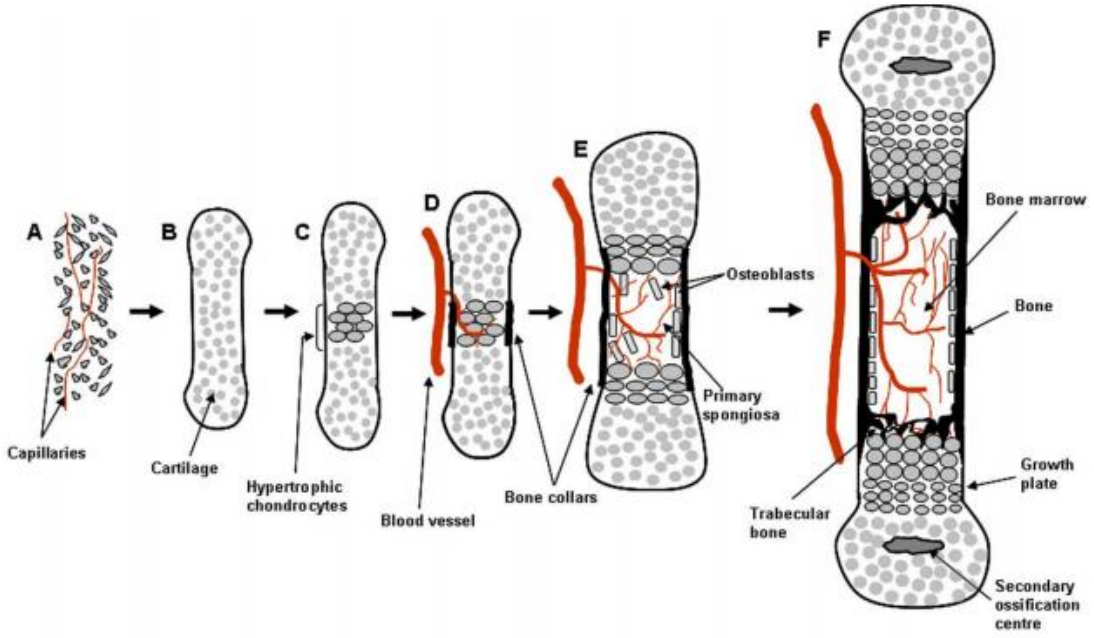

Figure 2.1: The Stages of Endochondral Ossification. A) MSCs condense. (B) MSCs differentiate into chondrocytes which form the cartilage model. (C) The primary ossification center forms and chondrocytes stop proliferating. (D) Osteoblasts form a bone collar. (E) The chondrocytes apoptose, and a cavity forms to allow for vascular infiltration to transport osteoblasts to the site. (F) Growth plates form at the secondary ossification centers after multiple cycles of chondrocyte hypertrophy, vascular invasion and osteoblast activity. Finally, trabecular and cortical bone are formed. (Image taken from Kanczler et al., Eur Cell Mater, 2008 [1])

Once a bone has fully developed, it continuously goes through a remodeling process in which old bone is removed by osteoclasts, and new bone is replaced by osteoblasts. Remodeling is needed to increase bone strength when there is extra stress applied and to release calcium to other parts of the body. Development and remodeling are not the only times that bone goes through regeneration. When bone tissue sustains an injury, such as a fracture, it progresses through a healing cycle. After the initial fracture, a

hematoma forms from the broken blood vessels, and an inflammatory response activates cytokines and growth factors which recruit osteoprogenitors and MSCs to the injury site (Figure 2.2A)[1-3]. Next, blood vessels and connective tissue stem cells infiltrate the fracture site to phagocytize the injury debris and form a fibrocartilaginous callus. Fibrous connective tissue and cartilage matrix is laid down so that new bone can form (Figure 2.2B). Osteoclasts then break down the fibrous and cartilaginous portions, and osteoblasts lay down a bone matrix to form a callus of spongy bone [1,4]. The new bone volume is generally greater than the fracture volume (Figure 2.2C). In the final stage, osteoclasts and osteoblasts remodel the bone until the original dimension is recreated (Figure 2.2D) [1].

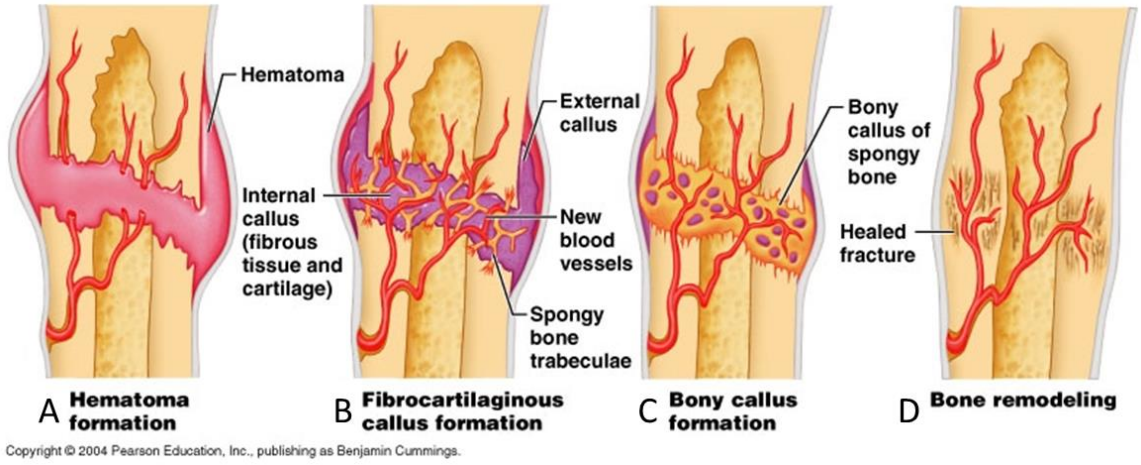

Figure 2.2: The Stages of Bone Fracture Healing. **A)** A hematoma forms at the fracture site. **B**) Neovascularization occurs, and the internal callus composed of fibrous tissue and cartilage forms. **C)** A boney callus is formed as osteoclasts remove the cartilage and osteoblasts lay down new bone. **D**) Bone remodeling occurs until the original geometry is achieved. (Image taken from: Cummings B. Figure 5.5. Stages in the Healing of a Bone Fracture: Pearson Education, Inc., 2004, [5])

During this complex fracture healing process, many growth factors and signals are expressed to recruit cells and guide cell gene expression to stimulate osteogenesis and

angiogenesis. These factors are typically utilized in methods to tissue engineer bone due to their natural involvement in bone healing.

Osteogenic Protein	Role in Bone Regeneration	References
BMPs (BMP-2,-4)	Influences MSCs to differentiate into osteoblasts	[1,6-9]
PDGF	Releases when the hematoma forms and stimulates osteoblast migration Increases MSC proliferation	[1,10-12]
βFGF (-2b)	Increases MSC proliferation Promotes an osteogenic response in progenitor cells by providing cytotoxic resistance to inflammatory oxidants	[1,12-15]
IGF (IGF-1)	Stimulates osteoblast chemotaxis and activity Expressed in proliferating chondrocytes	[12]
TGFβ	Influences MSCs to differentiate into the chondrogenic lineage and proliferate Involved in matrix production	[1,9,16-18]
Angiogenic Protein	**Role in Bone Regeneration**	**References**
VEGF	Coordinates metaphyseal and epiphyseal vascularization, cartilage formation, and ossification	[1]
βFGF (-2)	Accelerates fracture repair Stimulates angiogenesis and osteoblast differentiation	[14,19-23]
TGFβ	Released by endothelial cells and promotes bone deposition	[24]
Ang-1	Potentiates the BMP2 signaling pathways and stimulates angiogenesis Increases trabecular bone and vascularity	[25]
EPO	Influences HSCs to produce BMPs Activates MSCs to differentiate into osteoblasts Similar to VEGF and has angiogenic properties	[26-29]

Table 2.1: Osteogenic and Angiogenic Factors and their Role in Bone Regeneration. BMP: bone morphogenetic protein; PDGF: platelet derived growth factor, FGF: fibroblast growth factor; IGF: insulin like growth factor; TGF: transforming growth factor; VEGF: vascular endothelial growth factor; Ang-1: angiopoietin; EPO: erythropoietin; MSC: mesenchymal stem cells; HSC: hematopoietic stem cells

2.2 Bone Morphogenetic Protein-2 and Bone Regeneration

Bone morphogenetic proteins (BMPs) [30], fibroblast growth factors (FGFs) [31], insulin like growth factor-1 (IGF-1) [32], transforming growth factor-beta (TGF-β) [33], and platelet derived growth factor (PDGF) [34] are a few of the key factors temporally

expressed during bone healing that assist with the osteoblast recruitment, proliferation, and differentiation [35]. The most potent osteogenic proteins are the BMPs which induce cartilage and bone formation [36].

BMPs belong to the TGF-β superfamily and are naturally produced by MSCs, osteoblasts, and chondroblasts. MSCs [37], chondroblasts [38], osteoblasts [36], and fibroblasts [39] are present during bone regeneration and development, and if they are exposed to BMP2, they differentiate down an osteogenic lineage. BMP2 is a disulfide-linked homodimeric protein consisting of two 114 amino acid residue subunits (~26kDa dimer). Its glycosylated form is about 36kDa. Molecularly, BMP (-2,-4,-7) dimerizes and binds to a receptor complex containing type I and type II serine/threonine receptor kinases on the cell membrane as seen in Figure 2.3. This unit then phosphorylates SMAD1, 5 and 8 which forms a complex with SMAD 4 and translocates into the nucleus where it interacts with Runx2 transcription factor [40,41]. This interaction up-regulates gene expression such as osterix, collagen type 1, alkaline phosphatase, and matrix metalloproteinase (MMP-13).

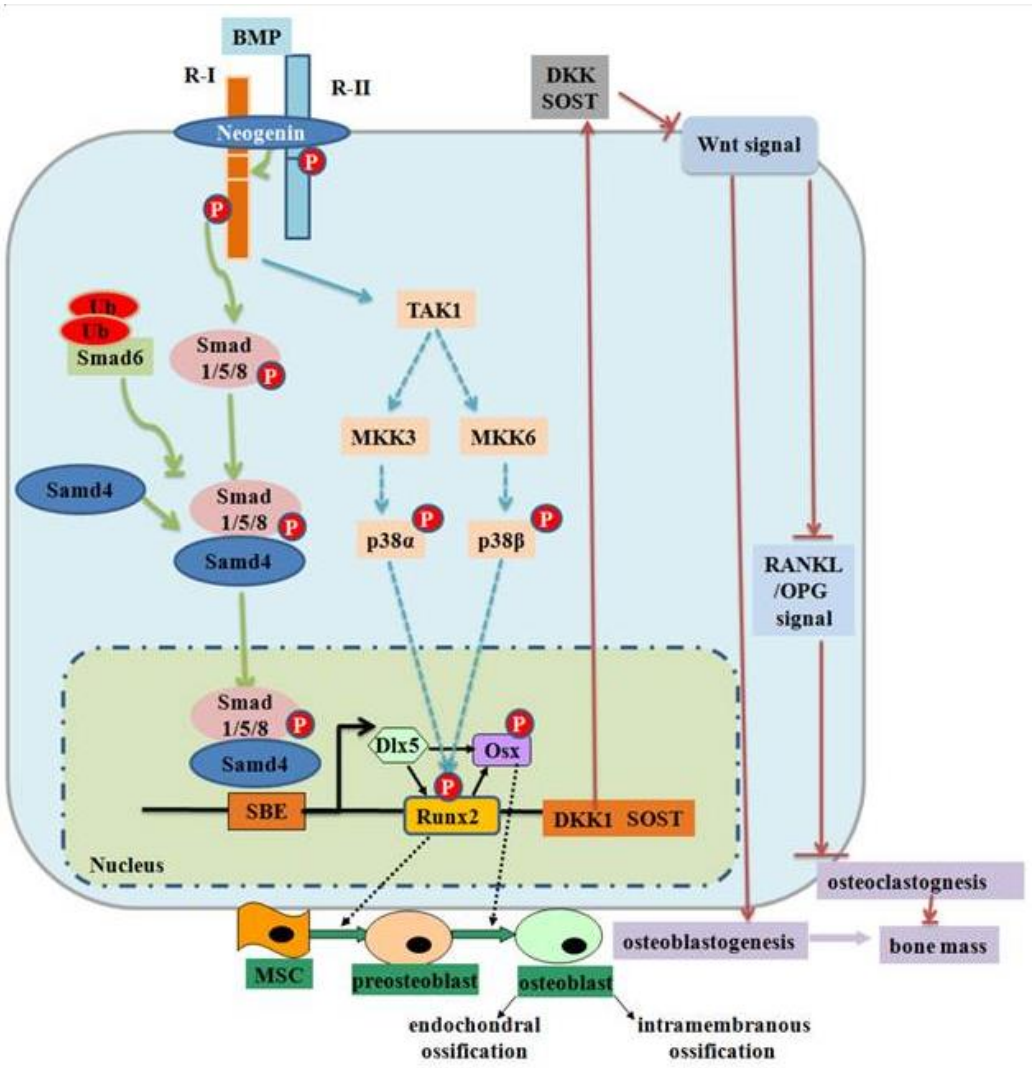

Figure 2.3: Cell Signaling Pathway for BMP2 Activity. (Chen et al., Int J Biol Sci, 2012 [42])

Recombinant forms of BMP2 and BMP7 are potent osteoinductive agents that stimulate healing in long bone critical sized defects [43,44]. The earliest skeletal need for BMP signaling is during chondroblast compaction. Signaling then mediates chondroblast proliferation and hypertrophy indicating a direct role in chondrogenesis which is the first stage in endochondral ossification [45]. In models lacking skeletal BMP2 production, there were significant delays in the formation of the secondary ossification centers and increased micro-fractures. Osteoprogenitor cells were also unable to proliferate and

differentiate into fully functional osteoblasts, indicating BMP's crucial role in progressing an osteoprogenitor cell into a mature osteocyte.

In relation to fracture healing, the BMP2 signaling cascade begins during the initial phases of bone healing which triggers an inflammatory response and periosteal activation. BMP2 is also important during later stages of osteogenesis [46]. In one study, mice lacking bone-specific expression of BMP2 were unable to initiate a healing response [47]. Those with BMP2 produced new bone at the trauma site, and a highly proliferative callus was present. Femurs without BMP2 produced some bone but there was no bridging callus. In a similar study that lacked BMP4 and BMP7, normal fracture healing occurred despite the missing proteins [45]. Finally, loss of endogenous BMP activity leads to osteopenia, bone fragility, and spontaneous fracture. Taken together, this information indicates that BMP2 plays a crucial role in osteogenesis and fracture healing [42,47-49].

Recombinant human BMP2 (glycosylated) can be manufactured in mammalian cells such as chinese hamster ovary cells (CHO); however, this purification method is associated with post-translational problems, low yields, and high cost [50]. BMP2 can also be purified from *Escherichia Coli* (*e-coli*) which results in a higher yield and lower cost. *E.coli* produced BMP2 is not glycosylated which alters the protein's solubility. When compared to glycosylated BMP2, the non-glycosylated version proves to be a more potent osteogenic agent that produces more bone *in vivo* [51].

Currently, two BMP devices are approved by the Food and Drug Administration (FDA) for clinical usage: BMP2 loaded into a collagen matrix (Infuse^{TM}, Medtronic Sofamor Danek, Inc) used for spinal fusion, open tibial fractures, sinus augmentation, and

dental procedures [52] and BMP7 (OP-1TM, Stryker Biotech) used for long bone defects and non-union treatment [35,53]. These products are costly due to high BMP doses (2-12mg) which greatly exceed the physical concentrations (18.8-22g/mL) present in defect areas by several orders of magnitude [35].

2.3 Vascular Endothelial Growth Factor and Bone Regeneration

When regenerating a large bone volume, it is crucial to develop a rich vascular network. Vasculature provides developing bone with necessary nutrients such as growth factors, hormones, cytokines, chemokines and metabolites. Of the angiogenic proteins that can stimulate neovascularization, vascular endothelial growth factor (VEGF) is the most potent, and VEGF is expressed during the early phases of bone healing.

VEGF has four isoforms: VEGF-A, VEGF-B, VEGF-C, and VEGF-D. VEGF-A (also known as VEGF-165) is a 34-46kD homodimeric glycoprotein produced by MSCs, osteoblasts, and chondrocytes. It has a high affinity receptor VEGFR2 (Flk-1/KDR) located on the cell membranes of monocytes, neurons, chondrocytes, osteoblasts, and osteoclasts. As seen in Figure 2.4, VEGF is involved in many cell signaling pathways. VEGF is essential in coordinating metaphyseal and epiphyseal vascularization, cartilage formation, and ossification during endochondral ossification [1]. During this time, VEGF promotes vascularization and regulates the survival and activity of endothelial, chondrogenic, and osteogenic cells [54]. Hypertrophic chondrocytes secrete VEGF which induces angiogenesis from the perichondrium and leads to the recruitment of osteoblasts, osteoclasts, and hematopoietic cells. These cells then assist with developing the primary ossification centers [1]. VEGF is responsible for forming a vascular network to provide nutrients, for recruiting endothelial progenitor cells [55], and for inducing osteoblast

migration and differentiation to produce bone [56]. On a molecular level, Runx2 expression (also important in pre-osteoblast differentiation) may regulate VEGF expression and angiogenesis at the growth plate/trabeculae junction [1].

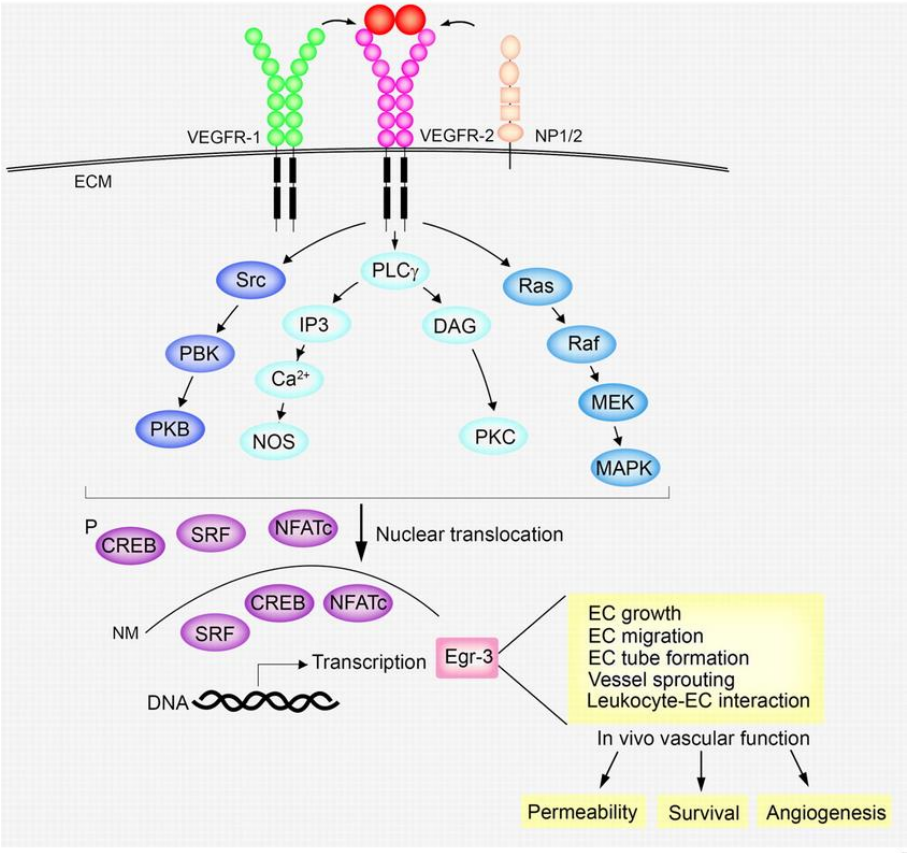

Figure 2.4: Cell Signaling Pathway for VEGF Activity. (Cao et al, Blood, 2010 [57])

When bone is healing, angiogenic factors are expressed at an earlier time point while osteogenic factors are continuously expressed [58,59]. VEGF is highly expressed during the first seven days but decreases in later phases [60]. The growth factor is expressed before blood vessels are detected, and its expression is linked to bone formation [4,61]. With respect to facture healing, VEGF is expressed in chondroblasts, chondrocytes [62], osteoprogenitor cells and osteoblasts in the fracture callus [63].

Recombinant human VEGF-165 can be purified using various methods. One efficient method is to produce the protein in the endosperm tissue of barley grain (hordeum valgare) [64]. Wheat-produced VEGF results in up to 50 times less protease activity when compared to VEGF produced in *e.coli* [65] or in CHO cells [66].

During bone development, there is a natural interaction between osteogenesis and angiogenesis [67]. Sojo et al. showed that angiogenesis occurs before osteogenesis in bone lengthening [68]. Furthermore, the rate that bone marrow stromal cells (BMSCs) differentiate into osteoblasts may be controlled by endothelial cells by initiating osteoprogenitor cell recruitment to the bone remodeling site [69]. Co-culture experiments find osteoblast-like cells stimulate endothelial cell proliferation by producing VEGF, and endothelial cells stimulate osteoprogenitor cell differentiation by producing BMP2 [70-72]. Exposing endothelial cells to VEGF increased BMP2 mRNA expression [73], indicating an interactive relationship between angiogenesis and osteogenesis. Overall, VEGF has the potential to synergistically interact with BMP2.

2.4 Erythropoietin and Bone Regeneration

Erythropoietin (EPO) is an acidic glycoprotein with a molecular weight of 30.4kDa. The core contains two bisulfide bridges composed of 165 amino acids [74]. EPO's main function is as a hematopoietic hormone that is secreted from the liver and kidneys in response to hypoxia. This release is initiated by activating HIF-1α [29,75]. EPO regulates red blood cell proliferation and has angiogenic properties in various tissues [26,27]. Interestingly, EPO shares some functional and structural similarities with VEGF [27]. Once secreted, EPO binds to EPO receptors (EPOR) on cellular membranes. EPOR are also expressed on cells not involved in hematopoietic functions such as on

endothelial cells [27,76], neurons, and trophoblast cells [28]. Brines et al. [75] found EPO-EPOR signaling was activated in response to neuronal injury, and several other studies find EPO induces cell proliferation in the kidney, intestine, and skeletal muscle [77-79]. Due to EPOR expression on many cell types, EPO may have specific functions for different tissues [29].

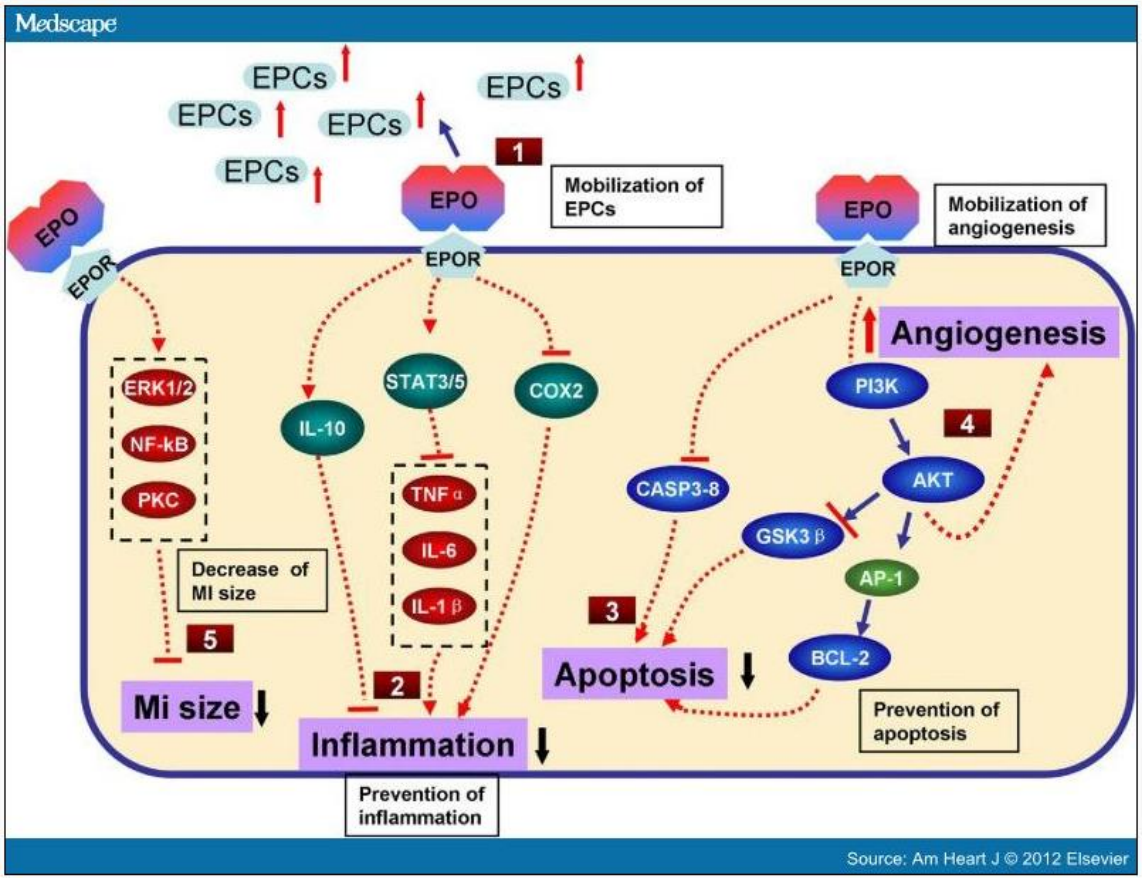

Figure 2.5: Cell Signaling Pathway for EPO Activity. (Gao et al., Am Heart J, 2012 [80])

There are several suggestions as to how EPO positively influences bone healing; however, the mechanisms regulating the process remain vague [29,81]. One study suggests EPO activates Jak-Stat signaling pathways in hematopoietic stem cells (HSCs) which leads to the production of BMPs. EPO also directly activates mesenchymal cells to differentiate into osteoblasts (*in vitro*). *In vivo*, mice treated systemically with

supraphysiological EPO doses had increased bone mineral density, bone volume fraction, and the osteoblasts that adhered to the bone surfaces [28,29]. EPO could increase bone healing directly by binding to EPOR on BMSCs to induce osteoblastic differentiation and/or indirectly by stimulating HSCs to produce BMPs which affects bone healing as mentioned in Section 2.2 [28,29]. Another method by which EPO could increase bone regeneration is EPO's ability to increase osteoclastogenesis [81]. Osteoclasts can recruit MSCs to the site of bone remodeling, and these MSCs have the potential to differentiate into osteoblasts [81].

Glycosylated EPO is required for its biological activity *in vivo*. For this reason, recombinant human EPO is manufactured in CHO cells. During glycosylation, several sugars are trimmed from the protein, it is folded and moved to the golgi complex, and then mannose elimination occurs before N-acetylglucosamine, galactose and sialic acid (*N*-acetylneuraminic acid) are added [74]. EPO's survival in circulation requires the presence of terminal sialic acid residues of its N-glycans [74]. Amgen's product EPOGEN® is produced in mammalian cells and is FDA approved. EPOGEN® uses EPO to increase the red blood cell levels caused by chronic kidney disease in anemic patients. Taking EPOGEN® avoids the need for red blood cell transfusions and is safe to use in oncology patients [82,83].

2.5 Conclusion

When engineering bone tissue, it is important to take into consideration the natural factors expressed during native bone development and bone fracture healing. Of all of the factors that stimulate bone healing, BMP2 is the most potent osteogenic factor that plays a key role in long bone development through its influence on a variety of cells.

VEGF is a widely studied potent angiogenic factor that stimulates vasculature development to transport MSCs to the bone formation site. Co-culture experiments find synergistic effects between BMP2 and VEGF which could positively influence bone healing. For this reason, we will use VEGF as the angiogenic protein to co-deliver with BMP2. EPO has shown to have positive effects on bone formation by directly influencing BMSCs to turn into osteoblasts or indirectly by influencing HSCs to produce BMPs. Since EPO is FDA approved and has shown to work synergistically with BMP2, we delivered it with BMP2. BMP2, VEGF, and EPO play a role in native bone healing; therefore, we delivered BMP2 alone and in combination with either VEGF or EPO to increase the bone regenerated on poly-Ɛ-caprolactone scaffolds that were implanted in an ectopic location.

2.6 References

[1] Kanczler JM, Oreffo RO. Osteogenesis and angiogenesis: the potential for engineering bone. Eur Cell Mater 2008 May 2;15:100-114.

[2] Glowacki J. Angiogenesis in fracture repair. Clin Orthop Relat Res 1998 Oct;(355 Suppl)(355 Suppl):S82-9.

[3] Rhinelander FW. Tibial blood supply in relation to fracture healing. Clin Orthop Relat Res 1974 Nov-Dec;(105)(105):34-81.

[4] Carano RA, Filvaroff EH. Angiogenesis and bone repair. Drug Discov Today 2003 Nov 1;8(21):980-989.

[5] Cummings B. Figure 5.5. Stages in the Healing of a Bone Fracture: Pearson Education, Inc.; 2004.

[6] Barnes GL, Kostenuik PJ, Gerstenfeld LC, Einhorn TA. Growth factor regulation of fracture repair. J Bone Miner Res 1999 Nov;14(11):1805-1815.

[7] Deckers MM, van Bezooijen RL, van der Horst G, Hoogendam J, van Der Bent C, Papapoulos SE, et al. Bone morphogenetic proteins stimulate angiogenesis through osteoblast-derived vascular endothelial growth factor A. Endocrinology 2002 Apr;143(4):1545-1553.

[8] Kloen P, Di Paola M, Borens O, Richmond J, Perino G, Helfet DL, et al. BMP signaling components are expressed in human fracture callus. Bone 2003 Sep;33(3):362-371.

[9] Rodrigues M, Griffith LG, Wells A. Growth factor regulation of proliferation and survival of multipotential stromal cells. Stem Cell Res Ther 2010 Oct 26;1(4):32.

[10] Mandracchia VJ, Nelson SC, Barp EA. Current concepts of bone healing. Clin Podiatr Med Surg 2001 Jan;18(1):55-77.

[11] Risau W, Drexler H, Mironov V, Smits A, Siegbahn A, Funa K, et al. Platelet-derived growth factor is angiogenic in vivo. Growth Factors 1992;7(4):261-266.

[12] Simpson AH, Mills L, Noble B. The role of growth factors and related agents in accelerating fracture healing. J Bone Joint Surg Br 2006 Jun;88(6):701-705.

[13] Rodan SB, Wesolowski G, Thomas KA, Yoon K, Rodan GA. Effects of acidic and basic fibroblast growth factors on osteoblastic cells. Connect Tissue Res 1989;20(1-4):283-288.

[14] Montesano R, Vassalli JD, Baird A, Guillemin R, Orci L. Basic fibroblast growth factor induces angiogenesis in vitro. Proc Natl Acad Sci U S A 1986 Oct;83(19):7297-7301.

[15] Cowan CM. Nell-1 - Microenvironment Induced Osteogenic Differentiation and Bone. Nell-1 - Microenvironment Induced Osteogenic Differentiation and Bone: ProQuest; 2007. p. 23.

[16] Rosier RN, O'Keefe RJ, Hicks DG. The potential role of transforming growth factor beta in fracture healing. Clin Orthop Relat Res 1998 Oct;(355 Suppl)(355 Suppl):S294-300.

[17] Bostrom MP, Asnis P. Transforming growth factor beta in fracture repair. Clin Orthop Relat Res 1998 Oct;(355 Suppl)(355 Suppl):S124-31.

[18] Erlebacher A, Filvaroff EH, Ye JQ, Derynck R. Osteoblastic responses to TGF-beta during bone remodeling. Mol Biol Cell 1998 Jul;9(7):1903-1918.

[19] Coffin JD, Florkiewicz RZ, Neumann J, Mort-Hopkins T, Dorn GW,2nd, Lightfoot P, et al. Abnormal bone growth and selective translational regulation in basic fibroblast growth factor (FGF-2) transgenic mice. Mol Biol Cell 1995 Dec;6(12):1861-1873.

[20] Montero A, Okada Y, Tomita M, Ito M, Tsurukami H, Nakamura T, et al. Disruption of the fibroblast growth factor-2 gene results in decreased bone mass and bone formation. J Clin Invest 2000 Apr;105(8):1085-1093.

[21] Kawaguchi H, Kurokawa T, Hanada K, Hiyama Y, Tamura M, Ogata E, et al. Stimulation of fracture repair by recombinant human basic fibroblast growth factor in normal and streptozotocin-diabetic rats. Endocrinology 1994 Aug;135(2):774-781.

[22] Nakamura K, Kawaguchi H, Aoyama I, Hanada K, Hiyama Y, Awa T, et al. Stimulation of bone formation by intraosseous application of recombinant basic fibroblast growth factor in normal and ovariectomized rabbits. J Orthop Res 1997 Mar;15(2):307-313.

[23] Hayek A, Culler FL, Beattie GM, Lopez AD, Cuevas P, Baird A. An in vivo model for study of the angiogenic effects of basic fibroblast growth factor. Biochem Biophys Res Commun 1987 Sep 15;147(2):876-880.

[24] Cenni E. ANGIOGENESIS AND BONE REGENERATION. The Bone and Joint Journal 2005;87-B.

[25] Zhou L, Yoon SJ, Jang KY, Moon YJ, Wagle S, Lee KB, et al. COMP-Angiopoietin1 Potentiates the Effects of Bone Morphogenic Protein-2 on Ischemic Necrosis of the Femoral Head in Rats. PLoS One 2014 Oct 17;9(10):e110593.

[26] Anagnostou A, Lee ES, Kessimian N, Levinson R, Steiner M. Erythropoietin has a mitogenic and positive chemotactic effect on endothelial cells. Proc Natl Acad Sci U S A 1990 Aug;87(15):5978-5982.

[27] Holstein JH, Menger MD, Scheuer C, Meier C, Culemann U, Wirbel RJ, et al. Erythropoietin (EPO): EPO-receptor signaling improves early endochondral ossification and mechanical strength in fracture healing. Life Sci 2007 Feb 13;80(10):893-900.

[28] Shiozawa Y, Jung Y, Ziegler AM, Pedersen EA, Wang J, Wang Z, et al. Erythropoietin couples hematopoiesis with bone formation. PLoS One 2010 May 27;5(5):e10853.

[29] McGee SJ, Havens AM, Shiozawa Y, Jung Y, Taichman RS. Effects of erythropoietin on the bone microenvironment. Growth Factors 2012 Feb;30(1):22-28.

[30] Groeneveld EH, Burger EH. Bone morphogenetic proteins in human bone regeneration. Eur J Endocrinol 2000 Jan;142(1):9-21.

[31] Du X, Xie Y, Xian CJ, Chen L. Role of FGFs/FGFRs in skeletal development and bone regeneration. J Cell Physiol 2012 Dec;227(12):3731-3743.

[32] Koch H, Jadlowiec JA, Campbell PG. Insulin-like growth factor-I induces early osteoblast gene expression in human mesenchymal stem cells. Stem Cells Dev 2005 Dec;14(6):621-631.

[33] Hong L, Tabata Y, Miyamoto S, Yamamoto M, Yamada K, Hashimoto N, et al. Bone regeneration at rabbit skull defects treated with transforming growth factor-beta1 incorporated into hydrogels with different levels of biodegradability. J Neurosurg 2000 Feb;92(2):315-325.

[34] Yu X, Hsieh SC, Bao W, Graves DT. Temporal expression of PDGF receptors and PDGF regulatory effects on osteoblastic cells in mineralizing cultures. Am J Physiol 1997 May;272(5 Pt 1):C1709-16.

[35] Santo VE, Gomes ME, Mano JF, Reis RL. Controlled Release Strategies for Bone, Cartilage, and Osteochondral Engineering-Part I: Recapitulation of Native Tissue Healing and Variables for the Design of Delivery Systems. Tissue Eng Part B Rev 2013 Feb 19.

[36] Hiraki Y, Inoue H, Shigeno C, Sanma Y, Bentz H, Rosen DM, et al. Bone morphogenetic proteins (BMP-2 and BMP-3) promote growth and expression of the differentiated phenotype of rabbit chondrocytes and osteoblastic MC3T3-E1 cells in vitro. J Bone Miner Res 1991 Dec;6(12):1373-1385.

[37] Dorman LJ, Tucci M, Benghuzzi H. In vitro effects of bmp-2, bmp-7, and bmp-13 on proliferation and differentation of mouse mesenchymal stem cells. Biomed Sci Instrum 2012;48:81-87.

[38] Liu T, Gao Y, Sakamoto K, Minamizato T, Furukawa K, Tsukazaki T, et al. BMP-2 promotes differentiation of osteoblasts and chondroblasts in Runx2-deficient cell lines. J Cell Physiol 2007 Jun;211(3):728-735.

[39] Umehara K, Iimura T, Sakamoto K, Lin Z, Kasugai S, Igarashi Y, et al. Canine oral mucosal fibroblasts differentiate into osteoblastic cells in response to BMP-2. Anat Rec (Hoboken) 2012 Aug;295(8):1327-1335.

[40] Shah P, Keppler L, Rutkowski J. Bone morphogenic protein: an elixir for bone grafting--a review. J Oral Implantol 2012 Dec;38(6):767-778.

[41] Garrett IR. Anabolic agents and the bone morphogenetic protein pathway. Curr Top Dev Biol 2007;78:127-171.

[42] Chen G, Deng C, Li YP. TGF-beta and BMP signaling in osteoblast differentiation and bone formation. Int J Biol Sci 2012;8(2):272-288.

[43] Nair MB, Kretlow JD, Mikos AG, Kasper FK. Infection and tissue engineering in segmental bone defects--a mini review. Curr Opin Biotechnol 2011 Oct;22(5):721-725.

[44] Murakami N, Saito N, Horiuchi H, Okada T, Nozaki K, Takaoka K. Repair of segmental defects in rabbit humeri with titanium fiber mesh cylinders containing recombinant human bone morphogenetic protein-2 (rhBMP-2) and a synthetic polymer. J Biomed Mater Res 2002 Nov;62(2):169-174.

[45] Rosen V. BMP2 signaling in bone development and repair. Cytokine Growth Factor Rev 2009 Oct-Dec;20(5-6):475-480.

[46] Fassbender M, Minkwitz S, Strobel C, Schmidmaier G, Wildemann B. Stimulation of bone healing by sustained bone morphogenetic protein 2 (BMP-2) delivery. Int J Mol Sci 2014 May 14;15(5):8539-8552.

[47] Tsuji K, Bandyopadhyay A, Harfe BD, Cox K, Kakar S, Gerstenfeld L, et al. BMP2 activity, although dispensable for bone formation, is required for the initiation of fracture healing. Nat Genet 2006 Dec;38(12):1424-1429.

[48] Bandyopadhyay A, Tsuji K, Cox K, Harfe BD, Rosen V, Tabin CJ. Genetic analysis of the roles of BMP2, BMP4, and BMP7 in limb patterning and skeletogenesis. PLoS Genet 2006 Dec;2(12):e216.

[49] Wang Q, Huang C, Xue M, Zhang X. Expression of endogenous BMP-2 in periosteal progenitor cells is essential for bone healing. Bone 2011 Mar 1;48(3):524-532.

[50] Bessa PC, Cerqueira MT, Rada T, Gomes ME, Neves NM, Nobre A, et al. Expression, purification and osteogenic bioactivity of recombinant human BMP-4, -9, -10, -11 and -14. Protein Expr Purif 2009 Feb;63(2):89-94.

[51] van de Watering FC, van den Beucken JJ, van der Woning SP, Briest A, Eek A, Qureshi H, et al. Non-glycosylated BMP-2 can induce ectopic bone formation at lower concentrations compared to glycosylated BMP-2. J Control Release 2012 Apr 10;159(1):69-77.

[52] Cahill KS, Chi JH, Day A, Claus EB. Prevalence, complications, and hospital charges associated with use of bone-morphogenetic proteins in spinal fusion procedures. JAMA 2009 Jul 1;302(1):58-66.

[53] Summary of typical bone-graft substitutes that are commercially available - 2010. Available at: http://www.aatb.org/aatb/files/ccLibraryFiles/Filename/000000000323/BoneGraftSubstituteTable2010.pdf.

[54] Coultas L, Chawengsaksophak K, Rossant J. Endothelial cells and VEGF in vascular development. Nature 2005 Dec 15;438(7070):937-945.

[55] Hankenson KD, Dishowitz M, Gray C, Schenker M. Angiogenesis in bone regeneration. Injury 2011 Jun;42(6):556-561.

[56] Huang YC, Kaigler D, Rice KG, Krebsbach PH, Mooney DJ. Combined angiogenic and osteogenic factor delivery enhances bone marrow stromal cell-driven bone regeneration. J Bone Miner Res 2005 May;20(5):848-857.

[57] Cao Y. Wake-up call for endothelial cells. Blood 2010 Mar 25;115(12):2336-2337.

[58] Sheetz MP, Felsenfeld DP, Galbraith CG. Cell migration: regulation of force on extracellular-matrix-integrin complexes. Trends Cell Biol 1998 Feb;8(2):51-54.

[59] Kaigler D, Wang Z, Horger K, Mooney DJ, Krebsbach PH. VEGF scaffolds enhance angiogenesis and bone regeneration in irradiated osseous defects. J Bone Miner Res 2006 May;21(5):735-744.

[60] Uchida S, Sakai A, Kudo H, Otomo H, Watanuki M, Tanaka M, et al. Vascular endothelial growth factor is expressed along with its receptors during the healing process of bone and bone marrow after drill-hole injury in rats. Bone 2003 May;32(5):491-501.

[61] Zelzer E, McLean W, Ng YS, Fukai N, Reginato AM, Lovejoy S, et al. Skeletal defects in VEGF(120/120) mice reveal multiple roles for VEGF in skeletogenesis. Development 2002 Apr;129(8):1893-1904.

[62] Pufe T, Petersen W, Tillmann B, Mentlein R. The splice variants VEGF121 and VEGF189 of the angiogenic peptide vascular endothelial growth factor are expressed in osteoarthritic cartilage. Arthritis Rheum 2001 May;44(5):1082-1088.

[63] Tatsuyama K, Maezawa Y, Baba H, Imamura Y, Fukuda M. Expression of various growth factors for cell proliferation and cytodifferentiation during fracture repair of bone. Eur J Histochem 2000;44(3):269-278.

[64] Magnusdottir A, Vidarsson H, Bjornsson JM, Orvar BL. Barley grains for the production of endotoxin-free growth factors. Trends Biotechnol 2013 Oct;31(10):572-580.

[65] Pizarro SA, Gunson J, Field MJ, Dinges R, Khoo S, Dalal M, et al. High-yield expression of human vascular endothelial growth factor VEGF(165) in Escherichia coli and purification for therapeutic applications. Protein Expr Purif 2010 Aug;72(2):184-193.

[66] Cass B, Pham PL, Kamen A, Durocher Y. Purification of recombinant proteins from mammalian cell culture using a generic double-affinity chromatography scheme. Protein Expr Purif 2005 Mar;40(1):77-85.

[67] Peng H, Wright V, Usas A, Gearhart B, Shen HC, Cummins J, et al. Synergistic enhancement of bone formation and healing by stem cell-expressed VEGF and bone morphogenetic protein-4. J Clin Invest 2002 Sep;110(6):751-759.

[68] Sojo K, Sawaki Y, Hattori H, Mizutani H, Ueda M. Immunohistochemical study of vascular endothelial growth factor (VEGF) and bone morphogenetic protein-2, -4 (BMP-2, -4) on lengthened rat femurs. J Craniomaxillofac Surg 2005 Aug;33(4):238-245.

[69] Meury T, Verrier S, Alini M. Human endothelial cells inhibit BMSC differentiation into mature osteoblasts in vitro by interfering with osterix expression. J Cell Biochem 2006 Jul 1;98(4):992-1006.

[70] Deckers MM, Karperien M, van der Bent C, Yamashita T, Papapoulos SE, Lowik CW. Expression of vascular endothelial growth factors and their receptors during osteoblast differentiation. Endocrinology 2000 May;141(5):1667-1674.

[71] Kaigler D, Krebsbach PH, West ER, Horger K, Huang YC, Mooney DJ. Endothelial cell modulation of bone marrow stromal cell osteogenic potential. FASEB J 2005 Apr;19(6):665-667.

[72] Wang DS, Miura M, Demura H, Sato K. Anabolic effects of 1,25-dihydroxyvitamin D3 on osteoblasts are enhanced by vascular endothelial growth factor produced by osteoblasts and by growth factors produced by endothelial cells. Endocrinology 1997 Jul;138(7):2953-2962.

[73] Bouletreau PJ, Warren SM, Spector JA, Peled ZM, Gerrets RP, Greenwald JA, et al. Hypoxia and VEGF up-regulate BMP-2 mRNA and protein expression in microvascular endothelial cells: implications for fracture healing. Plast Reconstr Surg 2002 Jun;109(7):2384-2397.

[74] Jelkmann W. Recombinant EPO production--points the nephrologist should know. Nephrol Dial Transplant 2007 Oct;22(10):2749-2753.

[75] Brines ML, Ghezzi P, Keenan S, Agnello D, de Lanerolle NC, Cerami C, et al. Erythropoietin crosses the blood-brain barrier to protect against experimental brain injury. Proc Natl Acad Sci U S A 2000 Sep 12;97(19):10526-10531.

[76] Anagnostou A, Liu Z, Steiner M, Chin K, Lee ES, Kessimian N, et al. Erythropoietin receptor mRNA expression in human endothelial cells. Proc Natl Acad Sci U S A 1994 Apr 26;91(9):3974-3978.

[77] Westenfelder C, Biddle DL, Baranowski RL. Human, rat, and mouse kidney cells express functional erythropoietin receptors. Kidney Int 1999 Mar;55(3):808-820.

[78] Ogilvie M, Yu X, Nicolas-Metral V, Pulido SM, Liu C, Ruegg UT, et al. Erythropoietin stimulates proliferation and interferes with differentiation of myoblasts. J Biol Chem 2000 Dec 15;275(50):39754-39761.

[79] Juul SE, Ledbetter DJ, Joyce AE, Dame C, Christensen RD, Zhao Y, et al. Erythropoietin acts as a trophic factor in neonatal rat intestine. Gut 2001 Aug;49(2):182-189.

[80] Gao D, Ning N, Niu X, Dang Y, Dong X, Wei J, et al. Erythropoietin treatment in patients with acute myocardial infarction: a meta-analysis of randomized controlled trials. Am Heart J 2012 Nov;164(5):715-727.e1.

[81] Sun H, Jung Y, Shiozawa Y, Taichman RS, Krebsbach PH. Erythropoietin modulates the structure of bone morphogenetic protein 2-engineered cranial bone. Tissue Eng Part A 2012 Oct;18(19-20):2095-2105.

[82] Luksenburg H, Weir A, Wager R. Safety Concerns Associated with Aranesp (darbepoetin alfa) Amgen, Inc. and Procrit (epoetin alfa) Ortho Biotech, L.P., for the Treatment of Anemia
Associated with Cancer Chemotherapy. 2004; Available at: http://www.fda.gov/ohrms/dockets/ac/04/briefing/4037b2_04_fda-aranesp-procrit.htm.

[83] Amgen Initiates Voluntary Nationwide Recall of Certain Lots Of Epogen® And Procrit® (Epoetin Alfa). 2013; Available at: http://www.fda.gov/Safety/Recalls/ucm227202.htm.

CHAPTER 3

SCAFFOLD TISSUE ENGINEERING-FABRICATION METHODS AND PROTEIN DELIVERY VEHICLES

3.1 Introduction

When designing a biologic carrier, it is helpful to consider native bone structure and material properties such as load bearing capabilities and porosity for nutrient diffusion. The scaffold should maintain incorporated biologic bioactivity, and the delivered growth factors (GFs) should stimulate bone development. Scaffold fabrication methods include salt leaching, solvent casting, phase separation, and rapid prototyping. Each of these has advantages and disadvantages for bone tissue engineering applications and meeting regulatory standards. Both natural and synthetic scaffold materials are currently utilized and employ numerous protein incorporation methods which result in varied GF release profiles. Sometimes two scaffold materials will be combined to deliver one or more proteins. This chapter will address scaffold manufacturing methods, protein incorporation methods, release profiles, and regenerated bone quality for bone morphogenetic protein-2 (BMP2), vascular endothelial growth factor (VEGF), and erythropoietin (EPO).

3.2 Fabricating Synthetic Scaffolds

To create a patient specific scaffold for the cranio-maxillofacial region, first a computed tomography (CT) image is taken of the face. Next, the image is translated into

a computer-aided design (CAD) model using software such as MIMICS™ (Materialise, Leuven, Belgium) or MATLAB™ (The Mathworks, Natick, MA). Using this software, a porous architecture is created to facilitate tissue ingrowth and to alter the mechanical properties. Finally, the scaffold is manufactured using a variety of 3-dimensional (3D) rapid prototyping techniques such as stereolithography, fused deposition modeling (FDM), or selective laser sintering (SLS). Other scaffold fabrication methods involve salt leaching, solvent casting, and thermal phase separation. Polylactic acid (PLA), polyglycolic acid (PLGA), and poly-Ɛ-caprolactone (PCL) are Food and Drug Administration (FDA) approved materials that are commonly utilized [1].

3.2.1 *Salt Leaching, Solvent Casting, and Phase Separation*

Commonly used scaffold fabrication methods involve spray/emulsion freeze drying, particulate leaching/solvent casting, and thermally induced phase separation [2]. Microspheres loaded with proteins or drugs can be prepared by a spray drying method which sprays a solid-in-oil dispersion or water-in-oil emulsion in a stream of heated air [2,3]. Drawbacks include low process efficacy and a risk of denaturing proteins due to dehydration. Microparticles could also adhere to the inner walls of the spray dryer [4]. Emulsion requires the use of hazardous organic solvents which need to be completely evaporated prior to using the scaffold. Due to this health risk, regulatory hurdles would increase if a fabrication method involves organic solvents. Furthermore, the high temperatures used in this process can damage or denature the loaded protein [2,4]. Particulate leaching is a popular method which uses porogens such as salt or sugar to create pores in a biomaterial. Briefly, the porogen is ground into particles of a certain size and poured into a mold. The polymer solution is then cast into the mold and the solvent is

evaporated such that the salt crystals are leached away to create pores. This method requires less polymer solution; however, the pore shape and inter-pore openings cannot be controlled [5]. Solvent casting dissolves a polymer and drug mixture into a solvent to the desired proportion. The solvent is then cast at about 60^{o}C until the toxic solvent is completely evaporated. One of the main drawbacks of this technique is that the solvent could denature the protein [4]. Phase separation uses temperature change to separate a polymer solution into two phases of either high or low polymer concentrations [5]. Since the process is mediated by a solvent and coacervate agent, the solutions can react with the protein and disrupt the secondary structure [2]. Phase separation techniques tend to produce agglomerated particles and also require the removal of large quantities of the organic phase from the microspheres [4].

Scaffolds fabricated by these aforementioned techniques may retain some solvent toxicity if it is not removed completely and would face increased regulatory hurdles to translate into the clinic [5]. Overall, these methods result in less reproducible external and internal geometries which translate to decreased control over scaffold geometry, mechanical properties, and surface area needed for protein integration [1].

3.2.2 *Rapid Prototyping: Stereolithography, FDM, and SLS*

Stereolithography, FDM, and SLS are rapid prototyping techniques that can produce more complex geometry scaffolds than the methods discussed in Section 3.2.1 [6-10]. Stereolithography selectively polymerizes photosensitive resin using ultraviolet (UV) light. The UV laser beam focuses on a layer of resin on a platform and polymerizes it. The platform then moves in the X and Y directions to form a 2D geometry. Next, a fresh layer of resin is added on top of the cured layer, and the laser is applied again.

Ultimately, the scaffold is built in the Z direction. Although stereolithography produces high resolution scaffolds with a good surface finish, it also requires post-curing steps, and there can be some shrinkage and curling due to the phase change. Furthermore, only photo polymers can be used with the machine which limits the number of compatible materials [11].

More materials are compatible with FDM which melts and selectively deposits a thin filament of thermoplastic polymer on a stage to form the scaffold layer by layer. The material is provided on a spool, and the wire is threaded through the FDM head. The table moves in the X and Y directions and a cross-hatch design is created with the filament. The table then moves down in the Z direction, and the next layer is added on top of the previous one. The two filament layers then fuse together due to the heat. Although FDM machines are economical and the material can be easily changed, this method is not compatible for high resolution details as the Z resolution is limited [11].

SLS requires a material that is in powder form and selectively fuses the particles with a high power laser into the desired shape from the digital information received from CAD data [10]. The table then moves down in the Z direction, and a fresh layer of powder is added to the top. The laser fuses the powder again, and the 3D scaffold is created layer by layer in the Z direction. SLS can repeatedly and reproducibly produce scaffolds with complex geometries, controlled pore size, and detailed stiffness. Scaffold resolution is limited by the laser spot size and the powder particle size. The SLS build time is faster than the other mentioned methods, and the machine is compatible with a variety of materials such as nylon, polyether ether ketone (PEEK), β tri-calcium phosphate (β-TCP), poly-l-lactide acid (PLLA), and PCL [11,12].

The bone tissue scaffolding material can be chosen based on the fabrication method and the mechanical properties needed. With respect to maintaining incorporated protein bioactivity, the degraded material's byproducts should also be taken into account. For example, as PLGA degrades, the released glycolic and lactic acids cause the pH to decrease, which results in a loss of protein bioactivity due to protein aggregation and chemical degradation [2]. PCL degradation generates less acidic byproducts and leads to less inflammation than the more rapidly-degrading polylactic acid based co-polymers [13].

3.2.3 *Poly-ℰ-caprolactone*

PCL is a biocompatible and bioresorbable polymer that can be utilized with image-based CAD and SLS manufacturing techniques. The ester linkages on PCL's backbone degrade via hydrolysis into non-toxic metabolites consisting mainly of 6-hydroxyl caproic acid [14]. PCL degrades over three years, and its mechanical properties support its use for bone tissue engineering applications in complex reconstruction sites where bone may take over a year to form. In these sites, a PCL scaffold's slower degradation time is an advantage to provide form and load bearing over a longer time period. When compared to other synthetic materials, it is significantly less expensive and available in large quantities. PCL has already been approved for cranioplasty bone filling applications by the FDA [15,16]. Thus, the polymer has been widely tested, utilized, and has achieved regulatory approval as a bone repair scaffold. We propose using PCL as an ideal biologic delivery vehicle for pre-fabricated flaps because of the polymer's mechanical properties and safe manufacturing method.

3.3 BMP2 Growth Factor Delivery Methods

BMP2 has the potential to increase bone growth, but it has a very short half-life when delivered systemically in a solution. To increase its effectiveness, BMP2 can be delivered locally using synthetic or natural carrier materials. Various release profiles are observed depending on the material and binding method utilized.

3.3.1 *BMP2 Delivery Vehicles & Binding Methods*

Natural materials (i.e. collagen, alginate, hyaluronic acid) mentioned in Section 1.2.2 are used as scaffolding for mineralized tissue; however, drawbacks include batch-to-batch variations, potential for immune reactions, and mechanical properties that are well below that of native bone tissue [17]. Collagen is FDA approved as a carrier for BMP2 with Medtronic's spinal fusion product INFUSE™; however, there is a large burst release within the first 2-3 days which can result in heterotopic bone growth [18]. Because of BMP2's short half-life, a 1.5 mg/ml BMP2 (2-12 mg) dose is needed which has caused adverse reactions in patients and resulted in a lawsuit.

Synthetic materials can be fabricated with controllable properties such as degradation rate, pore structure, and mechanical stability. A mineral coating like TCP can be added to alter the surface chemistry and to promote BMP2 binding and release [19]. BMP2 adsorbed onto PLLA/TCP scaffolds resulted in a 70% burst release during the first two days [20]. Jeon et al. compared slow and rapid BMP2 delivery from PLGA microspheres and found that sustained delivery resulted in enhanced bone formation [21].

There are a wide range of methods used to bind BMP2 to materials, and the release profiles depend on the method employed. For example, a more controlled release was achieved by chemically conjugating BMP2 to chitosan with a cross linker

sulfosuccinimidyl-4-(N-maleimidomethyl)cyclohexane-1-carboxylate (sulfo-SMCC) in comparison to adsorption. Sulfo-SMCC is a heterobifunctional crosslinker with an NHS-ester group that binds to amines and a maleimide group that binds to the cysteine group on BMP2. Since the cysteine is located in the BMP2 protein's inner core, the sulfo-SMCC may not be able to bind to the cysteine. In this situation, an unfavorable reaction occurs in which the maleimide interacts with free amines on the BMP2 protein. Conjugation enhanced the material's *in vitro* osteoinductive properties; however, chitosan is not an ideal carrier because it lacks mechanical integrity for bone tissue engineering applications [22]. In that study, the scaffold was exposed to BMP2 for 10 hours at 4^{o}C. Other studies combined sulfo-SMCC in combination with trauts reagent to bind BMP2 to a demineralized bone matrix or collagen [23,24]. In those scenarios, the protein was exposed to the material in a more clinically applicable time frame of 1 hour at room temperature.

Heparin [25,26], 1-ethyl-3-(3-dimethylaminopropyl) carbodiimide (EDC) [27], and poly(ethylene-glycol) (PEG) [28] chemistry has also been used to covalently crosslink BMP2. These methods use BMP2's N-terminal heparin binding site which creates a stronger bond than adsorption [29-31]. Heparin's negatively charged sulfate groups interact with the protein's positively charged amino acid residues. For these studies, the materials were exposed to BMP2 anywhere from 1 to 6 hours in room temperature or 4^{o}C environments. When using heparin, release rates have reported to vary from 80% released in 28 days [25] to 99% BMP2 bound to PLGA and 100% released in 14 days [26]. PEG bound about 82% BMP2 to a PLGA scaffold after which there was a sustained release for 8 days and a gradual release for 28 days [28].

Adsorption is a much simpler GF incorporation method. Adsorption utilizes electrostatic forces to bind the GF to the surface and can be adjusted by altering the pH or the material's surface roughness. PCL has a slightly negative charge which attracts the positively charged amino acid residues on BMP2's surface. Adsorption is associated with a burst release trend instead of the sustained release observed with conjugation methods. Generally, GF exposure time to the materials ranges from 1 to 24 hours in environments from 4^{o}C-37^{o}C [19,32,33]. There are a few studies which superficially compare adsorption versus conjugation methods [24,26-28]; however, there are no studies of which we are aware that use highly controlled geometry scaffolds and clinical settings (<1 hour protein to material exposure at room temperature) for protein binding. Previously in our laboratory we compared adsorption versus sulfo-SMCC conjugation on salt-leached PCL scaffolds in which the scaffolds were exposed to the BMP2 for 16 hours at 4^{o}C [24]. Studies assessing conjugation methods utilized either porogen leaching [24,26] or other fabrication methods resulting in large variations in pore architecture that may significantly affect release kinetics, not allowing a rigorous comparison of adsorption and conjugation methods [22,25,28]. Overall, there are many methods for incorporating BMP2 onto a biomaterial surface. When designing a binding method to use in the clinic, however, it is important to consider the conditions in an operating room (OR).

PCL can be modified to integrate BMP2 [24,34]; however, further studies are needed to refine a method to functionalize PCL scaffolds with BMP2 in a clinically realistic time frame to produce bone when placed in an ectopic site (i.e. pre-fabricated flap applications). It is likely that any clinically relevant BMP2 delivery method for the

near future must be performed in the OR environment at room temperature with loading times of 1 hour or less, or it will face regulatory hurdles such as unknown sterilization effects on GF bioactivity.

3.4 BMP2 & VEGF Dual Delivery

Transplanting bone stock alone is insufficient to maintain construct viability, and it is crucial to develop a rich vasculature. VEGF is a potent angiogenic factor that has the potential to stimulate blood vessel growth into the scaffold. Co-culture studies found that osteoblast-like cells stimulated endothelial cell proliferation by producing VEGF, and endothelial cells stimulated osteoprogenitor cell differentiation by producing BMP2 [35,36]. These results suggest that there is a coupling between osteogenesis and angiogenesis. The methods utilized to deliver these growth factors vary and could impact the regenerated bone quality.

3.4.1 *VEGF Delivery Vehicles & Binding Methods*

Some of the scaffold materials used to deliver VEGF include PCL, PEG diacrylate, collagen, and alginate. Solvent casting, particulate leaching, photopolymerizaion, and crosslinking are manufacturing methods associated with these materials [37-41]. VEGF can be crosslinked to a surface using heparin or Arg-Gly-Asp acid (RGD), mixed into a hydrogel, or incorporated into microparticles. The nano or microparticles can be made of hyaluronic acid/chitosan, PLGA, or collagen. Furthermore, these particles can be used alone or in combination with scaffolds that embed the particles [42-48]. To prepare the scaffold, a double emulsion or solvent evaporation method is employed, which can result in a highly variable VEGF release lasting from 1 day to 4 weeks. These growth factor integration and delivery methods are complex and

cannot be easily translated to the OR environment as mentioned in Section 3.2.1. It is important to note that because of VEGF's short half-life at 37^{o}C (approximately 90 minutes) [49], it is often difficult to create a reliable release profile that represents *in vivo* release. If the protein rapidly degrades, an *in vitro* assay would not accurately detect proteins released into the solution.

Sojo et al. found that angiogenesis occurs before the onset of osteogenesis and there is an interaction between the two stages [50]. Dual delivery of osteogenic and angiogenic proteins can further enhance the regenerative capacity of bone [51-53]. For example, when BMP2, VEGF, and bone marrow stromal cells (BMSCs) were delivered from a scaffold implanted in a critically sized mouse defect model, there was a significant increase in bone regeneration [53]. On one hand, simultaneous release studies have resulted in enhanced bone formation [51,54,55]. On the other hand, to mimic natural bone healing, sequential VEGF and BMP2 release systems are under investigation [56,57]. Polyelectrolyte multilayer films have been used to deliver both factors and resulted in 27% initial BMP2 release and 15% per day VEGF release for 5 days [58]. In another study, BMP2 was delivered from PLGA microspheres that were embedded in a polypropylene scaffold surrounded by a gelatin hydrogel that contained VEGF. There was a VEGF burst release in the first three days as the material degraded and sustained BMP2 delivery for 56 days [57]. Other studies use various dual delivery systems including: alginate/poly(D,L-lactic)(PDLLA) [54], biphasic CaP/PLGA microparticles/gelatin hydrogel [56], collagen sponge [55], gelatin microparticles/propylene fumarate (PPF) pores [59], and gelfoam disc [51]. In the study included in this dissertation, a collagen sponge was used to deliver VEGF with a

relatively rapid burst release since previous studies found that sponges release most of the growth factors or antibiotics within the first few days [60-64].

There are various systems used to attach VEGF to biomaterial surfaces: incorporation, encapsulation, conjugation, and adsorption. Incorporation involves mixing the GF into a coating or into a hydrogel. For example, VEGF in solution can be mixed into an alginate/fibrinogen based hydrogel or into a collagen gel and polymerized at 37^{o}C [47,65]. In these studies, the VEGF was bound to the delivery vehicle via physical entrapment or weak chemical interaction and was released as the material degraded.

Encapsulation incorporates the VEGF inside of synthetic or collagen microparticles. Nanoparticles, which are smaller than microparticles, could penetrate through capillaries and into the cell; this can have dangerous side effects. PLGA is commonly used to make microparticles, but the hydrophobic interactions between VEGF and PLGA can result in protein aggregation and denaturing. To decrease aggregation, PEG can be added to protect the protein and prevent hydrophobic interactions [2,66].

Conjugation uses a linking molecule to bind VEGF to the surface. Heparin is a widely studied protein used to bind VEGF to polymer surfaces [37,67]. Amino groups (-NH_2) on the material interact with heparin, and VEGF binds to the heparin because of the protein's high affinity for heparin. Heparin is localized to the carboxyl-terminal 55 residues [68]. Other studies utilize EDC chemistry [69], photoimmobilization [70], and cysteine conjugation [71] to link VEGF to the material surface. VEGF adsorbed onto polymer surfaces uses electrostatic interactions. The polymer is usually submerged in a GF solution for a period of time during which the protein binds to the surface. For PCL, the positively charged amino acid residues on VEGF interact with PCL's hydrophobic

surface. Another form of adsorption includes saturating a sponge with a VEGF solution [72,73].

3.4.2 *Pre-Clinical Studies*

The synergistic effect of BMP2 and VEGF are both time and location dependent (ectopic vs. orthotopic) [56,57,59], ratio dependent [74], and a high VEGF dose could inhibit osteogenesis [58,74]. Optimizing angiogenic and osteogenic protein delivery may increase bone regeneration. One study delivered both factors via gelatin microparticles in PPF pores implanted in a rat calvarial defect model and found no increase in bone formation [59]. Another study showed increased ectopic bone growth in rats with dual delivery, however, there was no increase in the orthotopic location [57]. Contrary to those results, another study implanted a dual delivery scaffold in a critical sized femur defect and found dual delivery regenerated significantly more bone. The studies which used microparticles in PPF pores and PLGA microparticles in a gelatin hydrogel for delivery systems found no difference in dual delivery versus BMP2 delivery alone [56,59,74]. Furthermore, they found that the timing of BMP2 release determined the speed and amount of ectopic bone formation in an intramuscular beagle model. The bone growth was independent of the VEGF release [56]. Studies delivering both BMP2 and VEGF use various animal models, implant locations, growth factor delivery methods (i.e. microparticle, gelatin), time points, and regenerated bone analyses methods making it difficult to draw a strong conclusion for pre-fabricated flap applications.

3.5 BMP2 & EPO Dual Growth Factor Delivery

In vitro, EPO directly influences mesenchymal stem cells to differentiate into osteoblasts and also influences hematopoietic stem cells (HSCs) to produce BMPs, which

indicates that EPO has the potential to influence bone regeneration [75,76]. Dual delivery of EPO and BMP2 has not been widely investigated. EPO has been delivered from gels, microspheres, and nanoparticles, however, for application other than bone regeneration.

3.5.1 *Delivery Vehicles and Binding Methods*

EPO is typically delivered systemically; however, drawbacks include serious side effects such as increased blood viscosity, hypertension, and thromboembolic events [77-79]. EPO has a relatively short half-life of 8.5 hours, which requires the patients to be dosed repeatedly to have an effect [80]. To overcome these drawbacks, local EPO delivery is a viable alternative to systemic injection. Kobayashi et al. delivered EPO using a gelatin hydrogel at the surface of a rabbit heart [81], and Chen et al. delivered EPO using a fibrin gel to increase neovascularization [82]. EPO has been delivered using injectable hydrogels [83,84] for angiogenesis purposes and via synthetic materials such as dextran microparticle-based PLGA/PLA microspheres. In the microsphere study, there was a 20% burst release on the first day followed by a sustained release, resulting in about 90% released in 60 days [85]. Similarly, Frayed et al. incorporated EPO into PLGA nanoparticles resulting in a 33% loading efficiency and 82% release over 24 hours [86]. When delivered from chitosan nanoparticles, 30% was released in the first 48 hours, and a total of 63% was released over 15 days in phosphate buffered saline at 37^{o}C [80]. With respect to dual BMP2 and EPO delivery, Nair et al. delivered both proteins from porogen-leached protein microbubble PLGA scaffolds that were implanted in a rat calvarial defect model. No binding efficiencies or release kinetics were characterized [87].

There is very limited information available on adsorption or conjugation EPO delivery methods. EPO adsorbed onto dialysis bags resulted in less than 7% bound [88], and EPO conjugated with PEG successfully lasted longer in solution. In the conjugation study, the maleimide on the PEG bound to the cysteine on the protein [89]. Another study successfully created benzaldehyde-terminated MPC polymers conjugated with EPO to extend the protein's half-life [90]. We were unable to find any studies which immobilized EPO onto a synthetic polymer surface for local *in vivo* delivery.

3.5.2 *Pre-Clinical Studies*

Interactions between EPO and BMP2 have been studied *in vitro* [75,76] and *in vivo* [87,91], and the results find synergistic effects on bone formation. The advantage of delivering both BMP2 and EPO is that both proteins are FDA approved and regulatory hurdles would potentially decrease. Delivering two proteins, however, could conversely make regulatory approval more difficult. In one study, BMP2 was delivered from a collagen scaffold implanted in a rat calvarial defect, and EPO was injected subcutaneously at the defect site every other day for 2 weeks. After 6 weeks the dual delivery group had a higher bone volume fraction than the BMP2 alone group [91]. In another study, microbubble PLGA scaffolds delivering BMP2 and EPO were implanted in a calvarial defect and resulted in complete bridging. Furthermore, the authors found that EPO loaded scaffolds implanted subcutaneously in mice recruited autologous mesenchymal stem cells to the implant site. The effect of local dual EPO and BMP2 delivery on bone regenerated in an ectopic location is still unknown.

3.6 Conclusion

Developing a bioengineered vascularized bone flap *in vivo* is a promising alternative to using autografts to reconstruct large bone defects. The fabrication method, mechanical properties, geometry resolution, and protein incorporation methods are a few factors that should be considered when designing a scaffold for bone tissue engineering applications. Scaffold fabrication methods utilizing organic salts or toxic solvents will face challenges when overcoming regulatory hurdles because of the potential health hazards. 3D-printed scaffolds have better control over geometry, porosity, and degradation rate. BMP2, VEGF, and EPO have been delivered alone and in combination using various scaffolding materials. It is important to keep in mind the clinical applicability when integrating the protein because complex machinery and a long preparation time will make the process difficult to execute in the OR environment. If the scaffold is prepared outside of the OR room, there are unknown sterilization effects on protein bioactivity and shelf life time which increase the number of regulatory hurdles.

3.7 References

[1] Bagheri S, Bell B, Khan HA. Current Therapy In Oral and Maxillofacial Surgery. : Elsevier Health Sciences; 2011.

[2] Simon-Yarza T, Formiga FR, Tamayo E, Pelacho B, Prosper F, Blanco-Prieto MJ. Vascular endothelial growth factor-delivery systems for cardiac repair: an overview. Theranostics 2012;2(6):541-552.

[3] Sollohub K, Cal K. Spray drying technique: II. Current applications in pharmaceutical technology. J Pharm Sci 2010 Feb;99(2):587-597.

[4] Makadia HK, Siegel SJ. Poly Lactic-co-Glycolic Acid (PLGA) as Biodegradable Controlled Drug Delivery Carrier. Polymers (Basel) 2011 Sep 1;3(3):1377-1397.

[5] Subia B, Kundu J, Kundu S. Biomaterial Scaffold Fabrication Techniques for Potential Tissue Engineering Applications. ; 2010.

[6] Partee B, Hollister SJ, Das S. Selective Laser Sintering Process Optimization for Layered Manufacturing of CAPA® 6501 Polycaprolactone Bone Tissue Engineering Scaffolds. Journal of Manufacturing Science and Engineering 2005 September 14;128(2):531-540.

[7] Smith MH, Flanagan CL, Kemppainen JM, Sack JA, Chung H, Das SS, et al. Computed tomography-based tissue-engineered scaffolds in craniomaxillofacial surgery. Int. J. Med. Robot 2007;3:207.

[8] Schantz JT, Lim TC, Ning C, Teoh SH, Tan KC, Wang SC, et al. Cranioplasty after trephination using a novel biodegradable burr hole cover: technical case report. Neurosurgery 2006;58.

[9] Hutmacher DW, Schantz T, Zein I, Ng KW, Teoh SH, Tan KC. Mechanical properties and cell cultural response of polycaprolactone scaffolds designed and fabricated via fused deposition modeling. Journal of Biomedical Materials Research 2001;55:203.

[10] Williams JM, Adewunmi A, Schek RM, Flanagan CL, Krebsbach PH, Feinberg SE, et al. Bone tissue engineering using polycaprolactone scaffolds fabricated via selective laser sintering. Biomaterials 2005 Aug;26(23):4817-4827.

[11] Protosys Technologies PVT.LTD: Services/Rapid Prototyping. Available at: http://www.protosystech.com/rapid-prototyping.htm.

[12] Bose S, Vahabzadeh S, Bandyopadhyay A. Bone tissue engineering using 3D printing. MaterialToday 2013;16(12):496.

[13] Wong DY, Hollister SJ, Krebsbach PH, Nosrat C. Poly(epsilon-caprolactone) and poly (L-lactic-co-glycolic acid) degradable polymer sponges attenuate astrocyte response and lesion growth in acute traumatic brain injury. Tissue Eng 2007 Oct;13(10):2515-2523.

[14] Woodruff MA, Hutmacher DW. The return of a forgotten polymer—Polycaprolactone in the 21st century. Progress in Polymer Science 2010.

[15] Fitzsimmons J. 510(k) Premarket Notification, Cover, Burr Hole, TRS CRANIAL BONE VOID FILLER. 2014; Available at: http://www.accessdata.fda.gov/scripts/cdrh/cfdocs/cfpmn/pmn.cfm?ID=K123633, 2014.

[16] Yeo A. 510(k) Premarket Notification, Methyl Methacrylate For Cranioplasty, OSTEOPORE PCL SCAFFOLD. 2014; Available at: http://www.accessdata.fda.gov/scripts/cdrh/cfdocs/cfpmn/pmn.cfm?ID=K051093, 2014.

[17] Bae JH, Song HR, Kim HJ, Lim HC, Park JH, Liu Y, et al. Discontinuous release of bone morphogenetic protein-2 loaded within interconnected pores of honeycomb-like polycaprolactone scaffold promotes bone healing in a large bone defect of rabbit ulna. Tissue Eng Part A 2011 Oct;17(19-20):2389-2397.

[18] Cahill KS, Chi JH, Day A, Claus EB. Prevalence, complications, and hospital charges associated with use of bone-morphogenetic proteins in spinal fusion procedures. JAMA 2009 Jul 1;302(1):58-66.

[19] Autefage H, Briand-Mesange F, Cazalbou S, Drouet C, Fourmy D, Goncalves S, et al. Adsorption and release of BMP-2 on nanocrystalline apatite-coated and uncoated hydroxyapatite/beta-tricalcium phosphate porous ceramics. J Biomed Mater Res B Appl Biomater 2009 Nov;91(2):706-715.

[20] Lee YM, Nam SH, Seol YJ, Kim TI, Lee SJ, Ku Y, et al. Enhanced bone augmentation by controlled release of recombinant human bone morphogenetic protein-2 from bioabsorbable membranes. J Periodontol 2003 Jun;74(6):865-872.

[21] Jeon O, Song SJ, Yang HS, Bhang SH, Kang SW, Sung MA, et al. Long-term delivery enhances in vivo osteogenic efficacy of bone morphogenetic protein-2 compared to short-term delivery. Biochem Biophys Res Commun 2008 May 2;369(2):774-780.

[22] Park YJ, Kim KH, Lee JY, Ku Y, Lee SJ, Min BM, et al. Immobilization of bone morphogenetic protein-2 on a nanofibrous chitosan membrane for enhanced guided bone regeneration. Biotechnol Appl Biochem 2006 Jan;43(Pt 1):17-24.

[23] Zhao Y, Zhang J, Wang X, Chen B, Xiao Z, Shi C, et al. The osteogenic effect of bone morphogenetic protein-2 on the collagen scaffold conjugated with antibodies. J Control Release 2010 Jan 4;141(1):30-37.

[24] Zhang H, Migneco F, Lin CY, Hollister SJ. Chemically-conjugated bone morphogenetic protein-2 on three-dimensional polycaprolactone scaffolds stimulates osteogenic activity in bone marrow stromal cells. Tissue Eng Part A 2010 Nov;16(11):3441-3448.

[25] Kim TH, Oh SH, Na SY, Chun SY, Lee JH. Effect of biological/physical stimulation on guided bone regeneration through asymmetrically porous membrane. J Biomed Mater Res A 2012 Jun;100(6):1512-1520.

[26] Jeon O, Song SJ, Kang SW, Putnam AJ, Kim BS. Enhancement of ectopic bone formation by bone morphogenetic protein-2 released from a heparin-conjugated poly(L-lactic-co-glycolic acid) scaffold. Biomaterials 2007 Jun;28(17):2763-2771.

[27] Gharibjanian NA, Chua WC, Dhar S, Scholz T, Shibuya TY, Evans GR, et al. Release kinetics of polymer-bound bone morphogenetic protein-2 and its effects on

the osteogenic expression of MC3T3-E1 osteoprecursor cells. Plast Reconstr Surg 2009 Apr;123(4):1169-1177.

[28] Liu HW, Chen CH, Tsai CL, Hsiue GH. Targeted delivery system for juxtacrine signaling growth factor based on rhBMP-2-mediated carrier-protein conjugation. Bone 2006 Oct;39(4):825-836.

[29] Zhao B, Katagiri T, Toyoda H, Takada T, Yanai T, Fukuda T, et al. Heparin potentiates the in vivo ectopic bone formation induced by bone morphogenetic protein-2. J Biol Chem 2006 Aug 11;281(32):23246-23253.

[30] Ruppert R, Hoffmann E, Sebald W. Human bone morphogenetic protein 2 contains a heparin-binding site which modifies its biological activity. Eur J Biochem 1996 Apr 1;237(1):295-302.

[31] Rider CC. Heparin/heparan sulphate binding in the TGF-beta cytokine superfamily. Biochem Soc Trans 2006 Jun;34(Pt 3):458-460.

[32] Kumagai T, Anada T, Honda Y, Takami M, Kamijyo R, Shimauchi H, et al. Osteoblastic Cell Differentiation on BMP-2 Pre-Adsorbed Octacalcium Phosphate and Hydroxyapatite. Key Engineering Materials 2007;361-363:1025.

[33] Apatite-Polymer Composite Particles for Controlled Delivery of BMP-2: *In Vitro* Release and Cellular Response. Proceedings of the Singapore-MIT Alliance Symposium; 2005.

[34] Mitsak AG, Kemppainen JM, Harris MT, Hollister SJ. Effect of polycaprolactone scaffold permeability on bone regeneration in vivo. Tissue Eng Part A 2011 Jul;17(13-14):1831-1839.

[35] Kaigler D, Krebsbach PH, West ER, Horger K, Huang YC, Mooney DJ. Endothelial cell modulation of bone marrow stromal cell osteogenic potential. FASEB J 2005 Apr;19(6):665-667.

[36] Wang DS, Miura M, Demura H, Sato K. Anabolic effects of 1,25-dihydroxyvitamin D3 on osteoblasts are enhanced by vascular endothelial growth factor produced by osteoblasts and by growth factors produced by endothelial cells. Endocrinology 1997 Jul;138(7):2953-2962.

[37] Singh S, Wu BM, Dunn JC. The enhancement of VEGF-mediated angiogenesis by polycaprolactone scaffolds with surface cross-linked heparin. Biomaterials 2011 Mar;32(8):2059-2069.

[38] Porter AM, Klinge CM, Gobin AS. Biomimetic hydrogels with VEGF induce angiogenic processes in both hUVEC and hMEC. Biomacromolecules 2011 Jan 10;12(1):242-246.

[39] Miyagi Y, Chiu LL, Cimini M, Weisel RD, Radisic M, Li RK. Biodegradable collagen patch with covalently immobilized VEGF for myocardial repair. Biomaterials 2011 Feb;32(5):1280-1290.

[40] Silva EA, Mooney DJ. Effects of VEGF temporal and spatial presentation on angiogenesis. Biomaterials 2010 Feb;31(6):1235-1241.

[41] Chiu LL, Radisic M. Scaffolds with covalently immobilized VEGF and Angiopoietin-1 for vascularization of engineered tissues. Biomaterials 2010 Jan;31(2):226-241.

[42] Chung YI, Kim SK, Lee YK, Park SJ, Cho KO, Yuk SH, et al. Efficient revascularization by VEGF administration via heparin-functionalized nanoparticle-fibrin complex. J Control Release 2010 May 10;143(3):282-289.

[43] Golub JS, Kim YT, Duvall CL, Bellamkonda RV, Gupta D, Lin AS, et al. Sustained VEGF delivery via PLGA nanoparticles promotes vascular growth. Am J Physiol Heart Circ Physiol 2010 Jun;298(6):H1959-65.

[44] Karal-Yilmaz O, Serhatli M, Baysal K, Baysal BM. Preparation and in vitro characterization of vascular endothelial growth factor (VEGF)-loaded poly(D,L-lactic-co-glycolic acid) microspheres using a double emulsion/solvent evaporation technique. J Microencapsul 2011;28(1):46-54.

[45] Formiga FR, Pelacho B, Garbayo E, Abizanda G, Gavira JJ, Simon-Yarza T, et al. Sustained release of VEGF through PLGA microparticles improves vasculogenesis and tissue remodeling in an acute myocardial ischemia-reperfusion model. J Control Release 2010 Oct 1;147(1):30-37.

[46] Nagai N, Kumasaka N, Kawashima T, Kaji H, Nishizawa M, Abe T. Preparation and characterization of collagen microspheres for sustained release of VEGF. J Mater Sci Mater Med 2010 Jun;21(6):1891-1898.

[47] des Rieux A, Ucakar B, Mupendwa BP, Colau D, Feron O, Carmeliet P, et al. 3D systems delivering VEGF to promote angiogenesis for tissue engineering. J Control Release 2011 Mar 30;150(3):272-278.

[48] Jay SM, Shepherd BR, Andrejecsk JW, Kyriakides TR, Pober JS, Saltzman WM. Dual delivery of VEGF and MCP-1 to support endothelial cell transplantation for therapeutic vascularization. Biomaterials 2010 Apr;31(11):3054-3062.

[49] Kleinheinz J, Jung S, Wermker K, Fischer C, Joos U. Release kinetics of VEGF165 from a collagen matrix and structural matrix changes in a circulation model. Head Face Med 2010 Jul 19;6:17-160X-6-17.

[50] Sojo K, Sawaki Y, Hattori H, Mizutani H, Ueda M. Immunohistochemical study of vascular endothelial growth factor (VEGF) and bone morphogenetic protein-2, -4 (BMP-2, -4) on lengthened rat femurs. J Craniomaxillofac Surg 2005 Aug;33(4):238-245.

[51] Peng H, Usas A, Olshanski A, Ho AM, Gearhart B, Cooper GM, et al. VEGF improves, whereas sFlt1 inhibits, BMP2-induced bone formation and bone healing through modulation of angiogenesis. J Bone Miner Res 2005 Nov;20(11):2017-2027.

[52] Geiger F, Bertram H, Berger I, Lorenz H, Wall O, Eckhardt C, et al. Vascular endothelial growth factor gene-activated matrix (VEGF165-GAM) enhances osteogenesis and angiogenesis in large segmental bone defects. J Bone Miner Res 2005 Nov;20(11):2028-2035.

[53] Kanczler JM, Oreffo RO. Osteogenesis and angiogenesis: the potential for engineering bone. Eur Cell Mater 2008 May 2;15:100-114.

[54] Kanczler JM, Ginty PJ, White L, Clarke NM, Howdle SM, Shakesheff KM, et al. The effect of the delivery of vascular endothelial growth factor and bone morphogenic protein-2 to osteoprogenitor cell populations on bone formation. Biomaterials 2010 Feb;31(6):1242-1250.

[55] Kakudo N, Kusumoto K, Wang YB, Iguchi Y, Ogawa Y. Immunolocalization of vascular endothelial growth factor on intramuscular ectopic osteoinduction by bone morphogenetic protein-2. Life Sci 2006 Oct 4;79(19):1847-1855.

[56] Geuze RE, Theyse LF, Kempen DH, Hazewinkel HA, Kraak HY, Oner FC, et al. A differential effect of bone morphogenetic protein-2 and vascular endothelial growth factor release timing on osteogenesis at ectopic and orthotopic sites in a large-animal model. Tissue Eng Part A 2012 Oct;18(19-20):2052-2062.

[57] Kempen DH, Lu L, Heijink A, Hefferan TE, Creemers LB, Maran A, et al. Effect of local sequential VEGF and BMP-2 delivery on ectopic and orthotopic bone regeneration. Biomaterials 2009 May;30(14):2816-2825.

[58] Shah NJ, Macdonald ML, Beben YM, Padera RF, Samuel RE, Hammond PT. Tunable dual growth factor delivery from polyelectrolyte multilayer films. Biomaterials 2011 Sep;32(26):6183-6193.

[59] Patel ZS, Young S, Tabata Y, Jansen JA, Wong ME, Mikos AG. Dual delivery of an angiogenic and an osteogenic growth factor for bone regeneration in a critical size defect model. Bone 2008 Nov;43(5):931-940.

[60] Wang AY, Leong S, Liang YC, Huang RC, Chen CS, Yu SM. Immobilization of growth factors on collagen scaffolds mediated by polyanionic collagen mimetic

peptides and its effect on endothelial cell morphogenesis. Biomacromolecules 2008 Oct;9(10):2929-2936.

[61] Uludag H, Gao T, Porter TJ, Friess W, Wozney JM. Delivery systems for BMPs: factors contributing to protein retention at an application site. J Bone Joint Surg Am 2001;83-A Suppl 1(Pt 2):S128-35.

[62] Seeherman H, Wozney JM. Delivery of bone morphogenetic proteins for orthopedic tissue regeneration. Cytokine Growth Factor Rev 2005 Jun;16(3):329-345.

[63] Mullen LM, Best SM, Brooks RA, Ghose S, Gwynne JH, Wardale J, et al. Binding and release characteristics of insulin-like growth factor-1 from a collagen-glycosaminoglycan scaffold. Tissue Eng Part C Methods 2010 Dec;16(6):1439-1448.

[64] Sorensen TS, Sorensen AI, Merser S. Rapid release of gentamicin from collagen sponge. In vitro comparison with plastic beads. Acta Orthop Scand 1990 Aug;61(4):353-356.

[65] Chen TT, Luque A, Lee S, Anderson SM, Segura T, Iruela-Arispe ML. Anchorage of VEGF to the extracellular matrix conveys differential signaling responses to endothelial cells. J Cell Biol 2010 Feb 22;188(4):595-609.

[66] Kratz F. Albumin as a drug carrier: design of prodrugs, drug conjugates and nanoparticles. J Control Release 2008 Dec 18;132(3):171-183.

[67] Masters KS. Covalent growth factor immobilization strategies for tissue repair and regeneration. Macromol Biosci 2011 Sep 9;11(9):1149-1163.

[68] Fairbrother WJ, Champe MA, Christinger HW, Keyt BA, Starovasnik MA. Solution structure of the heparin-binding domain of vascular endothelial growth factor. Structure 1998 May 15;6(5):637-648.

[69] Taguchi T, Kishida A, Akashi M, Maruyama I. Immobilization of Human Vascular Endothelial Growth Factor (VEGF165) onto Biomaterials: An Evaluation of the Biological Activity of Immobilized VEGF165. Journal of Bioactive and Compatible Polymers: Biomedical Applications 2000;15(4):309.

[70] Ito Y, Hasuda H, Terai H, Kitajima T. Culture of human umbilical vein endothelial cells on immobilized vascular endothelial growth factor. J Biomed Mater Res A 2005 Sep 15;74(4):659-665.

[71] Backer MV, Patel V, Jehning BT, Claffey KP, Backer JM. Surface immobilization of active vascular endothelial growth factor via a cysteine-containing tag. Biomaterials 2006 Nov;27(31):5452-5458.

[72] Schroeder JW,Jr, Rastatter JC, Walner DL. Effect of vascular endothelial growth factor on laryngeal wound healing in rabbits. Otolaryngol Head Neck Surg 2007 Sep;137(3):465-470.

[73] Sinnathamby T, Yun TJ, Clavet-Lanthier ME, Cheong C, Sirois MG. VEGF and angiopoietins promote inflammatory cell recruitment and mature blood vessel formation in murine sponge/Matrigel model. J Cell Biochem 2014 Aug 21.

[74] Young S, Patel ZS, Kretlow JD, Murphy MB, Mountziaris PM, Baggett LS, et al. Dose effect of dual delivery of vascular endothelial growth factor and bone morphogenetic protein-2 on bone regeneration in a rat critical-size defect model. Tissue Eng Part A 2009 Sep;15(9):2347-2362.

[75] Shiozawa Y, Jung Y, Ziegler AM, Pedersen EA, Wang J, Wang Z, et al. Erythropoietin couples hematopoiesis with bone formation. PLoS One 2010 May 27;5(5):e10853.

[76] Kim J, Jung Y, Sun H, Joseph J, Mishra A, Shiozawa Y, et al. Erythropoietin mediated bone formation is regulated by mTOR signaling. J Cell Biochem 2012 Jan;113(1):220-228.

[77] Saray A, Ozakpinar R, Koc C, Serel S, Sen Z, Can Z. Effect of chronic and short-term erythropoietin treatment on random flap survival in rats: an experimental study. Laryngoscope 2003 Jan;113(1):85-89.

[78] Maiese K, Chong ZZ, Shang YC. Raves and risks for erythropoietin. Cytokine Growth Factor Rev 2008 Apr;19(2):145-155.

[79] Bakhshi H, Rasouli MR, Parvizi J. Can local Erythropoietin administration enhance bone regeneration in osteonecrosis of femoral head? Med Hypotheses 2012 Aug;79(2):154-156.

[80] Bokharaei M, Margaritis A, Xenocostas A, Freeman DJ. Erythropoietin encapsulation in chitosan nanoparticles and kinetics of drug release. Curr Drug Deliv 2011 Mar;8(2):164-171.

[81] Kobayashi H, Minatoguchi S, Yasuda S, Bao N, Kawamura I, Iwasa M, et al. Post-infarct treatment with an erythropoietin-gelatin hydrogel drug delivery system for cardiac repair. Cardiovasc Res 2008 Sep 1;79(4):611-620.

[82] Chen F, Liu Q, Zhang ZD, Zhu XH. Co-delivery of G-CSF and EPO released from fibrin gel for therapeutic neovascularization in rat hindlimb ischemia model. Microcirculation 2013 Jul;20(5):416-424.

[83] Wang T, Jiang XJ, Lin T, Ren S, Li XY, Zhang XZ, et al. The inhibition of postinfarct ventricle remodeling without polycythaemia following local sustained

intramyocardial delivery of erythropoietin within a supramolecular hydrogel. Biomaterials 2009 Sep;30(25):4161-4167.

[84] Kang CE, Poon PC, Tator CH, Shoichet MS. A new paradigm for local and sustained release of therapeutic molecules to the injured spinal cord for neuroprotection and tissue repair. Tissue Eng Part A 2009 Mar;15(3):595-604.

[85] Rong X, Yang S, Miao H, Guo T, Wang Z, Shi W, et al. Effects of erythropoietin-dextran microparticle-based PLGA/PLA microspheres on RGCs. Invest Ophthalmol Vis Sci 2012 Sep 7;53(10):6025-6034.

[86] Fayed BE, Tawfik AF, Yassin AE. Novel erythropoietin-loaded nanoparticles with prolonged in vivo response. J Microencapsul 2012;29(7):650-656.

[87] Nair AM, Tsai YT, Shah KM, Shen J, Weng H, Zhou J, et al. The effect of erythropoietin on autologous stem cell-mediated bone regeneration. Biomaterials 2013 Oct;34(30):7364-7371.

[88] Schroder CH, Swinkels LM, Reddingius RE, Sweep FG, Willems HL, Monnens LA. Adsorption of erythropoietin and growth hormone to peritoneal dialysis bags and tubing. Perit Dial Int 2001 Jan-Feb;21(1):90-92.

[89] Long DL, Doherty DH, Eisenberg SP, Smith DJ, Rosendahl MS, Christensen KR, et al. Design of homogeneous, monopegylated erythropoietin analogs with preserved in vitro bioactivity. Exp Hematol 2006 Jun;34(6):697-704.

[90] Samanta D, McRae S, Cooper B, Hu Y, Emrick T, Pratt J, et al. End-functionalized phosphorylcholine methacrylates and their use in protein conjugation. Biomacromolecules 2008 Oct;9(10):2891-2897.

[91] Sun H, Jung Y, Shiozawa Y, Taichman RS, Krebsbach PH. Erythropoietin modulates the structure of bone morphogenetic protein 2-engineered cranial bone. Tissue Eng Part A 2012 Oct;18(19-20):2095-2105.

CHAPTER 4

BONE MORPHOGENETIC PROTEIN-2 ADSORPTION ONTO POLYCAPROLACTONE BETTER PRESERVES BIOACTIVITY *IN VITRO* AND PRODUCES MORE BONE *IN VIVO* THAN CONJUGATION UNDER CLINICALLY RELAVENT LOADING SCENARIOS

Colleen Flanagan and Scott Hollister assisted with the preparation of this chapter.

Accepted by Tissue Engineering Part C; Oct, 2014

4.1 Abstract

Background: One strategy to reconstruct large bone defects is to pre-fabricate a vascularized flap by implanting a biomaterial scaffold with associated biologics into the latissimus dorsi and then transplanting this construct to the defect site after a maturation period. This strategy, like all clinically and regulatory feasible biologic approaches to surgical reconstruction, requires the ability to quickly (<1 hour within an operating room) and efficiently bind biologics to scaffolds. It also requires the ability to localize biologic delivery. In this study we investigated the efficacy of binding bone morphogenetic protein-2 (BMP2) to poly-Ɛ-caprolactone (PCL) using adsorption and conjugation as a function of time.

Methods: BMP2 was adsorbed (Ads) or conjugated (Conj) to PCL scaffolds with the same 3D printed architecture while altering exposure time (0.5, 1, 5, 16hr), temperature (4^oC, 23^oC), and BMP2 concentration (1.4, 5, 20, 65µg/ml). The i*n vitro* release was

quantified and C2C12 cell alkaline phosphatase (ALP) expression was used to confirm bioactivity. Scaffolds with either 65 or 20 µg/ml Ads or Conj BMP2 for 1hr at 23^{o}C were implanted subcutaneously in mice to evaluate *in vivo* bone regeneration. MicroCT, compression testing, and histology were performed to characterize bone regeneration.

Results: After 1hr exposure to 65µg/ml BMP2 at 23^{o}C, Conj and Ads resulted in 12.83±1.78µg and 10.78±1.49µg BMP2 attached, respectively. Adsorption resulted in a positive ALP response and had a small burst release; whereas, conjugation provided a sustained release with negligible ALP production, indicating that the conjugated BMP2 may not be bioavailable. Adsorbed 65µg/ml BMP2 solution resulted in the greatest regenerated bone volume (15.0±3.0mm^{3}), elastic modulus (20.1±3.0MPa), and %bone ingrowth in the scaffold interior (17.2±5.4%) when compared to conjugation.

Conclusion: Adsorption may be optimal for the clinical application of pre-fabricating bone flaps due to BMP2 binding in a short exposure time, retained BMP2 bioactivity, bone growth adhering to scaffold geometry and into pores with healthy marrow development.

4.2 Introduction

The gold standard for reconstructing a bone defect is a vascularized autologous flap. However, this procedure results in donor site morbidity and poorly matched defect geometry, especially for craniofacial reconstruction. Alternatives to autografts include allografts and synthetic grafts. Allografts carry the risk of transferring diseases and eliciting an immune response. Synthetic grafts made from polymers or metal cages are alternatives being investigated to address the drawbacks of allografts and autografts. Particularly, polymers can be fabricated to match the patient's complex facial geometry and be integrated with biologics to induce bone growth when implanted into the defect-site. Although these grafts could be readily available and produced, they do not integrate as well as autografts into the host bone [1]. Chronically infected and irradiated wound sites are challenging to reconstruct and are not conducive to general wound healing, let alone being able to support a bone graft. Furthermore, blood vessels generally cannot penetrate the graft sufficiently to provide nutrients to the bone growing at the graft's core, especially in large volume defects. To increase viability and integration of grafts implanted directly into the defect site, researchers are investigating pre-fabrication of a synthetic flap that is assembled at a site remote from the defect [2-5]. As an alternative to creating the flap *in vitro* (in which patient cells are harvested, expanded, and seeded on the construct to mature in an external bioreactor), we are looking to tissue engineer a bone flap *in vivo* by using the patient's body as a bioreactor to achieve bone penetration into a biomaterial scaffold with associated biologics. There are few reports of this procedure in animal models [4,6-10] and even less in humans [2,3,11]. Previous studies have used BioOss/Hydroxyapatite blocks or titanium trays filled with BioOss blocks

soaked in growth factors [7,8]. A human mandibular case using a titanium mesh filled with hydroxyapatite blocks soaked in bone morphogenetic protein-7 (BMP7) fractured and failed [2].

Our goal is to advance this pre-fabricated flap procedure by integrating patient-specific computational design, 3D biomaterial printing, and post-fabrication biologic functionalization [12]. Poly-Ɛ-caprolactone (PCL) is a biocompatible and bioresorbable polymer that can be utilized with image-based computation aided design (CAD) and selective laser sintering (SLS) manufacturing techniques [13]. SLS can repeatedly and reproducibly produce PCL scaffolds with complex geometries, controlled pore size, and stiffness which degrade over three years. Its degradation profile and mechanical properties supports its use for bone tissue engineering in complex reconstruction sites where bone may take over a year to form. In these sites, a PCL scaffold's slower degradation time is an advantage to provide form and load bearing over a longer time period. Furthermore, PCL degradation generates less acidic byproducts and leads to less inflammation than more rapidly degrading polylactic acid based co-polymers [14]. PCL has been approved for cranioplasty bone filling applications by the FDA [15,16]. Thus, the polymer has been widely tested, utilized, and achieved regulatory approval as a bone repair scaffold. Furthermore, it may readily be formed into complex geometries by 3D printing techniques like SLS and Fused Deposition Modeling [13].

PCL can be modified to integrate the osteoinductive agent recombinant human bone morphogenetic protein-2 (BMP2) [17,18]. However, further studies are needed to refine a method of growth factor (GF) functionalization onto PCL scaffolds to produce bone when placed in the muscle bed (i.e. pre-fabricated flap applications) in a clinically

realistic time frame within the operating room (OR). Although a plethora of methods have been developed for conjugating and delivering BMP2 from scaffold materials, any conjugation technique requiring more than 1 hour performed outside the OR faces unknown sterilization effects on GF bioactivity and creates a significant uphill battle to be of any clinical relevance. It is likely that any clinically relevant BMP2 delivery method for the near future must be performed in the OR environment at room temperature with loading times of 1 hour or less. Current conjugation methods that more efficiently load BMP2 onto scaffolds than adsorption methods [19,20] do not fulfill these requirements. Additionally, studies that have assessed conjugation methods utilized either porogen leaching [18,19] or other methods resulting in large variations in pore architecture that may significantly affect release kinetics, not allowing a rigorous comparison of adsorption and conjugation methods [21-23]. Simpler adsorption methods have not been directly compared to conjugation methods [23-25]. Still, there is a lack of information on how conjugation methods compare directly to adsorption methods under OR relevant conditions on scaffolds with the exact same, rigorously controlled architecture in terms of not only *in vitro* loading efficiency and bioactivity, but also the direct translation into *in vivo* bone formation in terms of volume, localization and mechanical properties. The goal of this study was to investigate these questions both *in vitro* and in an *in vivo* ectopic model as a pre-cursor to large animal ectopic models for pre-fabricated flap construction.

4.3 Materials & Methods

PCL Fabrication

PCL discs (15mm Diameter, 2mm Height, 176mm^2 Surface Area) and 70% porous

scaffolds (6.35mm Diameter x 4mm Height, 170mm^2 Surface Area) with 2.15mm spherical pores (Figure 4.1) in a 2mm unit cell were fabricated using a Formiga P100 SLS machine (EOS, Inc., Novi, MI). The powder consisted of PCL (43-50kDa Polysciences, Warrington, PA) and 4 wt % hydroxyapatite (Plasma Biotal Limited, UK). Manufacturing conditions including bed temperature, laser power, particle size, PCL milling etc. followed protocols we previously developed and published for implantable PCL scaffolds [13,26-28]. After manufacturing, the discs and scaffolds were air blasted and then sonicated in 70% ethanol (EtOH) for 30 minutes to remove non-sintered powder, washed in distilled water (diH_20), and air-dried at room temperature.

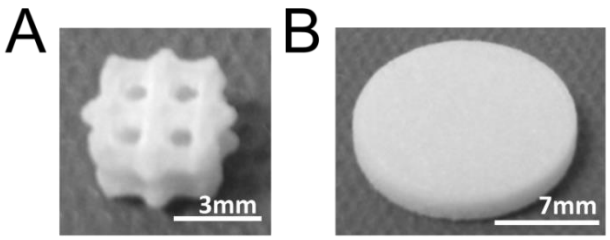

Figure 4.1: PCL Scaffold Geometries
A) PCL Scaffold C) PCL Disc

BMP2 Binding

For conjugation groups (Conj), PCL samples were exposed to 10% w/v 1,6-hexanediamine in isopropanol for 1 hour at 37^{o}C to add amine groups via aminolysis and then they were washed in diH_20. After air-drying overnight, 1M Ninhydrin reagent (Sigma), prepared with 100% EtOH, was used to confirm successful aminolysis in a representative specimen by the development of a purple stain. Note that this preparation can be done pre-sterilization and does not affect the capability to perform conjugation under OR relevant conditions. The samples were prewashed with activation buffer (BuPH Phosphate Buffered Saline Pack in diH_20, pH 7.2, Pierce Biotechnology). The

heterobifunctional cross-linker sulfosuccinimidyl 4-(N-maleimidomethyl) cyclohexane-1-carboxylate (sulfo-SMCC) (Pierce Biotechnology) was used to immobilize recombinant human BMP2 (e.coli derived, Creative Biomart, Shirley, NY) on the aminated surface. Samples were immersed in sulfo-SMCC (4mg/ml in activation buffer) for 1 hour at 23^{o}C, followed by activation and conjugation buffer washes. Conjugation buffer (pH 7.0) contained activation buffer and 0.1M EDTA. Adsorption groups (Ads) followed the same procedure as Conj but without the aminolysis and sulfo-SMCC reactions. E.coli derived BMP2 is non-glycosylated and has shown to produce more bone *in vivo* at a lower dose when compared to a glycosylated BMP2 [29]. BMP2 was dissolved in 20mM acetic acid (1mg/ml) and then further diluted in conjugation buffer to the desired concentration. Ads/Conj PCL discs (n=3/group) were immersed in 1ml of 1.43μg/ml BMP2 solution for 0.5, 1, 5, or 16 hours on a shaker at 4^{o}C or 23^{o}C. A simple disc geometry was used to understand initial binding trends prior to conducting concentration binding studies with a refined protocol on a more complex geometry. Ads/Conj PCL scaffolds (n=3/group) were immersed in 1ml of 1.4, 5, 20, or 65μg/ml BMP2 for the refined conditions of 1 hour exposure at 23^{o}C. Note, an ELISA was used to determine the detected BMP2 concentration (averaging 1.14, 3, 6.5, and 30μg/ml) with which to normalize binding values. Once BMP2 exposure was complete, samples were washed with di$H_2$0 and dried in a vacuum at 23^{o}C overnight. BMP2 solution supernatants and di$H_2$0 washes were collected in LoBind microcentrifuge tubes (Eppendorf) to analyze for BMP2 content. Bovine Serum Albumin 1% (BSA) was added to the collected solution to result in 0.1% BSA, and the samples were stored at -80^{o}C. BMP2 content was quantified using an indirect enzyme-linked immunoabsorbant assay (ELISA) kit (PeproTech) read at 405 and

650nm on a microplate reader (Multiskan Spectrum, Thermo Scientific, Pittsburg, PA). Results are reported as BMP2 bound (μg), BMP2 bound per mm^2 PCL surface area ($\mu g/mm^2$), or binding efficiency (%) and were calculated as shown below:

$$BMP2\ Bound\ (\mu g) = BMP2\ in\ original\ solution\ detected\ by\ ELISA - (BMP2\ in\ supernatant + washes)$$

$$Binding\ Efficiency\ (\%) = \left(\frac{original\ Amt - Amt\ remaining\ in\ sol'n}{original\ Amt}\right) * 100$$

Release Kinetics

Ads and Conj BMP2 release profiles were determined for PCL scaffolds exposed to 20μg/ml BMP2 for 1 hour at 23°C (n=3). After BMP2 exposure PCL samples were immersed in Dulbecco's Phosphate Buffered Saline (DPBS) and incubated in a sterile environment at 37°C, 5% CO_2, and 95% humidity. The supernatant was collected and replaced with fresh DPBS 1,3,5,7,14, and 21 days after initial exposure. Supernatant with added 0.1% BSA was stored at -80°C until BMP2 quantification by ELISA.

BMP2 Quantification

An e.coli derived BMP2 ELISA quantification kit (Peprotech) was used to indirectly quantify the amount of BMP2 bound to PCL and was conducted according to the manufacturer's instructions. High-binding 96-well plates (Costar) were coated with capture antibody overnight. Wells were blocked with 1% BSA in DPBS for 1 hour, thawed samples were added in triplicate wells for 2 hours, detection antibody for 2 hours, Avidin conjugated horseradish peroxidase for 0.5 hours, followed by the addition of ABTS liquid substrate solution (2,2'-azino-bis(3-ethylbenzthiazoline)-sulfonic acid) (Sigma) for colorimetric reading after 20 minutes. In between each step, wells were

washed four times with wash buffer (DPBS containing 0.05% Tween 20 (Sigma)). Absorbance was read at 405 and 650nm.

Cell Culture

C2C12 myoblastic cells are known to differentiate down an osteogenic lineage when exposed to active BMP2 and are extensively used in other studies as an initial screening for BMP2 bioactivity [30-33]. C2C12 cells (ATCC, Manassas, VA) were grown in high glucose Dulbecco's modified Eagle's medium (DMEM) containing 10% fetal bovine serum and 1% pennicillin/streptomycin and incubated in 37^{o}C, 5% CO_2 and 95% humidity (all reagents from Gibco, Carlsbad, CA). The Ads and Conj BMP2 discs were sterilized in 0.22µm filtered 70% EtOH for 30 min, washed with Hanks Balanced Salt Solution (HBSS), and maintained in DMEM under sterile conditions until cell seeding in a 24 well plate. Discs fit tightly into the well space. The DMEM was then replaced with culture medium and cells were added.

Alkaline Phosphatase Assay

C2C12 cells were seeded (1x10^{4}cells/disc or 57cells/mm^{2}) on discs with conjugated or adsorbed 0.7ml of 1.4µg/ml BMP2 for 1 hour at 23^{o}C. The simple disc geometry was used for cell studies because the aim of the study was to determine if the bound BMP2 maintained bioactivity and the extent of bioactivity was not compared. Positive controls were 1µg BMP2 in culture medium (sol BMP2) and 0.7ml of 1.4µg/ml BMP2 adsorbed for 16hr at 4^{o}C due to prior successful results in this laboratory for *in vivo* formation at that binding condition (n=4). The negative control was cells on PCL discs with no BMP2. After 4 days of static culture, cells were lysed with 700µl of CelLytic (Sigma) solution and (alkaline phosphatase) ALP production was quantified. The assay was conducted

using alkaline buffer solution, p-nitrophenol standard solution, and alkaline phosphatase substrate tablets (Sigma). Each sample (n=3/group) was read in triplicate wells at 405nm and results were normalized to total intracellular protein content (BCA, ThermoScientific) read at 562nm.

MTS Assay

An MTS assay was utilized to ensure cells attached and grew on the PCL to interact with the bound BMP2. Proliferation between groups was not compared. C2C12 cells were seeded ($2.5x10^4$ cells/disc) on discs with Conj or Ads 1.43µg/ml BMP2 for 1 hour at 23^oC and Ads at 4^oC (n=4). The positive control was cells seeded on PCL discs exposed to 1µg BMP2 in culture medium (sol BMP2). The negative control was cells on PCL discs with no BMP2. 260µl MTS solution (CellTiter96 Aqueous One Solution, Promega) was added to each disc after 72 hours of static culture. After incubating for two hours at 37^oC triplicates were read at 490nm.

In Vivo Bioactivity: Subcutaneous Implantation

Based on our *in vitro* studies, we chose the most clinically relevant conditions of 1 hour protein exposure at 23^oC and exposed scaffolds to 20 or 65µg/ml adsorbed or conjugated BMP2. After treatment, scaffolds were implanted subcutaneously in 5-7 week old NIHS bg-nu-xid mice (Harlan Laboratories, Indianapolis, IN). Negative controls for the adsorption group were PCL scaffolds soaked in conjugation buffer for 1 hour. Negative controls for the conjugation group were PCL scaffolds treated through the sulfo-SMCC reaction step without BMP2 exposure. Groups were sterilized with 70% EtOH and washed with HBSS prior to implanting. Four scaffolds were implanted in each mouse. An incision was made in the back and four pockets were created angling toward each limb.

Scaffolds were assigned a quadrant to be implanted in such that at least one sample from each group was implanted in all quadrants. Mice were then euthanized 8 weeks post-surgery to explant the specimen. Explanted specimen were placed in Z-Fix (Anatech, Battle Creek, MI) overnight, washed with diH_20 for 5 hours and stored in 70% EtOH until testing. Table 4.1 gives total sample numbers as well as the number of samples used for each specific assay (µCT scan, mechanical test, and histology). This study was conducted in compliance with the regulations set forth by the University Committee on Use and Care of Animals at the University of Michigan.

Group	µCT Scan	Mechanical Test	Histology	Total Samples
20µg/ml Conj	N=8	N=5	N=3	N=8
65µg/ml Conj	N=9	N=6	N=3	N=9
20µg/ml Ads	N=8	N=5	N=3	N=8
65µg/ml Ads	N=9	N=6	N=3	N=9
PCL-no BMP2	N=5	N=3	N=2	N=5
Sulfo-SMCC	N=9	N=6	N=3	N=9

Table 4.1: Sample Numbers for In Vivo Analyses
Number of explanted specimen used in each in vivo bone regeneration analysis method

Micro-Computed Tomography (MicroCT)

Fixed scaffolds were scanned in water with a high-resolution microCT scanner (Scanco Medical, Wayne, PA) at 16µm resolution and scans were calibrated to Hounsfield units (HU). Bone volume (BV), tissue mineral density (TMD), and tissue mineral content (TMC) data were determined. Bone was defined at a threshold of HU=1050 using Microview software (Parallax Innovations). TMD is an assessment of bone quality within the scaffold; the measure indicates the average density of the bone tissue (as defined by the threshold value of 1050HU) within a given 3D region of interest (or ROI) and is reported as the mass of hydroxyapatite per volume (mg HA/mm^3). TMC quantifies the amount of mineral present in the bone (as defined by the threshold value of 1050HU) in a

given ROI and reported as the mass of hydroxyapatite (mg HA). To obtain TMD and TMC values, Dicoms from Scanco were imported into Microview and greyscale values for each voxel were exported to excel and converted to HU values. The scaffold region was represented as a cylindrical ROI (6mmD x 3.615mmH). Bone formed outside the scaffold ROI boundary was quantified and defined as "external" bone growth and bone inside the scaffold ROI was defined as "internal" bone volume." External, internal and total BV, TMD, and TMC were calculated for each specimen.

To determine bone penetration into the scaffold radially, four concentric, cylindrical rings were defined as ROI's and were individually analyzed. The diameters of the 4 concentric rings are as follows: Ring 1: 6.00-4.84mm, Ring 2: 4.84-3.67mm, Ring 3: 3.67-2.5mm, Ring 4: 2.50-0.00mm. BV, TMC, and bone ingrowth of each ring was calculated using Microview Software. Bone ingrowth (%) was calculated as bone volume divided by the available pore volume for each ring. Available pore volume was calculated from the porosity of each ring based on the .STL design file for the scaffold.

Compression Mechanical Testing

Specimens were mechanically tested using an MTS Alliance RT30 electromechanical test frame (MTS Systems Corp, Minneapolis, MN) with a 500N load cell. Samples were compressed between two steel platens at a rate of 1.0 mm/min with a 0.5lbf preload. Data were collected and analyzed using TestWorks4 software (MTS Systems, Corp.). Data were collected to 25% strain, and the compressive elastic modulus was defined as the slope of linear region of the stress-strain curve prior to 15% strain. Data were normalized to scaffold area.

Histology

Fixed samples from each group were decalcified with RDO (Apex Engineering Products Corporation) and sent to the Histology Core at the University of Michigan Dental School to be embedded in paraffin, sectioned, and stained with hematoxylin and eosin (H&E). H&E was used to visualize cells, tissue matrix, blood vessels, and general tissue morphology. A light microscope was used to image sections with a 10x objective.

Statistical Analysis

Data are expressed as mean ± standard deviation of the mean. An analysis of variance (ANOVA) was used to determine statistical significance between groups. A *p-value <0.05 ($\alpha<0.05$) was considered statistically significant on a 95% confidence interval.

4.4 Results

Binding Environment Studies

At 4^{o}C, conjugation had significantly more BMP2 attached than adsorption at all exposure times. At 23^{o}C, conjugation still had significantly more binding at 0.5 and 1 hour exposures. Adsorption at 23^{o}C resulted in significantly more BMP2 bound than at 4^{o}C except at the 16 hour exposure. After 1 hour exposure at 23^{o}C, conjugated and adsorbed discs resulted in $0.0049\pm0.001\mu g/mm^2$ ($99.5\pm0.1\%$) and $0.0036\pm0.0001\mu g/mm^2$ ($73.3\pm1.3\%$) BMP2 attached, respectively (Figure 4.2). Based on these results, we examined Conj and Ads groups that were exposed to BMP2 for 1 hour at 23^{o}C in further studies.

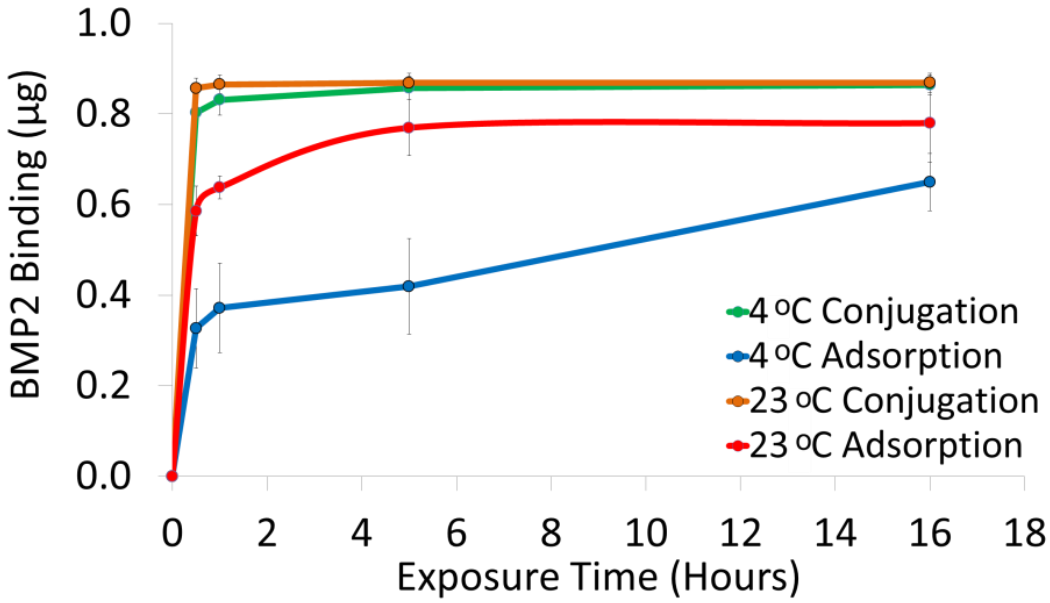

Figure 4.2: BMP2 Binding to PCL Discs via Adsorption or Conjugation
PCL discs were exposed to 1.4µg/ml BMP2 solution for 0.5, 1, 5, or 16 hours at 23°C or 4°C. BMP2 was quantified with an ELISA (n=3).

BMP2 *In Vitro* Bioactivity

To determine if the bound BMP2 was non-toxic and bioactive we seeded C2C12 myoblastic cells on BMP2 Ads or Conj PCL discs. We found cells on all PCL discs proliferated significantly more than the negative control (Figure 4.3A). Cells on adsorbed groups produced significantly higher ALP than the conjugated group. ALP production of cells on PCL without BMP2 was the same as conjugation and significantly less than adsorption. There was no difference between discs that had BMP2 adsorbed at 4°C or 23°C ($p=0.10$). Finally, the positive control of soluble BMP2 in cell culture medium showed significantly higher ALP (1.16nM ALP/mg protein/min) when compared to all other groups (Figure 4.3B).

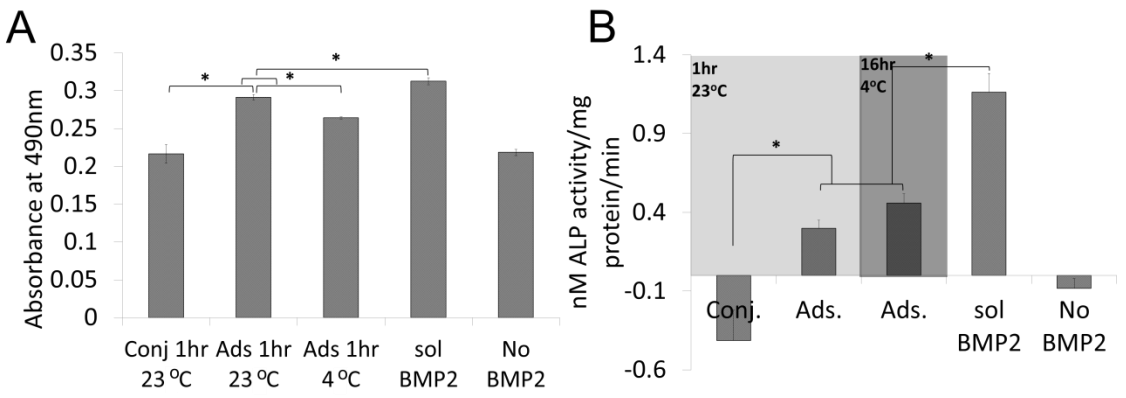

Figure 4.3: BMP2/PCL Cytotoxicity & Bioactivity
A) MTS assay results for relative C2C12 proliferation on BMP2/PCL discs. Cells were able to grow on PCL surface modified with BMP2. (n=4).
B) ALP production of C2C12 cells seeded on BMP2/PCL discs. Data is normalized to total intracellular protein content and based on linear curve fit. *$p<0.05$ was significant.

Concentration Binding Studies

To transition to *in vivo* bioactivity studies, 70% porous scaffolds (176mm^2) were exposed to increasing BMP2 concentrations for 1 hour at 23^{o}C (adsorbed and conjugated). The BMP2 bound to the scaffolds was compared to the amount adsorbed onto a disc (170mm^2). There was no significant difference in binding between adsorbed/conjugated scaffolds and discs at 5, 20, and 65µg/ml. Significantly more BMP2 bound to the surface as BMP2 concentration increased (Figure 4.4A). When exposed to 20µg/ml BMP2, 3.03±0.18µg (0.018±0.001µg /mm^2) BMP2 attached with conjugation and 2.49±0.35µg (0.015±0.002µg/mm^2) attached with adsorption. When exposed to 65µg/ml, conjugation and adsorption bound 12.83±1.78µg (0.076±0.01µg/mm^2) and 10.78±1.49µg BMP2 (0.063±0.01µg/mm^2), respectively. Figure 4.4B shows the percentage of BMP2 in the original solution that bound to the scaffold surface (% binding efficiency). Conjugation bound significantly more BMP2 than adsorption when exposed to 1.4µg/ml. There was

no difference in the amount bound between the two methods as BMP2 concentrations increased to 5, 20, and 65µg/ml.

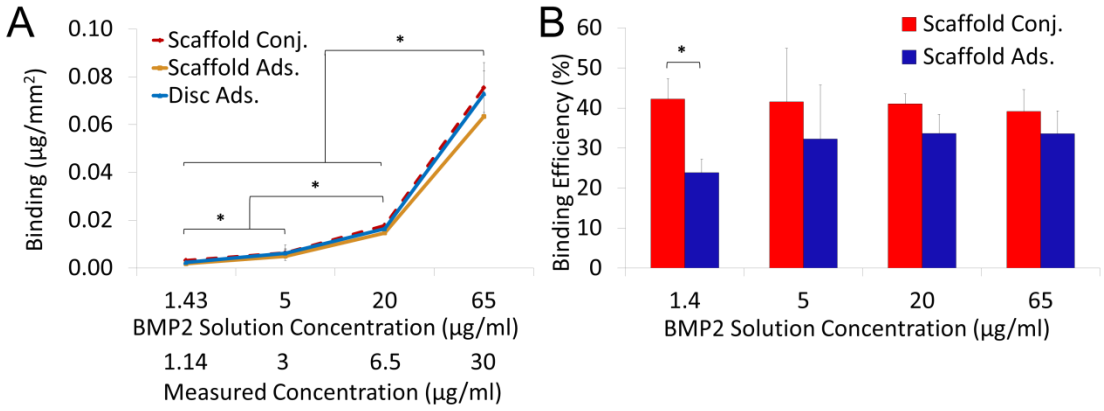

Figure 4.4: BMP2 Binding to PCL Discs and Scaffolds
A) PCL scaffolds were exposed to 1.43, 5, 20, or 65µg/ml BMP2 solution for 1 hour at 23°C. The data were normalized to the ELISA detected concentration which averaged at 1.14, 3, 6.5, 30µg/ml. *$p<0.05$
B) Bound BMP2 is expressed as a percentage of BMP2 in original solution (n=3).

In Vitro Release Kinetics

A carrier device's release kinetics plays a crucial role in the quality of engineered bone. PCL scaffolds exposed to 20µg/ml BMP2 solution for 1 hour at 23°C showed after 22 days, 0.0026± 0.0006µg and 0.0167±0.005µg of conjugated and adsorbed BMP2 was released, respectively (Figure 4.5A). A burst release commonly observed with adsorption occurred in the first 1-3 days during which about 0.0068µg BMP2 was released (Figure 4.5B).

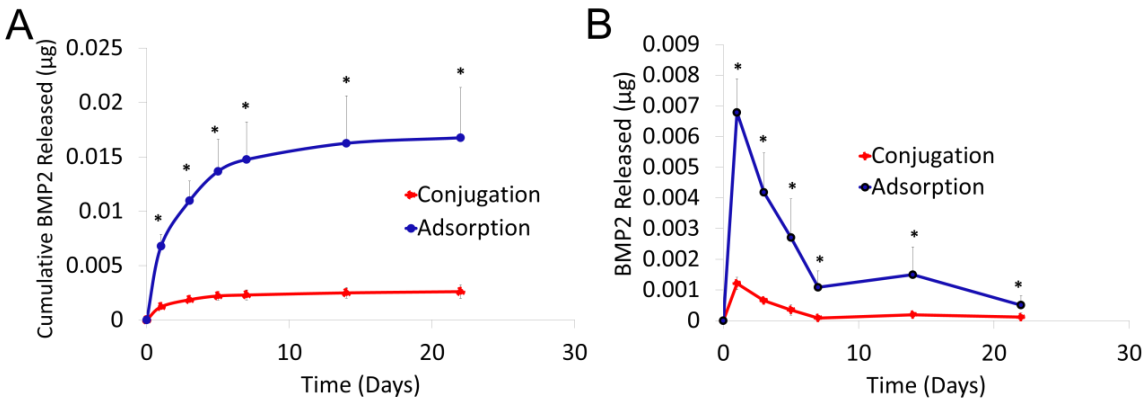

Figure 4.5: Conjugated and Adsorbed BMP2 Released from PCL
A) Cumulative release of BMP2 from PCL scaffolds into DPBS when exposed to 20µg/ml BMP2 for 1hr at 23°C. Release environment conditions were sterile, 37°C, 5% $C0_2$, and 95% humidity. *p<0.05
B) BMP2 (µg) released per day. The supernatant was analyzed for BMP2 content with an ELISA (n=3).

In Vivo Bone Formation

After 8 weeks subcutaneous implantation, we found adsorbed PCL scaffolds exposed to 20µg/ml and 65µg/ml BMP2 produced the greatest total bone volumes of 9.2±2.28mm^3 and 15.02±2.98mm^3, respectively. Conjugation produced 0.43±0.41mm^3 and 5.9±2.0mm^3 total bone when exposed to 20µg/ml or 65µg/ml respectively. Negative control blank PCL produced significantly less bone (0.14±0.03mm^3) than all other groups (Figure 4.6A). Using Microview to visualize µCT scans of explanted specimen, we found conjugation produced a shell of bone that followed scaffold geometry. Adsorption resulted in bone following scaffold geometry as well as filling into the pores (Figure 4.6B). The bone formed outside of the scaffold ROI for 65µg/ml adsorption (1.42±0.52 mm^3) and 65µg/ml conjugation (0.14±0.08 mm^3) was not excessive (Figure 4.6A&B). 65µg/ml adsorbed also had significantly higher tissue mineral content (8.44±1.7mg HA) than other groups. Finally, 65µg/ml conjugated, 20µg/ml adsorbed, and 65µg/ml

adsorbed produced bone that is within the normal density range of mandibular bone (551±25, 587±25, and 560±37mg HA/cm^3, respectively) [13,34].

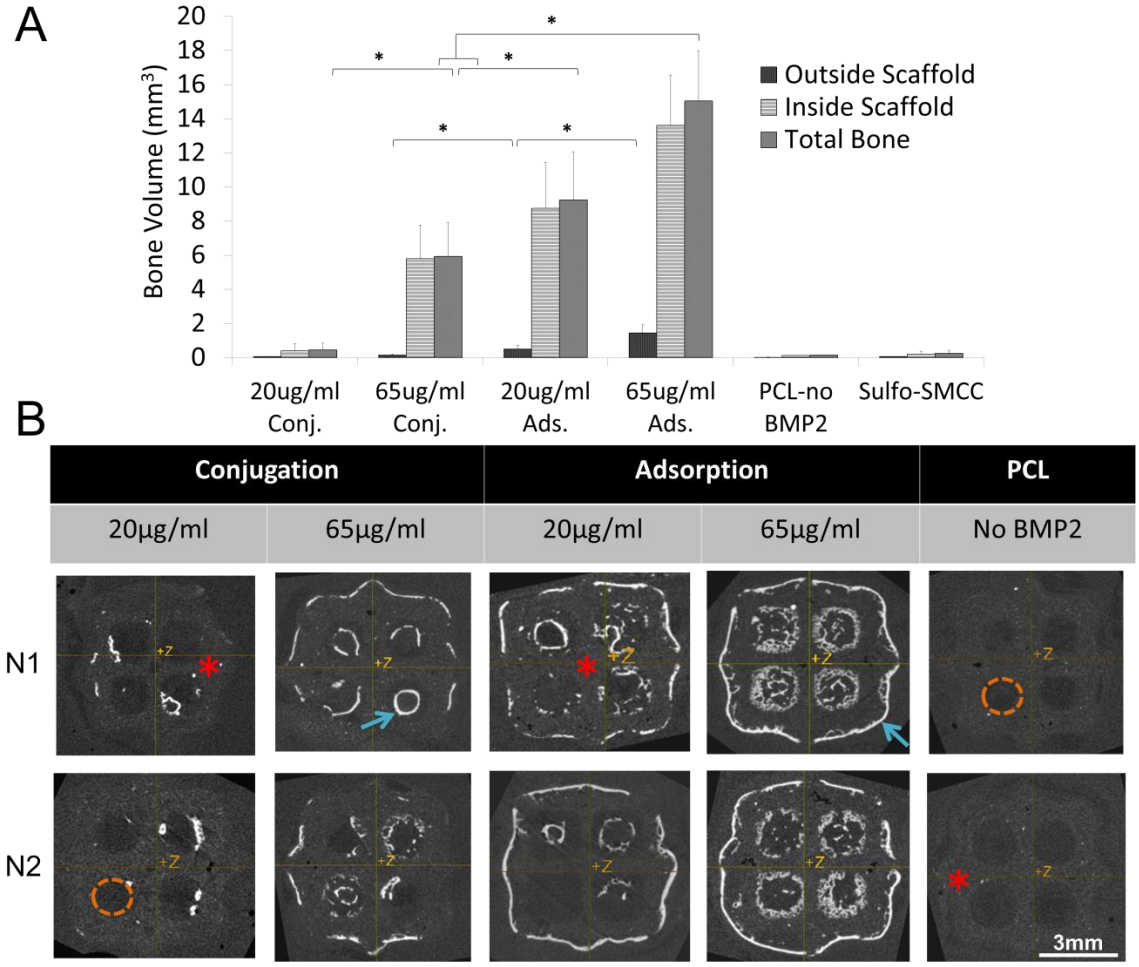

Figure 4.6: Regenerated Bone Analysis

A) Bone volume formed in explanted specimen using microCT scans (threshold=1050HU). "Inside scaffold" was defined as bone volume inside a cylindrical ROI (6mmD, 3.615mmH) and "outside scaffold" was the bone volume formed outside the ROI.

B) The microCT scans of two representative samples from each group are shown. Bright white areas indicate bone formation (blue arrow) and gray areas are scaffold (red*). Dark areas (orange dashed lines) indicate pores. Conjugation produced bone that closely followed PCL surface geometry. Adsorption produced bone growth into the pores in addition to following surface geometry.

Ring analysis showed a similar relationship in that adsorption resulted in higher %bone ingrowth in all rings when compared to conjugation. Percent bone ingrowth was the same

throughout the scaffold for 65µg/ml adsorption. In the center of the scaffold, 65µg/ml adsorption and conjugation had 17.2±5.4% and 7.5±3.07% ingrowth, respectively (Figure 4.7).

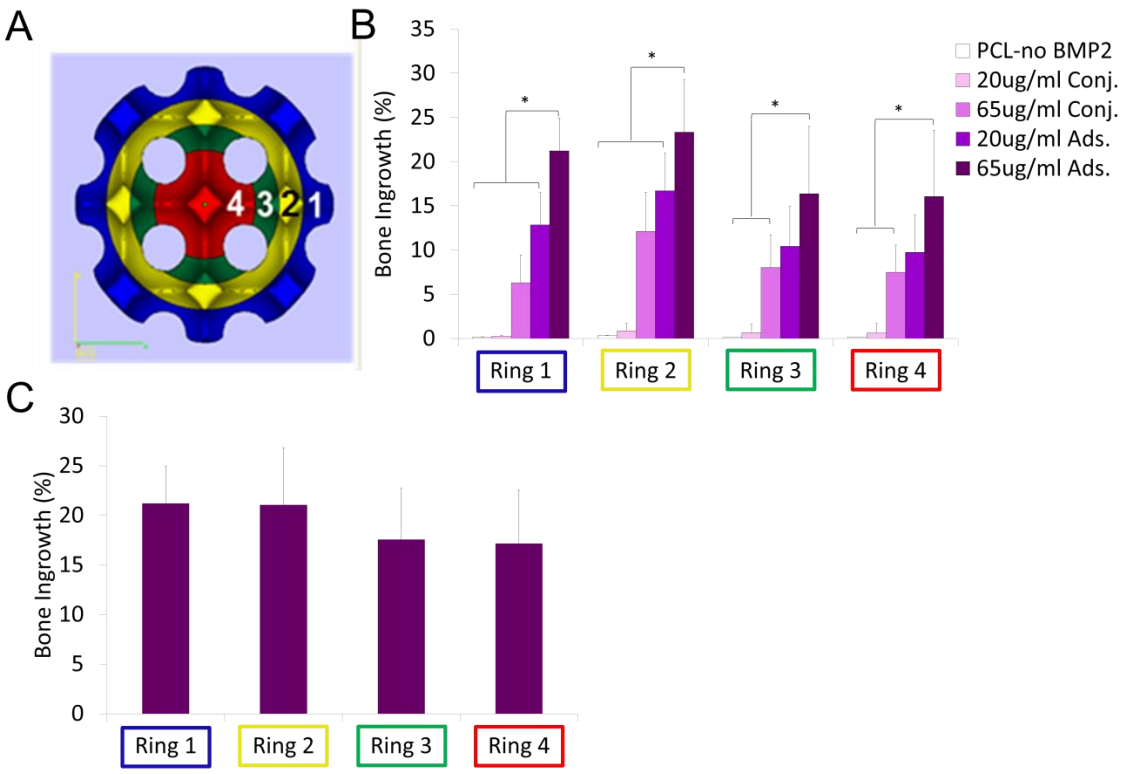

Figure 4.7: Ring Analysis for Bone Growth into Scaffold
A) Outer ROI diameters were 6.0, 4.84, 3.67, 2.50mm for Rings 1, 2, 3, and 4, respectively.
B) Percentage bone ingrowth (bone volume divided by available pore space) showed 65µg/ml adsorbed group had significantly more ingrowth than either conjugated groups.
C) 65µg/ml adsorbed group resulted in the same bone penetration throughout the scaffold.

Mechanical Testing

As seen in Figure 4.8, nearly all of the groups had significantly higher moduli when compared to the blank PCL (12.7±1.1MPa) or sulfo-SMCC negative controls, with the exception of 20µg/ml conjugated (p=0.12). The 65µg/ml adsorbed group had the highest elastic modulus of 20.1 ± 3.0 MPa, which was significantly higher than the 65µg/ml

conjugated group (15.1±1.3MPa). However, at the lower concentration level, there was no difference between 20µg/ml conjugated and 20µg/ml adsorbed moduli.

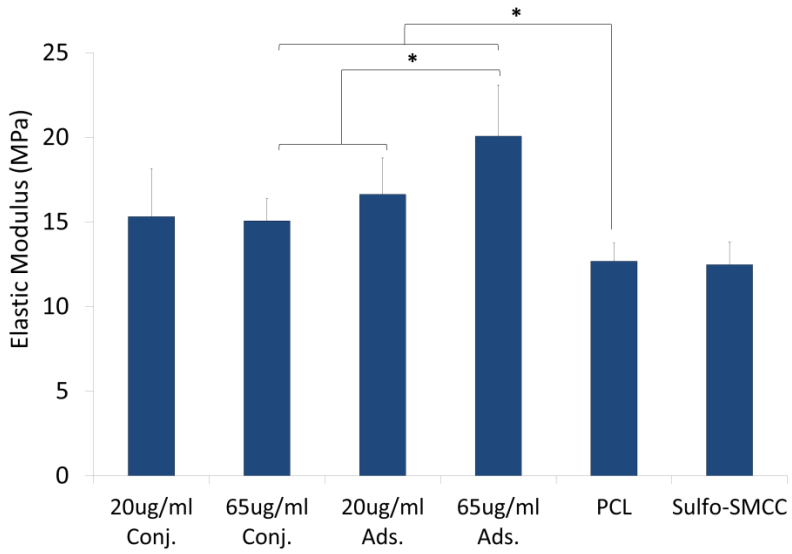

Figure 4.8: Compressive Mechanical Testing
Specimen elastic modulus measured in compression was defined as the slope of linear region prior to 15% strain level and normalized to specimen surface area.

Histology

Scaffold pores of sulfo-SMCC, blank PCL, and 20µg/ml conjugated BMP2 were infiltrated primarily with fibrous and fatty tissue (Figure 4.9). Negligible bone formation was observed in these groups. However, both of the adsorbed groups (20 and 65µg/ml) showed blood, bone and fatty marrow growth into the scaffold pore space. There were multiple osteocytes embedded in the osteoid as well as osteoblasts lining the matrix. The 65µg/ml conjugated group showed bone growth, fibrous tissue, and a little fatty marrow as well; however, the resulting bone was primarily localized to the pore surface and did not grow into the pores as well as the adsorbed group.

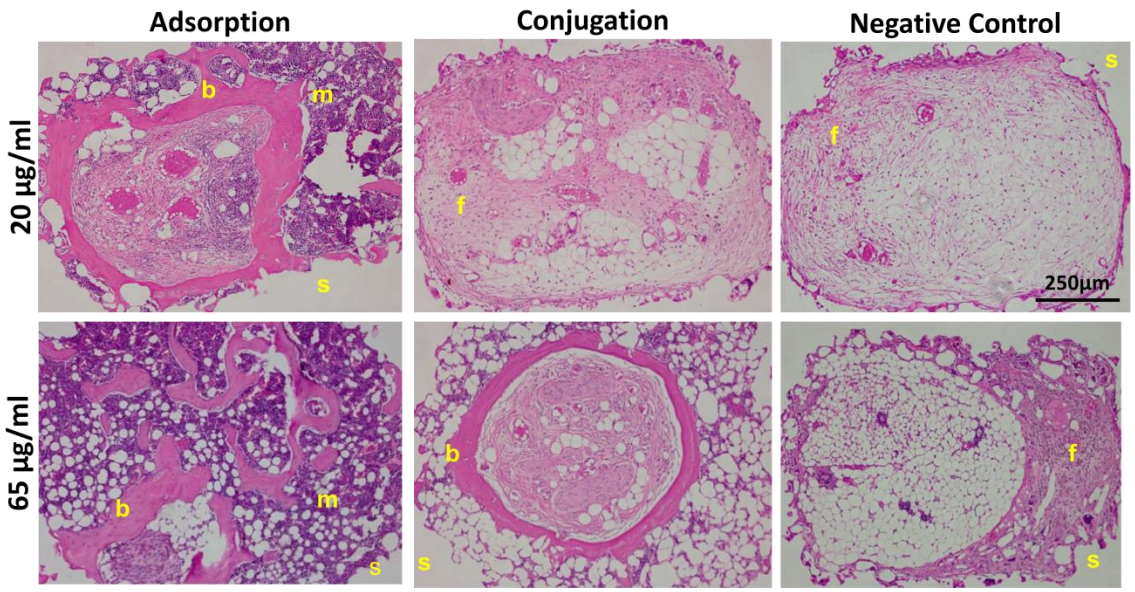

Figure 4.9: H&E Images of PCL/BMP2 Scaffold Pores
Bright field images of scaffold pores taken at 10x magnification. s=scaffold, b=bone, m=marrow, f=fibrous tissue. Negative controls consisted mainly of fibrous tissue.

4.5 Discussion

Prefabricating a bone flap *in vivo* has been completed in Europe and Asia but not yet in the United States to the best of our knowledge. For the foreseeable future this will likely be the method that can best generate large vascularized bone constructs for reconstruction. Medtronic's product Infuse™ has been FDA approved for delivery of BMP2 from a collagen type 1 sponge in treatment of spinal fusion, open tibial fractures, sinus augmentation, and dental procedures [35]. Due to BMP2's short half-life, a 1.5mg/ml BMP2 dose was needed (greatly exceeding native concentrations of 18.8-22pg/mL) which resulted in a large burst release during the first 2-3 days causing adverse reactions in some patients [36]. To control the release and prevent excessive bone growth, Park YJ et al chemically conjugated BMP2 to amine-containing chitosan with a sulfo-SMCC cross linker. Conjugation enhanced *in vitro* osteoinductive properties as determined by pre-osteoblast differentiation; however, chitosan would not be an ideal

carrier for creating a bone flap because it lacks mechanical integrity [21]. BMP2 adsorption and conjugation via heparin and sulfo-SMCC onto uncoated polymer surfaces (PLGA and PCL) has been superficially compared but a study was needed to refine a simple BMP2 binding method onto 3D SLS manufactured PCL scaffolds in a clinically applicable environment [18,19].

In this study we aimed to refine a protocol for binding BMP2 to PCL considering the constraints of intra OR use and to test bone regeneration using the sulfo-SMCC and simple adsorption binding protocols *in vivo*. Studies have used various methods to deliver BMP2 from biomaterials including sulfo-SMCC, heparin, trauts, adsorption, and incorporation into a coating or microparticles [20,22,25,33,37-41]. Temperatures and exposure times at which protein binding studies have been tested range from 4^{o}C-37^{o}C and 1-24 hours [21,33,42,43]. However, temperatures outside room temperature and long exposure times make it very difficult to use such BMP2 conjugation methods clinically. In this current study, we found chemical conjugation with sulfo-SMCC bound more BMP2 during a shorter exposure time and at ambient temperature in comparison to adsorption; however, the conjugated BMP2 did not maintain bioactivity once bound to the surface as determined by an absence of ALP production *in vitro*. This inactivity could be due to the sulfo-SMCC binding reaction binding BMP2 in a conformation that does not ideally present its cell binding moiety. Even though adsorbed BMP2 may not have bound as efficiently as conjugated BMP2 at 23^{o}C, it was shown to be bioactive *in vitro* and produced more bone that infiltrated the scaffold and pores *in vivo.* We also showed that adsorbed BMP2 bound more efficiently at 23^{o}C than at 4^{o}C, which is a clear advantage for the intra OR setting. This increased binding may have been due to

increased protein kinetics providing the protein with more opportunities to bind to the material surface.

GF delivery vehicle release kinetics are crucial to the resulting bone formed. Conjugation resulted in sustained GF release, whereas, adsorption had a slightly higher burst release after 1-3 days, followed by a sustained release over time. This burst release with adsorption is commonly seen in other studies [22,23,33]; however, in this case when BMP2 is delivered from laser sintered PCL the amount released, in a burst and during subsequent slower release, at the secondary site is extremely small (<1%)- much smaller than the other studies[22,33,43]. The released amount is still therapeutically relevant because the regenerated bone increased the scaffold's load bearing abilities. Since the *in vitro* release was at 37^{o}C, the remaining BMP2 could have degraded and the ELISA may not have detected the BMP2 fragments. Although an ELISA is a widely used method to detect low BMP2 concentrations, an alternate detection method that could be utilized to confirm the release kinetics would be to use ^{125}I-labeled BMP2 [21]. Overall, adsorption provided greater BMP2 release over time. A limitation to this study was that the *in vitro* release profile may not entirely accurately predict the *in vivo* release profile due to physiological factors such as enzymes cleaving BMP2 off of the surface.

To transition to *in vivo* studies and confirm BMP2 bioactivity, we increased the amount of BMP2 exposed to PCL and used the more complex geometry. We determined the same amount of BMP2 adsorbed onto discs as onto scaffolds and that samples bound increasingly more µg BMP2/mm^2 when they were exposed to increasing BMP2 concentrations. The higher concentrations may have caused a stronger concentration gradient that drove adsorption at a rate similar to that of conjugation. The *in vivo* study

showed that adsorption on PCL may be more clinically applicable because not only did bone formation follow scaffold surface geometry like conjugation but it also grew into the interior available pore space. This increased bone ingrowth is likely the reason adsorption had a higher elastic modulus than conjugation groups. This superior mechanical integrity will be crucial once the bone flap is transferred to the defect site. Adsorption also provided the most overall bone growth as well as bone formed at the center of the scaffold. When applied to a bone flap model it is important to produce as much bone as possible before transferring it to assist the flap to integrate into the defect site as well as facilitate further bone remodeling and growth. The ectopic model for bone regeneration was, due to our interest in pre-fabricated flaps, the process by which we wanted to test BMP2 delivery.

This scaffold was acellular when implanted, therefore, we speculate that circulating cells such as mesenchymal stem cells and fibroblasts that migrated through the vasculature in the wound bed could have interacted with the released BMP2 and were involved in endochondral bone formation. Due to a lack of bioactivity exhibited *in vitro,* but the presence of bone formed *in vivo*, we believe that conjugated BMP2 may be released via proteolytic activity and adsorption released the protein through weak molecular interactions. Overall, adsorption onto PCL makes BMP2 available faster to cells than conjugation via sulfo-SMCC. In the future, we would like to determine a dual GF delivery system to increase the bone growth rate into the scaffold so that the flap can be transplanted at an earlier time point for oncology patients waiting for adjunct therapy.

4.6 Conclusions

To address the drawbacks associated with autographs, allografts, and synthetic grafts we propose the idea of pre-fabricating a flap that is autologous in nature. The ability to create complex PCL geometries for craniofacial reconstruction is an advance in pre-fabricating flaps, as only crude geometries were utilized in other cases. Based on these studies, adsorbing BMP2 onto PCL may be more optimal for clinical use in comparison to conjugation via sulfo-SMCC due to BMP2 binding in a short exposure time at ambient temperature, retained BMP2 bioactivity, bone growth following geometry and into pores, and healthy marrow development. Further studies are currently being conducted to determine if these *in vivo* results can be replicated in a large porcine model and, furthermore, transplant the PCL implant to a mandibular angle defect. We will compare the pre-fabricated flap results to a PCL implant placed directly into the defect site.

Acknowledgements: This research was funded by the NIH/NIDCR Tissue Engineering at Michigan trainee grant (DE 007057), NIH R21 DE 022439, and NIH R01 AR 060892.

Author Disclosure Statement: Scott Hollister was a co-founder of Tissue Regeneration Systems (TRS), but is no longer affiliated.

4.7 References:

[1] Bhumiratana S, Vunjak-Novakovic G. Concise review: personalized human bone grafts for reconstructing head and face. Stem Cells Transl Med 2012 Jan;1(1):64-69.

[2] Warnke PH, Wiltfang J, Springer I, Acil Y, Bolte H, Kosmahl M, et al. Man as living bioreactor: fate of an exogenously prepared customized tissue-engineered mandible. Biomaterials 2006 Jun;27(17):3163-3167.

[3] Warnke PH, Springer IN, Wiltfang J, Acil Y, Eufinger H, Wehmoller M, et al. Growth and transplantation of a custom vascularised bone graft in a man. Lancet 2004 Aug 28-Sep 3;364(9436):766-770.

[4] Terheyden H, Knak C, Jepsen S, Palmie S, Rueger DR. Mandibular reconstruction with a prefabricated vascularized bone graft using recombinant human osteogenic protein-1: an experimental study in miniature pigs. Part I: Prefabrication. Int J Oral Maxillofac Surg 2001 Oct;30(5):373-379.

[5] Mesimaki K, Lindroos B, Tornwall J, Mauno J, Lindqvist C, Kontio R, et al. Novel maxillary reconstruction with ectopic bone formation by GMP adipose stem cells. Int J Oral Maxillofac Surg 2009 Mar;38(3):201-209.

[6] Alam MI, Asahina I, Seto I, Oda M, Enomoto S. Prefabrication of vascularized bone flap induced by recombinant human bone morphogenetic protein 2 (rhBMP-2). Int J Oral Maxillofac Surg 2003 Oct;32(5):508-514.

[7] Becker ST, Bolte H, Krapf O, Seitz H, Douglas T, Sivananthan S, et al. Endocultivation: 3D printed customized porous scaffolds for heterotopic bone induction. Oral Oncol 2009 Nov;45(11):e181-8.

[8] Terheyden H, Jepsen S, Rueger DR. Mandibular reconstruction in miniature pigs with prefabricated vascularized bone grafts using recombinant human osteogenic protein-1: a preliminary study. Int J Oral Maxillofac Surg 1999 Dec;28(6):461-463.

[9] Terheyden H, Menzel C, Wang H, Springer IN, Rueger DR, Acil Y. Prefabrication of vascularized bone grafts using recombinant human osteogenic protein-1--part 3: dosage of rhOP-1, the use of external and internal scaffolds. Int J Oral Maxillofac Surg 2004 Mar;33(2):164-172.

[10] Warnke PH, Springer IN, Acil Y, Julga G, Wiltfang J, Ludwig K, et al. The mechanical integrity of in vivo engineered heterotopic bone. Biomaterials 2006 Mar;27(7):1081-1087.

[11] Heliotis M, Lavery KM, Ripamonti U, Tsiridis E, di Silvio L. Transformation of a prefabricated hydroxyapatite/osteogenic protein-1 implant into a vascularised

pedicled bone flap in the human chest. Int J Oral Maxillofac Surg 2006 Mar;35(3):265-269.

[12] Hollister SJ, Murphy WL. Scaffold translation: barriers between concept and clinic. Tissue Eng Part B Rev 2011 Dec;17(6):459-474.

[13] Williams JM, Adewunmi A, Schek RM, Flanagan CL, Krebsbach PH, Feinberg SE, et al. Bone tissue engineering using polycaprolactone scaffolds fabricated via selective laser sintering. Biomaterials 2005 Aug;26(23):4817-4827.

[14] Wong DY, Hollister SJ, Krebsbach PH, Nosrat C. Poly(epsilon-caprolactone) and poly (L-lactic-co-glycolic acid) degradable polymer sponges attenuate astrocyte response and lesion growth in acute traumatic brain injury. Tissue Eng 2007 Oct;13(10):2515-2523.

[15] Fitzsimmons J. 510(k) Premarket Notification, Cover, Burr Hole, TRS CRANIAL BONE VOID FILLER. 2014; Available at: http://www.accessdata.fda.gov/scripts/cdrh/cfdocs/cfpmn/pmn.cfm?ID=K123633, 2014.

[16] Yeo A. 510(k) Premarket Notification, Methyl Methacrylate For Cranioplasty, OSTEOPORE PCL SCAFFOLD. 2014; Available at: http://www.accessdata.fda.gov/scripts/cdrh/cfdocs/cfpmn/pmn.cfm?ID=K051093, 2014.

[17] Mitsak AG, Kemppainen JM, Harris MT, Hollister SJ. Effect of polycaprolactone scaffold permeability on bone regeneration in vivo. Tissue Eng Part A 2011 Jul;17(13-14):1831-1839.

[18] Zhang H, Migneco F, Lin CY, Hollister SJ. Chemically-conjugated bone morphogenetic protein-2 on three-dimensional polycaprolactone scaffolds stimulates osteogenic activity in bone marrow stromal cells. Tissue Eng Part A 2010 Nov;16(11):3441-3448.

[19] Jeon O, Song SJ, Kang SW, Putnam AJ, Kim BS. Enhancement of ectopic bone formation by bone morphogenetic protein-2 released from a heparin-conjugated poly(L-lactic-co-glycolic acid) scaffold. Biomaterials 2007 Jun;28(17):2763-2771.

[20] Zhang Q, He QF, Zhang TH, Yu XL, Liu Q, Deng FL. Improvement in the delivery system of bone morphogenetic protein-2: a new approach to promote bone formation. Biomed Mater 2012 Aug;7(4):045002-6041/7/4/045002. Epub 2012 May 4.

[21] Park YJ, Kim KH, Lee JY, Ku Y, Lee SJ, Min BM, et al. Immobilization of bone morphogenetic protein-2 on a nanofibrous chitosan membrane for enhanced guided bone regeneration. Biotechnol Appl Biochem 2006 Jan;43(Pt 1):17-24.

[22] Kim TH, Oh SH, Na SY, Chun SY, Lee JH. Effect of biological/physical stimulation on guided bone regeneration through asymmetrically porous membrane. J Biomed Mater Res A 2012 Jun;100(6):1512-1520.

[23] Liu HW, Chen CH, Tsai CL, Hsiue GH. Targeted delivery system for juxtacrine signaling growth factor based on rhBMP-2-mediated carrier-protein conjugation. Bone 2006 Oct;39(4):825-836.

[24] Rai B, Teoh SH, Hutmacher DW, Cao T, Ho KH. Novel PCL-based honeycomb scaffolds as drug delivery systems for rhBMP-2. Biomaterials 2005 Jun;26(17):3739-3748.

[25] Gharibjanian NA, Chua WC, Dhar S, Scholz T, Shibuya TY, Evans GR, et al. Release kinetics of polymer-bound bone morphogenetic protein-2 and its effects on the osteogenic expression of MC3T3-E1 osteoprecursor cells. Plast Reconstr Surg 2009 Apr;123(4):1169-1177.

[26] Partee B, Hollister SJ, Das S. Selective Laser Sintering Process Optimization for Layered Manufacturing of CAPA® 6501 Polycaprolactone Bone Tissue Engineering Scaffolds. Journal of Manufacturing Science and Engineering 2005 September 14;128(2):531-540.

[27] Dias MR, Guedes JM, Flanagan CL, Hollister SJ, Fernandes PR. Optimization of scaffold design for bone tissue engineering: A computational and experimental study. Med Eng Phys 2014 Apr;36(4):448-457.

[28] Zopf DA, Hollister SJ, Nelson ME, Ohye RG, Green GE. Bioresorbable airway splint created with a three-dimensional printer. N Engl J Med 2013 May 23;368(21):2043-2045.

[29] van de Watering FC, van den Beucken JJ, van der Woning SP, Briest A, Eek A, Qureshi H, et al. Non-glycosylated BMP-2 can induce ectopic bone formation at lower concentrations compared to glycosylated BMP-2. J Control Release 2012 Apr 10;159(1):69-77.

[30] Katagiri T, Yamaguchi A, Komaki M, Abe E, Takahashi N, Ikeda T, et al. Bone morphogenetic protein-2 converts the differentiation pathway of C2C12 myoblasts into the osteoblast lineage. J Cell Biol 1994 Dec;127(6 Pt 1):1755-1766.

[31] Jiao X, Billings PC, O'Connell MP, Kaplan FS, Shore EM, Glaser DL. Heparan sulfate proteoglycans (HSPGs) modulate BMP2 osteogenic bioactivity in C2C12 cells. J Biol Chem 2007 Jan 12;282(2):1080-1086.

[32] Pohl TL, Boergermann JH, Schwaerzer GK, Knaus P, Cavalcanti-Adam EA. Surface immobilization of bone morphogenetic protein 2 via a self-assembled monolayer formation induces cell differentiation. Acta Biomater 2012 Feb;8(2):772-780.

[33] Zhao Y, Zhang J, Wang X, Chen B, Xiao Z, Shi C, et al. The osteogenic effect of bone morphogenetic protein-2 on the collagen scaffold conjugated with antibodies. J Control Release 2010 Jan 4;141(1):30-37.

[34] Kontogiorgos E, Elsalanty ME, Zapata U, Zakhary I, Nagy WW, Dechow PC, et al. Three-dimensional evaluation of mandibular bone regenerated by bone transport distraction osteogenesis. Calcif Tissue Int 2011 Jul;89(1):43-52.

[35] Cahill KS, Chi JH, Day A, Claus EB. Prevalence, complications, and hospital charges associated with use of bone-morphogenetic proteins in spinal fusion procedures. JAMA 2009 Jul 1;302(1):58-66.

[36] Santo VE, Gomes ME, Mano JF, Reis RL. Controlled Release Strategies for Bone, Cartilage, and Osteochondral Engineering-Part I: Recapitulation of Native Tissue Healing and Variables for the Design of Delivery Systems. Tissue Eng Part B Rev 2013 Feb 19.

[37] Han J, Cao RW, Chen B, Ye L, Zhang AY, Zhang J, et al. Electrospinning and biocompatibility evaluation of biodegradable polyurethanes based on L-lysine diisocyanate and L-lysine chain extender. J Biomed Mater Res A 2011 Mar 15;96(4):705-714.

[38] Kumagai T, Anada T, Honda Y, Takami M, Kamijyo R, Shimauchi H, et al. Osteoblastic Cell Differentiation on BMP-2 Pre-Adsorbed Octacalcium Phosphate and Hydroxyapatite. Key Engineering Materials 2007;361-363:1025.

[39] Bae SE, Choi J, Joung YK, Park K, Han DK. Controlled release of bone morphogenetic protein (BMP)-2 from nanocomplex incorporated on hydroxyapatite-formed titanium surface. J Control Release 2012 Jun 28;160(3):676-684.

[40] Hosseinkhani H, Hosseinkhani M, Khademhosseini A, Kobayashi H. Bone regeneration through controlled release of bone morphogenetic protein-2 from 3-D tissue engineered nano-scaffold. J Control Release 2007 Feb 26;117(3):380-386.

[41] Kirby GTS, White LJ, Rahman CV, Cox HC, Qutachi O, Rose, Felicity R. A. J., et al. PLGA-Based Microparticles for the Sustained Release of BMP-2. Polymers 2011;3:571.

[42] Apatite-Polymer Composite Particles for Controlled Delivery of BMP-2: *In Vitro* Release and Cellular Response. Proceedings of the Singapore-MIT Alliance Symposium; 2005.

[43] Autefage H, Briand-Mesange F, Cazalbou S, Drouet C, Fourmy D, Goncalves S, et al. Adsorption and release of BMP-2 on nanocrystalline apatite-coated and uncoated hydroxyapatite/beta-tricalcium phosphate porous ceramics. J Biomed Mater Res B Appl Biomater 2009 Nov;91(2):706-715.

CHAPTER 5

DUAL DELIVERY OF BMP2 AND VEGF FROM A POLYCAPROLACTONE/COLLAGEN SPONGE CONSTRUCT TO INCREASE BONE GROWTH IN ECTOPIC SITES FOR FLAP PREFABRICATION

Rui Fan, Sean Miller, Colleen Flanagan, Sean Edwards, and Scott Hollister assisted with the preparation of this chapter.

Submitted to Journal of Biomedical Materials Research Part B. Dec 2014

5.1 Abstract

Background: Pre-fabricated bone flaps produced in vivo require the ability to grow relatively large bone volumes with associated vasculature to reconstruct large craniofacial defects. Polycaprolactone (PCL) with adsorbed bone morphogenetic protein-2 (BMP2) regenerates bone in soft tissue pockets. With the goal of further optimizing bone ingrowth for prefabricated flap applications, this study investigates dual delivery of BMP2 and vascular endothelial growth factor (VEGF) from a composite PCL/collagen sponge construct.

Methods: BMP2 (65µg/ml) was first adsorbed onto PCL scaffolds. Next, a lyophilized collagen sponge was created within the scaffold, and VEGF (5µg) was pipetted onto the sponge. BMP2 and VEGF bioactivity were confirmed using alkaline phosphatase and endothelial cell proliferation assays. The constructs were then implanted subcutaneously in mice.

Results: At 8 weeks, bone volume was greater for BMP2+VEGF (10.1±3.7mm3) compared to BMP2 (7.9±3.8mm3). Bone volume significantly increased from 4 to 8 weeks with BMP2+VEGF and corresponded to a significant increase in construct modulus from 4 weeks (10.5±2.3MPa) to 8 weeks (14.7±2.7MPa).

Conclusion: BMP2+VEGF delivery from PCL/collagen sponge constructs resulted in a greater increase in regenerated bone volume from 4 to 8 weeks when compared to BMP2 alone. Dual delivery is a potential method to regenerate bone faster and in greater volume for a tissue engineered bone flap.

Keywords: Bone morphogenetic protein-2, vascular endothelial growth factor, polycaprolactone, tissue engineering, protein delivery

5.2 Introduction

The gold standard for reconstructing a large bone defect is to use an autograft (typically from the iliac crest or fibula). In cases with large bone defects with compromised vascularity in the recipient site, a vascularized flap is used. When vascularity is required, a vascular pedicle is taken from the donor site to attach to a vein and artery at the recipient site to ensure immediate perfusion. Major drawbacks to autografts include donor site morbidity and geometry mismatch for craniofacial reconstruction. Furthermore, chronically infected and irradiated wound sites are challenging to reconstruct and are not conducive to general wound healing, let alone being able to support a bone graft. An alternative to using an autograft or vascularized flap is to tissue engineer a bone flap *in vivo*. Pre-fabricating a patient-specific bone flap for large craniofacial defects involves implanting a biomaterial scaffold with associated biologics into the patient's latissimus dorsi and then transplanting it to the defect site after a maturation period. There are few reports of this type of surgery in animals and humans [1-9]. It is important to note that for large defects, a large bone volume would be needed in the flap.

Our goal is to advance the current pre-fabricated flap process by integrating patient-specific computational design, 3D biomaterial printing, and dual biologic functionalization [10]. Poly-Ɛ-caprolactone (PCL) is a biocompatible and bioresorbable polymer that has been approved for cranioplasty bone filling applications by the Food and Drug Administration (FDA) [11,12]. PCL is compatible with image-based computational aided design (CAD) and selective laser sintering (SLS) manufacturing techniques to repeatedly produce scaffolds with complex geometries, controlled pore

size, and stiffness [13] and degrades over three years. Its degradation profile and mechanical properties support its use for bone tissue engineering in complex reconstruction sites where bone may take over a year to form; however, PCL is not osteoconductive.

Bone morphogenetic protein-2 (BMP2) is a potent osteoinductive growth factor which has been used to induce osteogenesis with various biomaterials [14-18]. Previously in our laboratory we adsorbed BMP2 onto PCL scaffolds and found that the resultant PCL/BMP2 scaffold regenerates bone when implanted in soft pockets in mice [19].

Since the PCL/BMP2 constructs will be implanted without cells, the host's cells need to migrate into the construct and differentiate into osteoblasts. Angiogenesis plays a key role in the bone regeneration process by providing transportation for nutrients, oxygen, and cells migrating to the construct. Many studies find vascular endothelial growth factor (VEGF) is a key mediator in angiogenesis by playing a role in early fracture repair and endochondral and intramembranous ossification [20-22]. Transplanting bone stock alone is insufficient to maintain construct viability, especially in large defects, and it is crucial to develop a supporting vascular network. To mimic natural bone healing many investigators have developed VEGF and BMP2 sequential release systems in which VEGF is incorporated into rapidly degrading gels and BMP2 is delivered slowly from poly(lactic-co-glycolic acid) (PLGA) microspheres embedded in scaffolds [23,24]. Studies which successfully increase bone growth with dual growth factor delivery used collagen sponge, PLGA microspheres/gelatin hydrogel, or poly-DL-lactide (PDLLA)/alginate scaffolds and implanted the scaffolds in murine intramuscular, rat subcutaneous or rat critical size femur defects [24-27].

On the contrary, some studies find that dual VEGF and BMP2 delivery has no effect on bone regeneration when implanted in beagle intramuscular or rat calvarial defect sites [23,28]. Furthermore, the studies suggest that it is the BMP2 release rate and implant location (ectopic vs. orthotopic), not the VEGF delivery, that effects the resulting bone growth [23,24]. Specifically, ectopic delivery locations resulted in increased bone formation with VEGF inclusion when compared to orthotopic sites. Due to these conflicting results of these studies, the suggestion that VEGF delivery may be more effective in an ectopic location, and the need to implement designed structured scaffolds for prefabricated flap generation, we applied the dual BMP2 and VEGF delivery method to our PCL/BMP2 system.

Specifically, this study investigated the effect of dual BMP2 and VEGF delivery from a two phase composite scaffold system on subcutaneous regenerated bone volume in mice in comparison to BMP2 delivery alone. The construct consisted of a designed structural PCL scaffold and an integrated collagen sponge scaffold. Adsorbed BMP2 was delivered from the PCL scaffold surface and VEGF was delivered from the internal collagen sponge. The integration and testing of multiple biologics from a designed scaffold construct with controlled anatomic shape and porous architecture is a novel approach in pre-fabricating bone flaps.

5.3 Methods & Materials

PCL Scaffold Fabrication

Selective laser sintered 3D 70% porous PCL scaffolds (6.35mm D x 4mm H, 170mm^2 surface area) with 2.15mm spherical pores were fabricated as previously described (Figure 5.1A)[19].

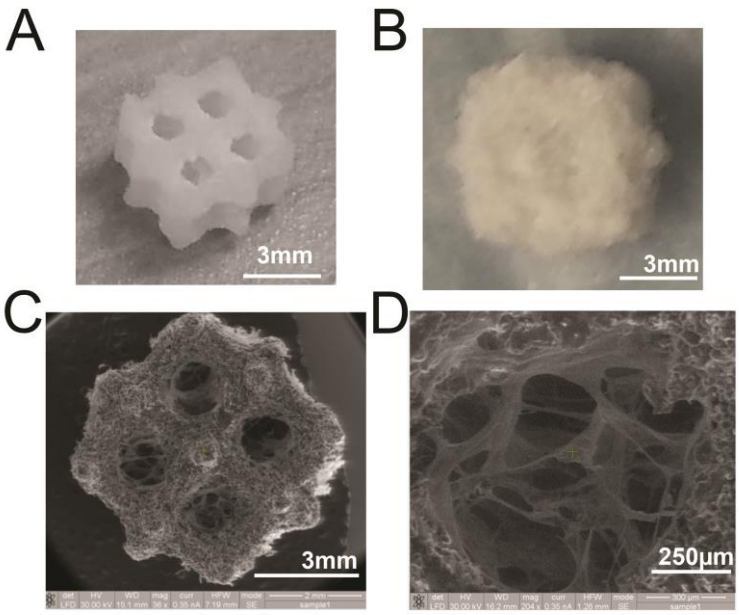

Figure 5.1: PCL/Collagen Sponge Construct
A) PCL scaffold
B) PCL scaffold filled with a collagen type 1 sponge
C) SEM image of PCL/collagen sponge construct taken at 36x magnification and
D) 204x magnification of the pore space in construct.

BMP2 Binding

BMP2 adsorption was completed as previously described [19]. Briefly, scaffolds were pre-washed in activation buffer (BuPH Phosphate Buffered Saline Pack in diH_20, pH 7.2 Pierce Biotechnology) and then washed in conjugation buffer (activation buffer plus 0.1M EDTA) to wet the surface. They were then exposed to 1ml of 65µg/ml BMP2 (Creative Biomart, Shirley, NY) for 1 hour at 23^{o}C, washed in distilled water (diH_20), and dried overnight. BMP2 was provided in lyophilized form and suspended to 1mg/ml in 20mM Acetic Acid. The BMP2 solution was diluted to 65µg/ml in conjugation buffer.

PCL/Collagen Sponge Construct Fabrication

Rat tail collagen type 1 gel was made according to the manufacturer's instructions (BD Bioscience). The collagen gel consisted of 5mg/ml collagen, 10% 10x Dulbeccos

Phosphate Buffered Saline (DPBS), 1N sodium hydroxide (NaOH), and diH_20. The volume of 1N NaOH added was equal to 0.023*(volume of collagen) and diH_20 was used to adjust the final solution volume.

BMP2 adsorbed PCL scaffolds were washed in DPBS under vacuum and placed into form-fitting Sylgard184 (Dow Corning) molds. Sylgard molds were created using solid PCL cylinders (6.35mmD, 5mmH) in the uncured Sylgard. The cylinders were removed with acetone after the Sylgard cured. Next, 80µl collagen gel was pipetted into the macroporous space within the scaffold, and the molds were placed in a vacuum for 2 minutes. The PCL/collagen gel combination will now be referred to as a construct. The constructs were then incubated at 37^oC for 30 minutes and frozen at -80^oC for 12 hours. Finally, constructs were lyophilized for 24 hours to form a collagen sponge within the scaffold pores (Figure 5.1B).

SEM Imaging

Constructs were imaged at the Electron Beam Analysis Laboratory at the University of Michigan using a Philips/FEI XL30 FEG environmental scanning electron microscope (Figure 5.1C&D). Images were taken this 36x and 204x objectives to visualize the construct and the pore space, respectively.

BMP2 Bioactivity-Alkaline Phosphatase Stain

Cell studies used PCL discs (15mm diameter, 2mm height, 176 mm^2 surface area) for simplicity. C2C12 myoblastic cells are known to differentiate down an osteogenic lineage when exposed to active BMP2 [29,30]. Since the adsorbed BMP2 will be subjected to the conditions to fabricate the collagen sponge, we next determined if BMP2 was bioactive at the end of the process. C2C12 cells (ATCC, Manassas, VA) were grown in high glucose

Dulbecco's modified Eagle's medium (DMEM) containing 10% fetal bovine serum and 1% penicillin/streptomycin and incubated in 37^{o}C, 5% CO_2 and 95% humidity (all reagents from Gibco, Carlsbad, CA).

An Alkaline phosphatase (ALP) assay is commonly used to measure the activity of osteoblast-specific protein ALP which corresponds to cells differentiating down an osteogenic lineage. PCL discs adsorbed with 1µg BMP2 (n=3, 1.4x10^{4}cells/cm^{2}) were subjected to the conditions required to create a collagen sponge (30 min at 37^{o}C, 12 hours at -80^{o}C, and 24 hours lyophilization), and then C2C12 cells were seeded on them. The positive control was 1µg BMP2 adsorbed discs that did not go through the collagen sponge production process (n=3). The negative control was cells seeded on PCL discs without the addition of BMP2 (n=3). All of the sterile discs were washed with Hanks Balanced Salt Solution (HBSS), and maintained in DMEM under sterile conditions until cell seeding in a 24 well plate. Discs fit tightly into the well space. The DMEM was then replaced with culture medium, and cells were seeded. After 4 days of static culture, discs were stained using an Alkaline Phosphatase kit (Sigma) and carried out according to manufacturer's directions. Briefly, discs were fixed, dyed with alkaline dye mixture, and counterstained with hematoxylin solution to stain the cell nuclei. A red/pink stain was produced if cells expressed ALP.

VEGF Incorporation and Bioactivity

Human umbilical vein endothelial cells (HUVECs) were a generous gift from Dr. Andrew Putnam's laboratory and were harvested fresh from patients at the University of Michigan Hospital. HUVECs (second passage) were cultured using the EGM-2 Bullet kit (Lonza CC-3162) for 4 days in a T-75cm^{2} flask (BD Falcon) incubated at 37^{o}C, 5% CO_2

and 95% humidity. Cells were detached using 0.05% EDTA Trypsin (Gibco) and quantified with a hemocytometer.

100µg Vascular Endothelial Growth Factor-165 (VEGF-165) produced in the endosperm tissue of barley grain (Novus Biologicals) was dissolved in 1ml sterile diH_20 to 0.1mg/ml. Constructs were placed in an ultra-low bind 24 well plate and 0 or 5µg VEGF in 50µl diH_20 (n=4) was added drop-wise onto each construct such that the collagen sponge was saturated without excess liquid. Constructs were placed in 37^oC for 25 minutes and then 50µl of cell medium was added to the constructs to ensure a wetted surface. After 20 min, $4.0x10^4$ cells were added drop-wise on one side, and the construct was incubated at 37^oC for 2 hours. Next, constructs were flipped over, $4.0x10^4$ cells were added to the other side, and after incubating for another 2 hours 500µl HUVEC medium was added to each well. The negative control was constructs with no cells added. After 72 hours of static culture, 100µl MTS solution (CellTiter96 Aqueous One Solution Promega) was added to each construct. Constructs were then incubated at 37^oC for 4 hours and triplicate aliquots from each specimen were read at 490nm.

A standard curve (cell number vs. absorbance) was created by seeding 0, $2x10^4$, $4x10^4$, $8x10^4$, $16x10^4$ HUVECs per well in standard tissue culture treated polystyrene wells (24 well plate) in triplicate. After 1 hour, 100µl MTS solution was added to each well and triplicate aliquots from each specimen was read at 490nm after 4 hour incubation at 37^oC using a microplate reader.

In Vivo Bioactivity: Subcutaneous Implantation

This study was conducted in compliance with the regulations set forth by the University Committee on Use and Care of Animals at the University of Michigan. Constructs

containing both 65µg/ml BMP2 and 5µg VEGF (BMP2+VEGF group) were implanted subcutaneously in 5-6 week old NIHS bg-nu-xid mice (Harlan Laboratories, Indianapolis, IN). An immunocompromised model was used previously in our laboratory for bone regeneration studies involving cells delivered on the scaffolds. Therefore, we used the same model so that the results from this study could be compared to previous results. To provide a more challenging environment for the scaffold to regenerate bone, scaffolds were implanted in a subcutaneous region rather than intramuscular. The negative control was constructs with 5µg VEGF delivered via collagen sponge and no BMP2 delivered from the PCL (VEGF group). The positive control was a construct with BMP2 adsorbed onto the PCL scaffold and no VEGF in the collagen sponge (BMP2 group) (Table 5.1). Less sample numbers were used for the negative control group because that group was not expected to regenerate bone in an ectopic site and would not be included in the bone regeneration analyses. 50µl HBSS was added to each group prior to implanting to keep the surface wet. A dorsal incision was made and four subcutaneous pockets were created angling toward each limb. Four constructs were implanted in each mouse. Constructs were randomly assigned a quadrant to be implanted in such that at least one sample from each group was implanted in all quadrants. Mice were then euthanized at 4 or 8 weeks post-surgery to assess the regenerated bone. Explanted specimens were placed in Z-Fix (Anatech, Battle Creek, MI) overnight, washed with diH_20 for 24 hours and stored in 70% EtOH until testing. Table 5.1 describes total sample numbers as well as the number of samples used for each specific analysis method (µCT scan, mechanical testing, and histology). Two constructs broke during fabrication in the 4 week BMP2+VEGF and BMP2 groups and they were not included in the study.

	µCT Scan		Mechanical Test		Histology		Total Samples	
	4wk	8wk	4wk	8wk	4wk	8wk	4wk	8wk
BMP2+VEGF	7	8	5	6	2	2	7	8
BMP2	7	8	5	6	2	2	7	8
VEGF	4	4	2	3	2	1	4	4

Table 5.1: Sample Numbers for In Vivo Analyses
Number of explanted specimen used in each in vivo bone regeneration analysis method.

Micro-Computed Tomography (µCT)

Constructs were scanned in water at 16µm voxel resolution with a µCT scanner (Scanco Medical, Wayne, PA). Scan data was generated in calibrated Hounsfield units (HU). Data from Microview software (Parallax Innovations, Ilderton, Canda) were used to analyze bone volume (BV), tissue mineral density (TMD), and tissue mineral content (TMC) using a 1050HU threshold value. The construct region was represented as a cylindrical region of interest (ROI) defined as 6mmD x 3.615mmH. Bone regenerated outside of the construct ROI boundary was defined as external bone growth and bone regenerated inside the construct ROI was defined as internal bone growth.

To determine bone formation in the middle of the construct, the construct was divided into three planar zones as described in Figure 5.5A. Microview was used to calculate the bone volume formed in Zone 2 (6mmD, 1.205mmH ROI). This location was chosen because it is more challenging to regenerate bone inside of the construct. To determine bone penetration into the construct radially, four concentric, cylindrical ring ROIs were defined and were individually analyzed with respect to bone ingrowth (Figure 5.7A). The diameters of the 4 rings were as follows: Ring 1: 6.00-4.84mm, Ring 2: 4.84-3.67mm, Ring 3: 3.67-2.5mm, Ring 4: 2.50-0.00mm. Bone ingrowth for each ring was defined as:

$$Bone\ Ingrowth\ (\%) = \frac{Bone\ Volume}{Available\ Pore\ Volume} * 100$$

Available pore volume was calculated from the porosity of each ring based on the construct's .STL design file.

Compression Mechanical Testing

Specimens were compressed between a fixed bottom and self-aligning upper steel platen at a rate of 1.0 mm/min after application of a 0.5lbf preload. Tests were conducted using an MTS Alliance RT30 electromechanical test frame (MTS Systems Corp, Minneapolis, MN) and a 500N load cell. Data were collected to 20% strain and analyzed using TestWorks4 software (MTS Systems, Corp.). The compressive elastic modulus was defined as the slope of linear region of the stress-strain curve prior to 15% strain. Stiffness was defined as the slope of the load vs. displacement curve. Explanted construct dimensions were measured with calipers prior to testing, and the stress was calculated from the measured construct cross-sectional area.

Histology

Fixed samples from each group were decalcified with RDO (Apex Engineering Products Corporation), processed through a graded ethanol series, embedded in paraffin, and stored at -20^{o}C. Samples were then sectioned using a microtome (MICRON HM 325, Thermo Scientific) and slides were dried overnight at 37^{o}C. Sections were stained with hematoxylin and eosin (H&E) to visualize cells, tissue matrix, blood vessels, and general tissue morphology. Blood vessels were clearly observed in histology sections and manually counted using ImageJ software. Vessels were quantified from sections taken from the same location within constructs.

Statistical Analysis

Data are expressed as mean ± standard deviation of the mean. An analysis of variance

(ANOVA) was used to determine statistical significance between groups. A p-value less than 0.05 ($\alpha<0.05$) was considered statistically significant.

5.4 Results

Protein Bioactivity

BMP2 bioactivity was confirmed with a noticeable red stain on BMP2 adsorbed PCL discs (Figure 5.2A). The negative control of cells seeded on PCL discs (without BMP2) produced little to no stain. Bioactivity of VEGF released from the internal collagen sponge was determined by HUVEC proliferation. Constructs with 5µg VEGF delivered via collagen sponge resulted in significantly increased HUVECs (6.83±0.91 x 10^4 cells) in comparison to the negative control (2.89±0.64 x 10^4 cells) as seen in Figure 5.2B. Based on these results we determined that BMP2 could be exposed to the sponge fabrication process and still be bioactive, and VEGF was bioactive when released from the collagen sponge.

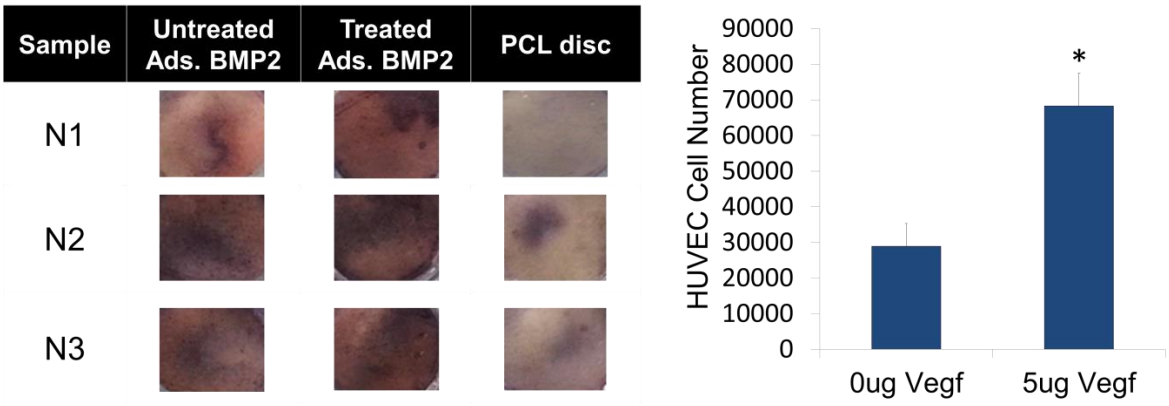

Figure 5.2: BMP2 and VEGF Bioactivity
A) ALP stain of C2C12 cells seeded on PCL/BMP2 discs subjected to the conditions for creating a collagen sponge
B) HUVEC proliferation on constructs with no VEGF and constructs with 5µg VEGF in the collagen sponge. *$p<0.05$

Regenerated Bone Volume

At both 4 and 8 weeks, the BMP2+VEGF and BMP2 groups regenerated significantly more BV than the VEGF group ($p<0.005$, volume < $0.3mm^3$). For the BMP2+VEGF group, there was a significant increase in both total and internal BV from 4 to 8 weeks, which was not the case for the BMP2 group. As a trend, at 4 weeks the BMP2+VEGF group produced less bone ($4.9\pm1.9mm^3$) than BMP2 ($5.7\pm2.4mm^3$), while at 8 weeks the BMP2+VEGF group produced more bone ($10.1\pm3.7mm^3$) than BMP2 ($7.9\pm3.9mm^3$) (Figure 5.3). MicroCT scans illustrated the quantitative results that the BMP2+VEGF and BMP2 groups produced visibly more bone than the negative VEGF control. Both of the BMP+VEGF and BMP2 groups resulted in bone growth into construct pores and followed the surface geometry as seen in Figure 5.4**.**

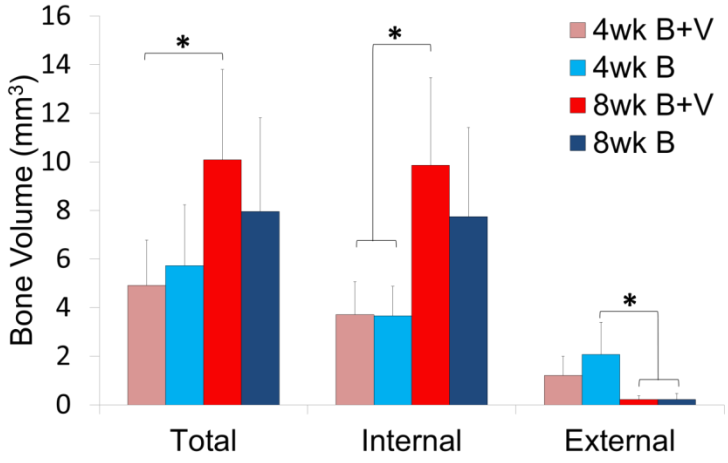

Figure 5.3: Bone Volume Analysis
Regenerated bone volume (at a 1050HU threshold) was calculated for the whole explanted specimen (total), inside the 6mmD, 3.615mmH construct ROI (internal), and outside of the construct ROI (external). There was a significant increase in bone volume from 4 to 8 weeks for BMP2+VEGF but not for BMP2. B=BMP2, B+V=BMP2+VEGF, *$p<0.05$

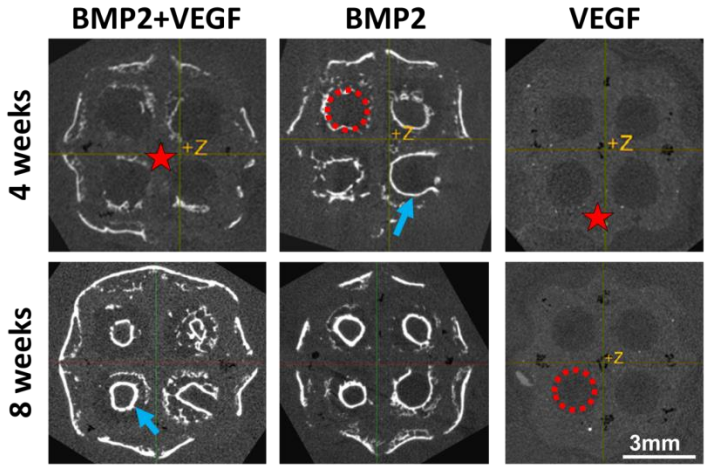

Figure 5.4: Microview Images of Explanted Specimen MicroCT Scans
Bright white areas indicate bone formation (blue arrow) and gray areas indicate the PCL scaffold (red star). Dark areas (red dashed lines) indicate pores. BMP2+VEGF and BMP2 resulted in bone growth into construct pores and followed surface geometry. VEGF produced little to no visible bone.

To further investigate the bone distribution throughout the construct, the BV regenerated in the middle third of the construct was calculated (Figure 5.5A). There was a significant increase in bone volume from 4 to 8 weeks (4.9±1.9mm^3 to 10.1±3.7mm^3) for BMP2+VEGF as seen in Figure 5.5B, whereas, there was no significant increase for the BMP2 group (p=0.67).

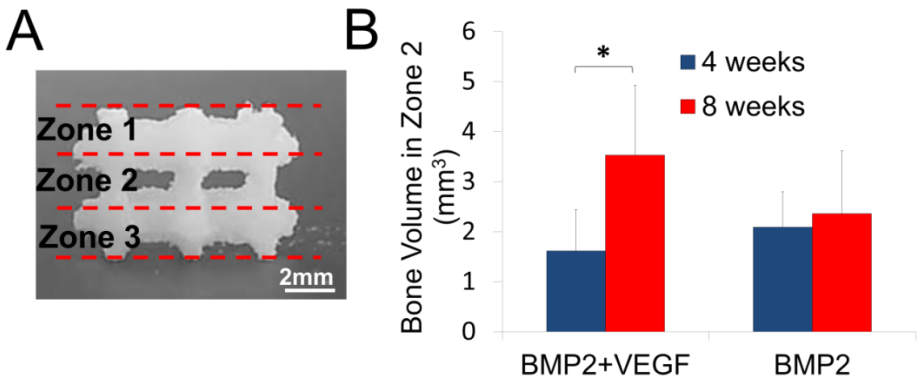

Figure 5.5: Regenerated Bone Volume in the Middle of Construct
A) Side view of the construct which was divided into three Zones.
B) Bone volume (1050HU threshold) regenerated in cylindrical Zone 2 ROI (6mmD, 1.205mmH). BMP2+VEGF had a significant increase in bone formed from 4 to 8 weeks. *p<0.05

TMC, TMD, & Ingrowth

TMC significantly increased over time for BMP2+VEGF from 2.4±1.0mg HA to 5.8±2.1mg HA but not for BMP2 (Figure 5.6A). The TMD was not significantly different between groups at either time point, and both groups showed a significant increase in TMD from 4 to 8 weeks (Figure 5.6B). BMP2+VEGF TMD increased from 493.5±33.7mg HA/cm^3 to 575.4±31.3mg HA/cm^3 and these values are within the range of native mandibular bone [13,31].

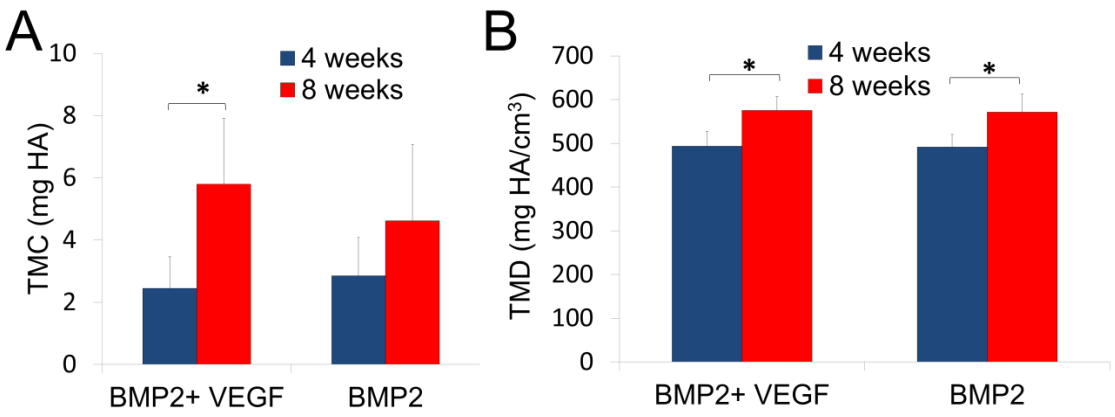

Figure 5.6: Explanted Construct TMC and TMD Analysis
A) Tissue mineral content of the whole construct. There was a significant increase in TMC from 4 to 8 weeks for BMP2+VEGF but not for BMP2.
B) Tissue mineral density of whole construct. BMP2+VEGF and BMP2 showed a significant increase from 4 to 8 weeks. There was no difference between groups at either time point. *$p<0.05$

A ring analysis was conducted to determine the extent of bone ingrowth into the construct radially (Figure 5.7A). Only the BMP2+VEGF group showed a significant increase in ingrowth from 4 to 8 weeks in the outer ring, Ring 1, from 5.2±2.9% to 13.5±7.8% (Figure 5.7B). For both single and dual delivery groups, there was no significant increase in %ingrowth from 4 to 8 weeks in Rings 2-4 (Figure 5.7B).

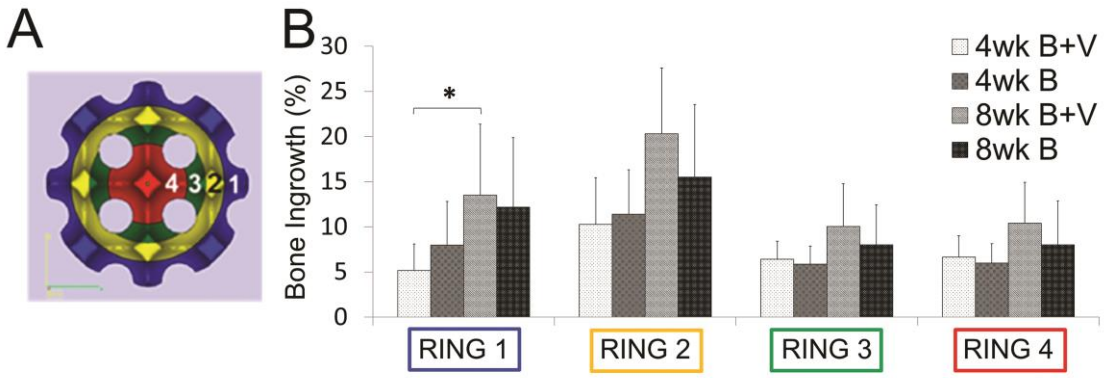

Figure 5.7: Cylindrical Ring Analyses for Bone Ingrowth
A) .STL file image of the Ring ROIs.
B) Percentage bone ingrowth (bone volume divided by available pore space). BMP2+VEGF %ingrowth in Ring 1 significantly increased from 4 to 8 weeks. There was no difference in ingrowth throughout all of the Rings at 4 weeks and at 8 weeks for BMP2 and BMP2+VEGF. B=BMP2, B+V=BMP2+VEGF, *$p<0.05$

Mechanical Testing

The elastic modulus and geometric stiffness of BMP2+VEGF increased significantly from 10.5±2.3MPa to 14.7±2.7MPa and from 81.5±16.35N/mm to 115.2±20.1N/mm, respectively at 4 & 8 weeks (Figure 5.8). There was no significant increase for the BMP2 group. The elastic modulus for the BMP2 group increased from 11.4±1.7MPa to 13.1±3.4MPa and stiffness increased from 91.3±13.3N/mm to 101.5±26.6N/mm.

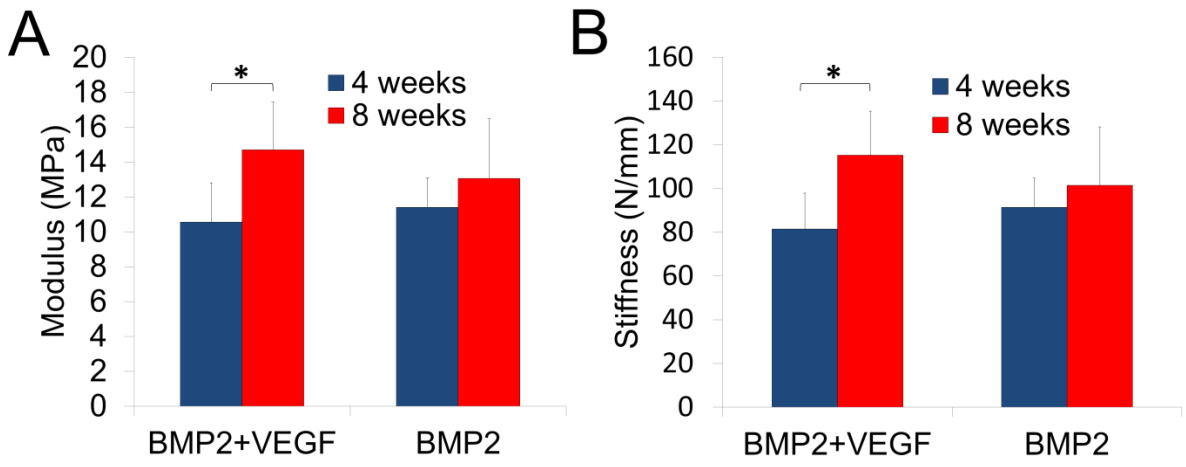

Figure 5.8: Explanted Specimen Compressive Mechanical Testing
A) Elastic modulus defined as the slope of the linear region prior to 15% strain level and normalized to specimen surface area. There was a significant increase in modulus and for BMP2+VEGF from 4 to 8 weeks.
B) Stiffness increased for BMP2+VEGF from 4 to 8 weeks but not for BMP2. *$p<0.05$

Histology

General tissue morphology was observed with H&E staining (Figure 5.9). BMP2+VEGF and BMP2 constructs produced bone with embedded osteocytes and healthy cellular marrow. VEGF constructs consisted mostly of blood vessels and fibrous tissue. The average blood vessel density increased over time for both BMP2+VEGF (29 to 49 vessels) and BMP2 (27 to 41 vessels) groups (Figure 5.10); however, with n=2 there could be more variability.

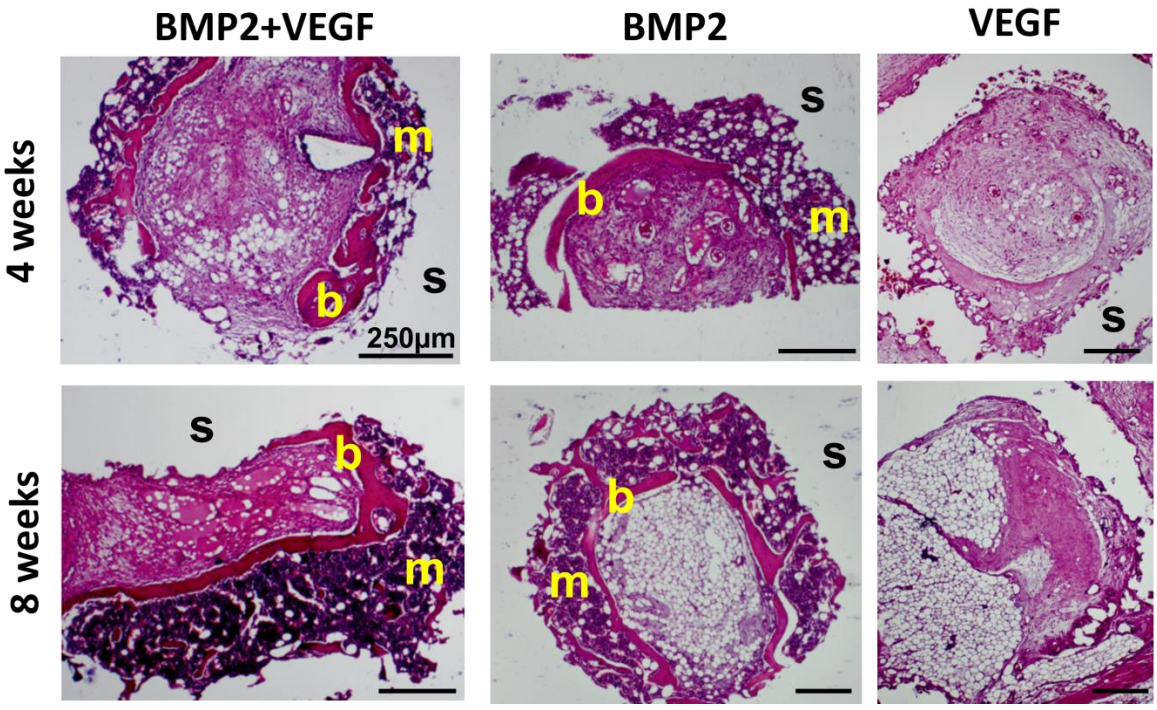

Figure 5.9: H&E Stain of Construct Sections
Bright field images of tissue formed in available construct pore space. Images were taken with a 4x objective. s=scaffold, b=bone, m=marrow. BMP2+VEGF and BMP2 had healthy fatty bone marrow and osteoid formation. VEGF constructs consisted mostly of fibrous tissues

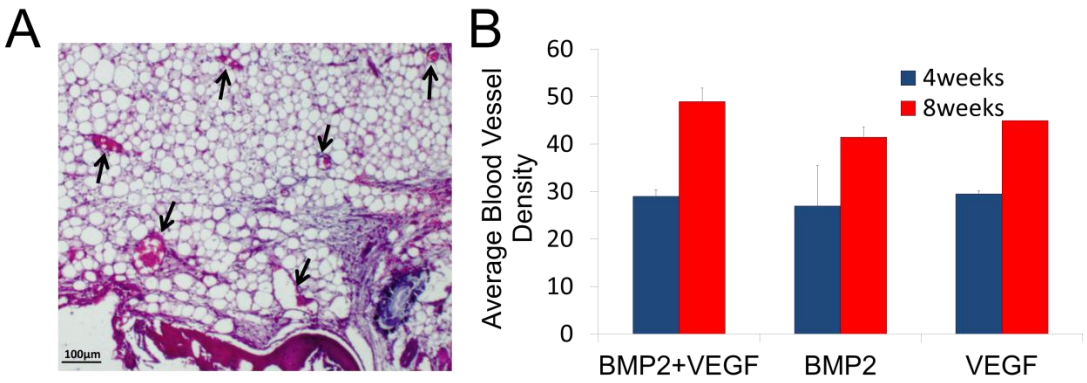

Figure 5.10: Blood Vessel Density
A) Blood vessels seen on H&E stained sections. B) The average number of blood vessels normalized over the construct area (n=2/group; n=1 for 8week VEGF). There was an increase in blood vessel density over time for BMP2+VEGF and BMP2.

5.5 Discussion

Co-culture experiments find that osteoblast-like cells stimulate endothelial cell proliferation by producing VEGF, and endothelial cells stimulate osteoprogenitor cell differentiation by producing BMP2 [32,33]. These results suggest that there is a BMP2/VEGF coupling between osteo/angiogenesis [34]. Simultaneous release studies have resulted in enhanced bone formation [20,28,35]. The release profiles of these studies show a burst release of VEGF in the first 3-5 days and a sustained delivery of BMP2 [24,36]. Some researchers suggest that the synergistic effect of BMP2/VEGF is both time and location dependent (ectopic vs. orthotopic) [23,24,28], the dose ratio utilized is important [37], and a high VEGF dose inhibits osteogenesis [36]. Other studies that delivered both factors via gelatin microparticles in propylene fumerate (PPF) pores and implanted the scaffold in a rat calvarial defect showed no increase in bone formation for the dual delivery group [28].

Studies investigating dual BMP2 and VEGF delivery use various animal models, implant locations, growth factor delivery methods (i.e. microparticle, gelatin), time points, and methods to analyze the regenerated bone. Our study is novel in that utilizing a PCL/collagen sponge construct to deliver VEGF and BMP2 in a subcutaneous implantation site has not been investigated to the best of our knowledge. Furthermore, dual delivery of growth factors for pre-fabricating bone flap applications is advancement to the current process.

In this study, we used a collagen sponge to deliver VEGF with a relatively rapid burst release due to previous studies showing sponges release most of the growth factors or antibiotics within the first few days [38-42]. Adsorbed BMP2 onto PCL was

previously characterized in our laboratory, and the release profile resulted in a relatively small burst release in the first few days followed by a sustained release [19]. Based on this information, we expect VEGF to diffuse out of the sponge relatively faster than the release of adsorbed BMP2. The 65µg/ml BMP2 dose was chosen because in previous studies it regenerated bone *in vivo* [19]. The 5µg VEGF dose was used because lower doses did not cause a significant increase in HUVEC proliferation, *in vitro*.

Using the composite delivery system in this study, we showed that BMP2 released from a PCL scaffold and VEGF released from a collagen sponge are bioactive. After 8 weeks implanted subcutaneously, the BMP2+VEGF group regenerated significantly more BV when compared to its 4 week time point. This increase may be attributed to increased vasculature to the construct site to facilitate cell, nutrition, and waste transportation. Although not significantly different, at 4 weeks BMP2+VEGF resulted in less bone than BMP2, and at 8 weeks, BMP2+VEGF resulted in more bone than BMP2. Overall, dual delivery of BMP2 and VEGF increased the regenerated BV from 4 to 8 weeks, whereas, there was no significant increase with the BMP2 group. The average increase in the regenerated BV for dual delivery was 2.3 times higher than with single BMP2 delivery. As illustrated by µCT images, the spatial distribution of the regenerated bone varied (i.e. more bone in the outer ring and in the middle of the construct). This variability could be attributed to the internal collagen sponge affecting the BMP2 diffusion route upon release from the scaffold.

In addition to a significant increase in BV over time for the dual delivery group, there was also a significant increase in elastic modulus, stiffness, and TMC from 4 to 8 weeks. Mechanical integrity is crucial for a craniofacial bone flap to support load while

integrating into the defect site and regenerating more bone. When the construct was divided into concentric rings, we found that when VEGF was delivered with BMP2, the bone ingrowth in the outer part of the construct increased from 4 to 8 weeks. BMP2 and BMP2+VEGF both had a significant increase in TMD over time and both groups regenerated bone in the range of native mandibular bone [13,31]. Investigating longer *in vivo* time points in a future study may result in significant difference between BMP2+VEGF and BMP2 regenerated BV.

Finally, we showed that BMP2+VEGF increased blood vessels density when compared to BMP2 alone. However, due to the small sample sizes, the results were not statistically significant. Since the constructs were implanted without added cells in an ectopic location, it is crucial for the host cells to migrate to the construct and interact with the released BMP2 to form bone tissue. The increased vasculature with the dual factor group could explain the increased bone regeneration rate and bone volume at 8 weeks because vessels would provide more nutrients and transportation for cells migrating to the construct. Future studies should look at an earlier time point to quantify neovascularization. Overall, dual factor delivery shows promise for increasing the amount of regenerated bone volume for pre-fabricated flap applications.

5.6 Conclusion

Tissue engineering a bone flap by using the patient's body as a bioreactor is a potential alternative to using autografts, allografts, and synthetic bone grafts. Delivering two growth factors is advancement in the pre-fabrication process, and this study concluded that dual delivery of BMP2 and VEGF from a PCL/collagen sponge composite construct increased the regenerated bone volume from 4 to 8 weeks, whereas, BMP2

delivery alone did not. Dual factor delivery also resulted in an increased elastic modulus, TMD, and healthy bone marrow. Future studies should investigate the VEGF to BMP2 dose ratio and develop another dual growth factor delivery system in hopes to further increase the regenerated bone volume while maintaining clinical applicability.

Acknowledgements: This research was funded by the Tissue Engineering at Michigan trainee grant and NIH R21 DE 022439. We would like to thank Manasa Amancherla and Jane Modes for their assistance with data analysis and histology.

Author Disclosure Statement: Scott Hollister was a co-founder of Tissue Regeneration Systems (TRS), but is no longer affiliated with TRS.

5.7 References

[1] Heliotis M, Lavery KM, Ripamonti U, Tsiridis E, di Silvio L. Transformation of a prefabricated hydroxyapatite/osteogenic protein-1 implant into a vascularised pedicled bone flap in the human chest. Int J Oral Maxillofac Surg 2006 Mar;35(3):265-269.

[2] Warnke PH, Springer IN, Wiltfang J, Acil Y, Eufinger H, Wehmoller M, et al. Growth and transplantation of a custom vascularised bone graft in a man. Lancet 2004 Aug 28-Sep 3;364(9436):766-770.

[3] Warnke PH, Wiltfang J, Springer I, Acil Y, Bolte H, Kosmahl M, et al. Man as living bioreactor: fate of an exogenously prepared customized tissue-engineered mandible. Biomaterials 2006 Jun;27(17):3163-3167.

[4] Alam MI, Asahina I, Seto I, Oda M, Enomoto S. Prefabrication of vascularized bone flap induced by recombinant human bone morphogenetic protein 2 (rhBMP-2). Int J Oral Maxillofac Surg 2003 Oct;32(5):508-514.

[5] Becker ST, Bolte H, Krapf O, Seitz H, Douglas T, Sivananthan S, et al. Endocultivation: 3D printed customized porous scaffolds for heterotopic bone induction. Oral Oncol 2009 Nov;45(11):e181-8.

[6] Terheyden H, Jepsen S, Rueger DR. Mandibular reconstruction in miniature pigs with prefabricated vascularized bone grafts using recombinant human osteogenic protein-1: a preliminary study. Int J Oral Maxillofac Surg 1999 Dec;28(6):461-463.

[7] Terheyden H, Knak C, Jepsen S, Palmie S, Rueger DR. Mandibular reconstruction with a prefabricated vascularized bone graft using recombinant human osteogenic protein-1: an experimental study in miniature pigs. Part I: Prefabrication. Int J Oral Maxillofac Surg 2001 Oct;30(5):373-379.

[8] Terheyden H, Menzel C, Wang H, Springer IN, Rueger DR, Acil Y. Prefabrication of vascularized bone grafts using recombinant human osteogenic protein-1--part 3: dosage of rhOP-1, the use of external and internal scaffolds. Int J Oral Maxillofac Surg 2004 Mar;33(2):164-172.

[9] Warnke PH, Springer IN, Acil Y, Julga G, Wiltfang J, Ludwig K, et al. The mechanical integrity of in vivo engineered heterotopic bone. Biomaterials 2006 Mar;27(7):1081-1087.

[10] Hollister SJ, Murphy WL. Scaffold translation: barriers between concept and clinic. Tissue Eng Part B Rev 2011 Dec;17(6):459-474.

[11] Fitzsimmons J. **510(k) Premarket Notification, Cover, Burr Hole, TRS CRANIAL BONE VOID FILLER**. 2014; Available at:

http://www.accessdata.fda.gov/scripts/cdrh/cfdocs/cfpmn/pmn.cfm?ID=K123633, 2014.

[12] Yeo A. **510(k) Premarket Notification, Methyl Methacrylate For Cranioplasty, OSTEOPORE PCL SCAFFOLD**. 2014; Available at: http://www.accessdata.fda.gov/scripts/cdrh/cfdocs/cfpmn/pmn.cfm?ID=K051093, 2014.

[13] Williams JM, Adewunmi A, Schek RM, Flanagan CL, Krebsbach PH, Feinberg SE, et al. Bone tissue engineering using polycaprolactone scaffolds fabricated via selective laser sintering. Biomaterials 2005 Aug;26(23):4817-4827.

[14] Murakami N, Saito N, Horiuchi H, Okada T, Nozaki K, Takaoka K. Repair of segmental defects in rabbit humeri with titanium fiber mesh cylinders containing recombinant human bone morphogenetic protein-2 (rhBMP-2) and a synthetic polymer. J Biomed Mater Res 2002 Nov;62(2):169-174.

[15] Kim TH, Oh SH, Na SY, Chun SY, Lee JH. Effect of biological/physical stimulation on guided bone regeneration through asymmetrically porous membrane. J Biomed Mater Res A 2012 Jun;100(6):1512-1520.

[16] Jeon O, Song SJ, Kang SW, Putnam AJ, Kim BS. Enhancement of ectopic bone formation by bone morphogenetic protein-2 released from a heparin-conjugated poly(L-lactic-co-glycolic acid) scaffold. Biomaterials 2007 Jun;28(17):2763-2771.

[17] Liu HW, Chen CH, Tsai CL, Hsiue GH. Targeted delivery system for juxtacrine signaling growth factor based on rhBMP-2-mediated carrier-protein conjugation. Bone 2006 Oct;39(4):825-836.

[18] Park YJ, Kim KH, Lee JY, Ku Y, Lee SJ, Min BM, et al. Immobilization of bone morphogenetic protein-2 on a nanofibrous chitosan membrane for enhanced guided bone regeneration. Biotechnol Appl Biochem 2006 Jan;43(Pt 1):17-24.

[19] Patel JJ, Flanagan CL, Hollister S. Bone Morphogenetic Protein-2 Adsorption onto Poly-E-caprolactone Better Preserves Bioactivity in vitro and Produces More Bone in vivo than Conjugation under Clinically Relevant Loading Scenarios. Tissue Eng Part C Methods 2014 Oct 25.

[20] Huang YC, Kaigler D, Rice KG, Krebsbach PH, Mooney DJ. Combined angiogenic and osteogenic factor delivery enhances bone marrow stromal cell-driven bone regeneration. J Bone Miner Res 2005 May;20(5):848-857.

[21] Hankenson KD, Dishowitz M, Gray C, Schenker M. Angiogenesis in bone regeneration. Injury 2011 Jun;42(6):556-561.

[22] Yang YQ, Tan YY, Wong R, Wenden A, Zhang LK, Rabie AB. The role of vascular endothelial growth factor in ossification. Int J Oral Sci 2012 Jun;4(2):64-68.

[23] Geuze RE, Theyse LF, Kempen DH, Hazewinkel HA, Kraak HY, Oner FC, et al. A differential effect of bone morphogenetic protein-2 and vascular endothelial growth factor release timing on osteogenesis at ectopic and orthotopic sites in a large-animal model. Tissue Eng Part A 2012 Oct;18(19-20):2052-2062.

[24] Kempen DH, Lu L, Heijink A, Hefferan TE, Creemers LB, Maran A, et al. Effect of local sequential VEGF and BMP-2 delivery on ectopic and orthotopic bone regeneration. Biomaterials 2009 May;30(14):2816-2825.

[25] Kanczler JM, Ginty PJ, White L, Clarke NM, Howdle SM, Shakesheff KM, et al. The effect of the delivery of vascular endothelial growth factor and bone morphogenic protein-2 to osteoprogenitor cell populations on bone formation. Biomaterials 2010 Feb;31(6):1242-1250.

[26] Peng H, Usas A, Olshanski A, Ho AM, Gearhart B, Cooper GM, et al. VEGF improves, whereas sFlt1 inhibits, BMP2-induced bone formation and bone healing through modulation of angiogenesis. J Bone Miner Res 2005 Nov;20(11):2017-2027.

[27] Kakudo N, Kusumoto K, Wang YB, Iguchi Y, Ogawa Y. Immunolocalization of vascular endothelial growth factor on intramuscular ectopic osteoinduction by bone morphogenetic protein-2. Life Sci 2006 Oct 4;79(19):1847-1855.

[28] Patel ZS, Young S, Tabata Y, Jansen JA, Wong ME, Mikos AG. Dual delivery of an angiogenic and an osteogenic growth factor for bone regeneration in a critical size defect model. Bone 2008 Nov;43(5):931-940.

[29] Katagiri T, Yamaguchi A, Komaki M, Abe E, Takahashi N, Ikeda T, et al. Bone morphogenetic protein-2 converts the differentiation pathway of C2C12 myoblasts into the osteoblast lineage. J Cell Biol 1994 Dec;127(6 Pt 1):1755-1766.

[30] Jiao X, Billings PC, O'Connell MP, Kaplan FS, Shore EM, Glaser DL. Heparan sulfate proteoglycans (HSPGs) modulate BMP2 osteogenic bioactivity in C2C12 cells. J Biol Chem 2007 Jan 12;282(2):1080-1086.

[31] Kontogiorgos E, Elsalanty ME, Zapata U, Zakhary I, Nagy WW, Dechow PC, et al. Three-dimensional evaluation of mandibular bone regenerated by bone transport distraction osteogenesis. Calcif Tissue Int 2011 Jul;89(1):43-52.

[32] Kaigler D, Krebsbach PH, West ER, Horger K, Huang YC, Mooney DJ. Endothelial cell modulation of bone marrow stromal cell osteogenic potential. FASEB J 2005 Apr;19(6):665-667.

[33] Wang DS, Miura M, Demura H, Sato K. Anabolic effects of 1,25-dihydroxyvitamin D3 on osteoblasts are enhanced by vascular endothelial growth factor produced by osteoblasts and by growth factors produced by endothelial cells. Endocrinology 1997 Jul;138(7):2953-2962.

[34] Peng H, Wright V, Usas A, Gearhart B, Shen HC, Cummins J, et al. Synergistic enhancement of bone formation and healing by stem cell-expressed VEGF and bone morphogenetic protein-4. J Clin Invest 2002 Sep;110(6):751-759.

[35] Peng H, Usas A, Olshanski A, Ho AM, Gearhart B, Cooper GM, et al. VEGF improves, whereas sFlt1 inhibits, BMP2-induced bone formation and bone healing through modulation of angiogenesis. J Bone Miner Res 2005 Nov;20(11):2017-2027.

[36] Shah NJ, Macdonald ML, Beben YM, Padera RF, Samuel RE, Hammond PT. Tunable dual growth factor delivery from polyelectrolyte multilayer films. Biomaterials 2011 Sep;32(26):6183-6193.

[37] Young S, Patel ZS, Kretlow JD, Murphy MB, Mountziaris PM, Baggett LS, et al. Dose effect of dual delivery of vascular endothelial growth factor and bone morphogenetic protein-2 on bone regeneration in a rat critical-size defect model. Tissue Eng Part A 2009 Sep;15(9):2347-2362.

[38] Wang AY, Leong S, Liang YC, Huang RC, Chen CS, Yu SM. Immobilization of growth factors on collagen scaffolds mediated by polyanionic collagen mimetic peptides and its effect on endothelial cell morphogenesis. Biomacromolecules 2008 Oct;9(10):2929-2936.

[39] Uludag H, Gao T, Porter TJ, Friess W, Wozney JM. Delivery systems for BMPs: factors contributing to protein retention at an application site. J Bone Joint Surg Am 2001;83-A Suppl 1(Pt 2):S128-35.

[40] Seeherman H, Wozney JM. Delivery of bone morphogenetic proteins for orthopedic tissue regeneration. Cytokine Growth Factor Rev 2005 Jun;16(3):329-345.

[41] Mullen LM, Best SM, Brooks RA, Ghose S, Gwynne JH, Wardale J, et al. Binding and release characteristics of insulin-like growth factor-1 from a collagen-glycosaminoglycan scaffold. Tissue Eng Part C Methods 2010 Dec;16(6):1439-1448.

[42] Sorensen TS, Sorensen AI, Merser S. Rapid release of gentamicin from collagen sponge. In vitro comparison with plastic beads. Acta Orthop Scand 1990 Aug;61(4):353-356.

CHAPTER 6

DUAL DELIVERY OF BMP2 AND VEGF FROM A MODULAR POLYCAPROLACTONE SCAFFOLD FOR THE TREATMENT OF LARGE BONE DEFECTS

Joshua Deuel, Colleen Flanagan, Paul Krebsbach, Sean Edwards, and Scott Hollister assisted with the preparation of this chapter

Will be submitted after patent approval

6.1 Abstract

Background: An alternative to using autografts to fix large craniofacial bone defects is to tissue engineer a replacement that is patient specific and composed of bone and blood. Previously in this laboratory we delivered absorbed bone morphogenetic protein-2 (BMP2) from a poly-Ɛ-caprolactone (PCL) scaffold and found that bone regenerated in an ectopic location. A large defect requires a large volume of bone and vasculature to provide nutrients and transportation for cells migrating to the scaffold. Vascular endothelial growth factor (VEGF) is a potent angiogenic protein. In this study we investigate dual delivery of adsorbed VEGF and BMP2 from the outer and inner portions of a modular scaffold with the goal of increasing bone regeneration and further optimizing the pre-fabrication process.

Methods: The inner porous PCL module was exposed to 65µg/ml BMP2 and the outer porous PCL module was exposed to either 5µg/ml VEGF (B+5V) or

10µg/ml VEGF (B+10V). The modules were exposed to the protein solution for 1 hour and then assembled. Protein binding was quantified with ELISA, Nanoorange, and Fluoroprofile assays. Adsorbed VEGF bioactivity was determine by endothelial cell proliferation. B+5V, B+10V, BMP2, and VEGF groups were implanted subcutaneously in mice for 4 & 8 weeks. Bone distribution and histology were then assessed.

Results: 8.6±1.4µg BMP2 attached to the inner module and 0.0316±0.0053µg BMP2 was released after 21 days. 3.1±0.9µg and 8.8±0.9µg VEGF bound to outer modules exposed to 5µg/ml or 10µg/ml VEGF, respectively. There was increased endothelial cell proliferation on VEGF adsorbed PCL indicating protein bioactivity. B+10V had a significant increase in bone volume and ingrowth from 4 to 8 weeks (2.7±1.2 mm^3 to 4.6±1.8mm^3 and 1.8±0.8% to 3.16±1.2%, respectively). No increase was seen with B+5V or BMP2. The TMD for all experimental groups were in the range of native bone. Histology shows healthy marrow, osteoid, and blood vessel formation.

Conclusion*:* VEGF delivered locally with BMP2 increased the bone regenerated from 4 to 8 weeks. B+10V also produced the most bone volume after 8 weeks indicating that dual delivery could be a potential method to grow more bone for pre-fabrication applications.

Keywords: BMP2, VEGF, Polycaprolactone

6.2 Introduction

Large craniofacial bone defects are currently treated with an autograft which involves transferring a bone from one area in the patient's body to the defect site as a bony and vascularized flap. Autografts have the drawbacks of donor site morbidity and poorly matched defect geometry. Synthetic scaffolds modified with cells and growth factors can overcome these drawbacks; however, these scaffolds do not integrate as well into the host bone if implanted directly [1]. If the scaffold is placed directly into a large defect site, the surrounding vasculature is limited in its ability to grow into the scaffold, and the bone regenerating at the graft's core can turn necrotic without a sufficient blood supply. To overcome this challenge, methods to tissue engineer a bone flap are under investigation so that the scaffold is partially remodeled when implanted into the defect site [1]. Tissue regeneration can occur *in vitro* in an external bioreactor (which requires an optimal environment and nutritional flow throughout the scaffold), or the flap can be regenerated *in vivo*.

Pre-fabricating a bone flap *in vivo* involves implanting a patient-specific biomaterial scaffold with associated biologics in a patient's latissimus dorsi and then transplanting it to the defect site after a maturation period as a vascularized bone flap [2-5]. A few animal [4,6-10] and human [2,3,11] studies have been completed but not in the United States to the best of our knowledge. Some of these studies used titanium mesh trays filled with BioOs/hydroxyapetite blocks to deliver bone morphogenetic protein-7. These implants had a crude geometry with the potential to fracture [2,7,8]. Poly-Ɛ-caprolactone (PCL) is a biocompatible and biodegradable material that can be 3D printed into patient specific complex geometries using selective laser sintering (SLS)

manufacturing technique [12,13]. PCL is Food and Drug Administration (FDA) approved for cranioplasty applications [14,15] and has mechanical properties that are ideal for bone tissue engineering. Its slow degradation rate allows for bone regeneration while supporting load. Previously in our laboratory, PCL was integrated with osteogenic agent bone morphogenetic protein-2 (BMP2) under clinically relevant conditions (1 hour protein exposure at room temperature) to increase PCL's osteoinductive properties, and the scaffold produced bone when subcutaneously implanted in mice [16].

An ideal flap requires a large bone volume as well as a rich vascular network to provide the regenerating bone with the necessary nutrients and to remove wastes. Since the scaffold is implanted without cells, the scaffold relies on recruited host cells to interact with the released BMP2. Vascular endothelial growth factor (VEGF) is a potent angiogenic protein that is a key mediator in angiogenesis by playing a role in early fracture repair [17-19]. By delivering VEGF with the BMP2, we hope to increase vascularization and cellular access to the released BMP2. Studies that have delivered VEGF with BMP2 have conflicting results regarding if bone volume increases [20-22] or does not change with the added VEGF delivery [23-25]. These studies vary in animal model, implant location, time points, protein dose, and delivery vehicle. Additionally, the scaffold fabrication and protein incorporation methods utilized are complex and not easily conducted in an operating room (OR) environment. Attaching growth factors outside of the OR room will increase regulatory challenges significantly due to unknown effects of sterilization on growth factor bioactivity. There is a lack of knowledge as to the quality of ectopic bone regenerated when BMP2 and VEGF are co-delivered via adsorption from PCL. To make the prefabrication process more clinically applicable (1

hour protein exposure to the scaffold at room temperature), in this study we investigated the effect of delivering adsorbed BMP2 and VEGF from the inner and outer portions of a modular PCL construct, respectively, and assessed the regenerated bone distribution and histology.

6.3 Methods & Materials

PCL Scaffold Fabrication

Solid PCL discs (6mmD, 2mmH), 44% porous inner modules (3.5mm sides, 4.3mmH, 106mm^{2}SA), and 79% porous outer PCL modules (7mm sides, 4.3mmH, 357mm^{2}SA) were fabricated using a Formiga P100 SLS machine (EOS, Inc., Novi, MI) (Figure 6.1). Combined inner and outer modular portions resulted in a 70% porous scaffold. PCL powder (43-50kDa Polysciences, Warrington, PA) and 4% hydroxyapatite (Plasma Biotal Limited, UK) were mixed. After manufacturing, the scaffolds were air blasted, sonicated in 70% ethanol (EtOH) for 30 minutes to remove non-sintered powder, sterilized in 0.22µm filtered 70% EtOH for 30 minutes, and air-dried under sterile conditions at room temperature.

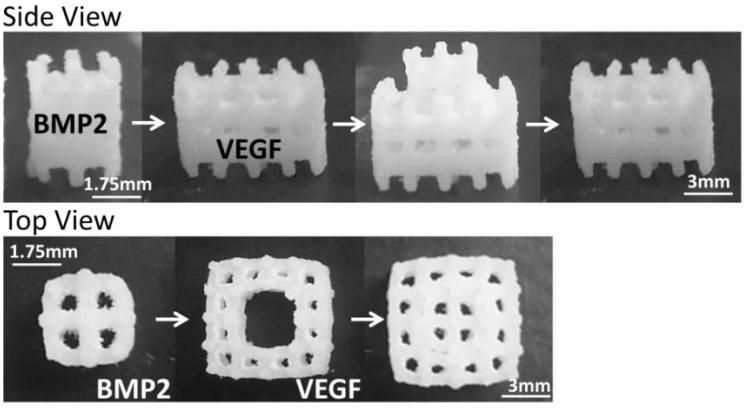

Figure 6.1: Modular Scaffold Assembly
65µg/ml BMP2 was adsorbed onto the inner scaffold module and either 5µg/ml or 10µg/ml VEGF was adsorbed onto the outer scaffold module. The scaffolds were then manually assembled.

BMP2 Binding and Quantification

BMP2 was adsorbed onto the inner module as previously described [16]. Briefly, 1mg lyophilized BMP2 (Creative Biomart, Shirley, NY) was dissolved in 1ml 20mM acetic acid and diluted in a BuPH (#28372, Pierce) buffer containing 0.1M EDTA (pH 7.0) to 65µg/ml. An *e-coli* derived BMP2 ELISA (Peprotech) kit was used to quantify the protein content in the 65µg/ml BMP2 solution (average detected concentration was 28.12±4.6µg/ml), and the binding studies were normalized to this value. Briefly, the scaffolds were washed in BuPH buffer (pH 7.2) followed by BuPH+0.1M EDTA buffer to wet the surface and then exposed to 1ml 65µg/ml BMP2 for 1 hour at 23^{o}C. Finally, they were washed in distilled water (di$H_2$0) to remove loosely bound protein. After the protein exposure, the remaining solution and washes were collected, 1% Bovine Serum Albumin (BSA) was added to result in 0.1% BSA content and samples were stored at -80^{o}C until ELISA analysis for BMP2 content.

$$BMP2\ Bound\ (\mu g) = (BMP2\ in\ original\ solution\ detected\ by\ ELISA) - (BMP2\ in\ remaining\ solution + BMP2\ in\ washes)$$

The ELISA was carried out according to the manufacturer's directions. Samples were read at 405nm and 650nm using a microplate reader.

VEGF Binding and Quantification

100µg VEGF-165 (Novus Biologicals, Littleton, CO) produced from the endosperm tissue of barley grain was dissolved in 1ml sterile di$H_2$0 and then further diluted to either 5µg/ml or 10µg/ml in di$H_2$0. The outer modules were placed in ultra low bind 24 well plates (Costar), washed in di$H_2$0 and exposed to 1ml VEGF solution for 1 hour at 23^{o}C,

and washed again in diH_20. The remaining solution and washes were collected and stored for protein analysis using NanoOrange and Fluoroprofile. These highly sensitive protein assays can detect low protein concentrations and were conducted according to the manufacturers' directions. Briefly, a VEGF standard curve was created from 5µg/ml to 0µg/ml and unknown samples were mixed with either 2x NanoOrange reagent (diluted in 3x diluent) or with Fluoroprofile reagent and buffer. A volume of working solution (NanoOrange or Fluoroprofile reagent) was added to the same volume of the unknown concentration sample. Samples were read in triplicates in a 96 well plate with a fluorometric reader (NanoOrange: 485 excitation, 590nm emission; Fluoroprofle: 520nm excitation, 620 emission).

$$VEGF\ Bound\ (\mu g) = (VEGF\ in\ original\ solution) - (VEGF\ in\ remaining\ solution + VEGF\ in\ washes)$$

BMP2 Release

BMP2 adsorbed inner scaffolds were assembled with a PCL outer scaffold (without VEGF), submerged in Dulbeccos Phosphate Buffered Saline (DPBS), and incubated at 37^{o}C, 5% CO_2, and 95% humidity. The supernatant was collected and replenished 1, 2, 3, 5, 7, 14, 21 days after the initial exposure. Supernatants with a final 0.1% BSA content were stored at -80^{o}C until BMP2 quantification with an ELISA.

Growth Factor Bioactivity

Previous studies in the laboratory show that BMP2 adsorbed onto PCL is bioactive as seen by C2C12 cell alkaline phosphatase (ALP) production [16]. Pre-myoblastic C2C12 cells differentiate down an osteoblastic lineage when exposed to active BMP2, and this is

a well-established model for determining BMP2 bioactivity. Endothelial cell proliferation is widely used as a measure of VEGF bioactivity. Human umbilical vein endothelial cells (HUVECs) were a generous gift from Dr. Andrew Putnam's laboratory and were harvested fresh from patients at the University of Michigan Hospital. HUVECs at second passage were grown in an EGM-2 Bullet kit (Lonza CC-3162) for 4 days at 37^{o}C, 5% CO_2 and 95% humidity. Cells were trypsinized using 0.05% Trypsin with EDTA (Gibco) and quantified with an automatic cell counter MoxieZ (Orflo,Ketchum, ID). Proliferation studies were completed on a disc geometry with a flat surface to understand adsorbed VEGF bioactivity prior to using a complex geometry used for *in vivo* studies.

1ml EGM media was added to PCL discs that had 5µg/ml VEGF adsorbed (n=4) and then $2.5x10^4$ HUVECs were added to each disc (11,765 cells/cm^2). The negative control was cells seeded on PCL discs without any VEGF exposure. After 72hrs of static culture to allow for attachment and growth, the medium was replaced with 500µl fresh EGM Medium and 100µl MTS solution (CellTiter96 Aqueous One Solution Promega) was added to each sample. PCL discs were incubated with the reagent at 37^{o}C for 4 hours after which triplicates were read at 490nm. Cells were also seeded at 0, $2x10^4$, $4x10^4$, $8x10^4$, $16x10^4$ cells/well in triplicate to create a standard curve (cell number vs. absorbance reading). After 1 hour, 100µl MTS solution was added to the 500µl EGM medium in each well and absorbance was read at 490nm.

In Vivo Bioactivity: Subcutaneous Implantation

65µg/ml BMP2 inner scaffold modules were assembled with 5µg/ml VEGF (B+5V) or 10µg/ml VEGF (B+10V) outer scaffold modules, and the scaffolds were implanted subcutaneously in 5-6 week old female C57BL/6N mice. The negative control was

5µg/ml VEGF outer modules combined with inner modules that had no adsorbed BMP2. The positive control was 65µg/ml BMP2 inner modules combined with outer modules that had no adsorbed VEGF. Scaffolds were randomly assigned a side to be implanted such that at least one sample from each group was implanted on each left and ride side. The dorsal hair was shaved, an incision was made, and two pockets were created angling toward the left and right front paws. One assembled scaffold was implanted into each soft tissue pocket. Mice were sacrificed at 4 and 8 weeks post-surgery, and the scaffolds were explanted for bone growth analysis. The specimens were placed in Z-Fix (Anatech, Battle Creek, MI) overnight, washed in diH_20 for 24 hours, and stored in 70% EtOH until testing. Table 6.1 describes the total sample numbers and the number of samples used for microCT and histology analysis methods. This study was conducted in compliance with the regulations set forth by the University Committee on Use and Care of Animals at the University of Michigan. N=6 samples from each group were used in mechanical testing; however, the results of this test were inconclusive because the machine was not sensitive enough to detect changes in scaffold mechanical properties due to low regenerated bone volume. Four samples were used for the negative control because no bone was expected to regenerate in an ectopic site and these samples would not be utilized in bone volume analyses.

Group	µCT Scan		Histology		Total Samples	
Time Point	4wk	8wk	4wk	8wk	4wk	8wk
BMP2+5µg/ml VEGF	9	8	3	2	9	8
BMP2+10µg/ml VEGF	9	8	3	2	9	8
BMP2	8	9	2	2	8	9
VEGF	4	5	1	2	4	5

Table 6.1: Sample Numbers for *In Vivo* Analyses
Number of samples used in explanted specimen analysis methods

Micro-Computed Tomography (MicroCT)

Fixed scaffolds were scanned in water with a high-resolution (16 μm) microCT scanner (Scanco Medical, Wayne, PA), and scans were calibrated to Hounsfield units (HU). Bone volume (BV) was defined at a threshold of 1050 HU and calculated using Microview software (Parallax Innovations). Tissue mineral content (TMC) and tissue mineral density (TMD) data were determined by using exported grayscale data. The total scaffold region was represented as a cubical region of interest (ROI) defined as 7mm x 7mm x 4.3mm height. Bone formed inside of the inner module ROI (3.5mmx 3.5mm x 4.3mmH) was quantified and defined as "inner" module bone volume, and the ROI for bone regenerated in the outer module was defined as the inner module BV subtracted from the total BV. We chose these ROI's because the BMP2 was coated on the inner module and bone grown outside of this area would be of interest. To determine the quantity of bone regenerated in the central region of the inner module pores instead of on the PCL scaffold surface, a 0.6750mmD, 4.3mmH cylinder ROI was created in all 4 vertical pores, and the total BV in the inner module pores was calculated. Bone ingrowth was defined as the ROI BV divided by the available pore volume in that ROI. The available pore volume was calculated from the porosity of each module based on a microCT scan of a PCL scaffold scanned in air.

Histology

Fixed samples from each group were demineralized with RDO Rapid Decalcifier (Apex Engineering Products), processed, embedded in paraffin, and stored at -20^{o}C. Samples were then sectioned at 7μm thickness using a MICRON HM 325 (Thermo Scientific, Waltham, WA) and slides were dried overnight at 37^{o}C. Sections were stained with

hematoxylin and eosin (H&E) to visualize cells, tissue matrix, blood vessels, and general tissue morphology. Sections were imaged with a 4x objective.

Statistical Analysis

Data are expressed as mean ± standard deviation of the mean. An analysis of variance (ANOVA) was used to determine statistical significance between groups. A p-value less than 0.05 ($\alpha<0.05$) was considered statistically significant on a 95% confidence interval.

6.4 Results

Protein Binding & Release Kinetics

8.6±1.4µg BMP2 (0.081±0.013µg/mm^2, 22%) attached to the inner module. After 1 hour exposure to 5µg/ml or 10ug/ml VEGF, 3.1±0.9µg (0.0086±0.0025µg/mm^2, 62%) and 8.8±0.9µg (0.0246±0.0026µg/mm^2, 88%) VEGF bound to the outer module, respectively (Figure 6.2A). There was significantly less VEGF bound to the 5µg/ml VEGF group when compared to 10µg/ml VEGF group (p=0.00076). There was no significant difference in the protein quantity bound between BMP2 and 10µg/ml VEGF. BMP2 release kinetics show a trend of a relatively small burst release in the first two days (0.0233±0.007µg) followed by a sustained release (Figure 6.2B). After 21 days, 0.0316±0.005µg BMP2 (<1%) was released (Figure 6.2C).

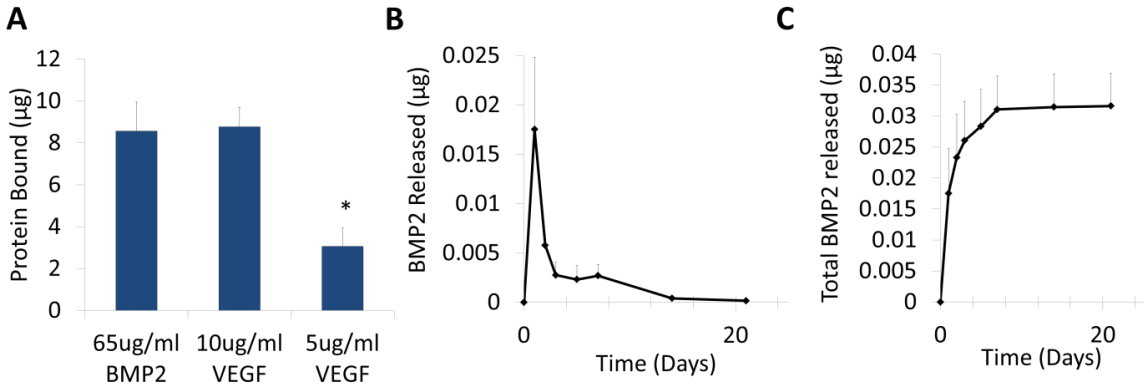

Figure 6.2: Protein Binding and Release Kinetics

A) Protein bound to the inner and outer scaffold modules after 1 hour exposure was quantified. 5µg/ml VEGF bound significantly less protein than the 10µg/ml VEGF and 65µg/ml BMP2 groups.
B) Adsorbed BMP2 has a small burst release trend in the first two days followed by a sustained release.
C) Cumulative release shows 0.032±0.005µg BMP2 was delivered after 21 days (n=3).

VEGF Bioactivity

Increased HUVEC proliferation was detected for cells seeded on 5µg/ml VEGF adsorbed PCL discs when compared to the negative control. Cells seeded on PCL discs with or without any adsorbed VEGF resulted in $1.77\pm0.17x10^4$ cells and $1.4\pm0.09x10^4$ cells after 3 days of static culture, respectively (Figure 6.3).

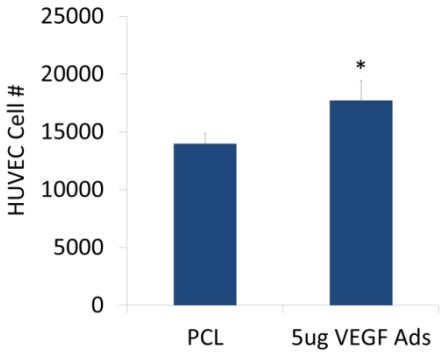

Figure 6.3: Adsorbed VEGF Bioactivity
HUVECs seeded on PCL discs with adsorbed 5µg/ml VEGF resulted in significantly increased proliferation in comparison to cells on PCL discs with no VEGF exposure. (n=4,*p<0.05)

MicroCT Analysis

Figure 6.4A shows representative microCT images of the explanted specimen. Bone regeneration was localized to the inner module for all of the groups except for the VEGF alone group that did not form any visible bone. The bone observed in the microCT scans was quantified using Microview (Figure 6.4B) at a 1050 HU threshold. The B+10V group had a significant increase in BV from 4 to 8 weeks in the total scaffold (2.7±1.2 to

4.6±1.8mm^3; p=0.031) and inner module (1.6±0.7 to 3.0±0.9mm^3; p=0.011). No significant increase was seen for the B+5V and BMP2 groups from 4 to 8 weeks.

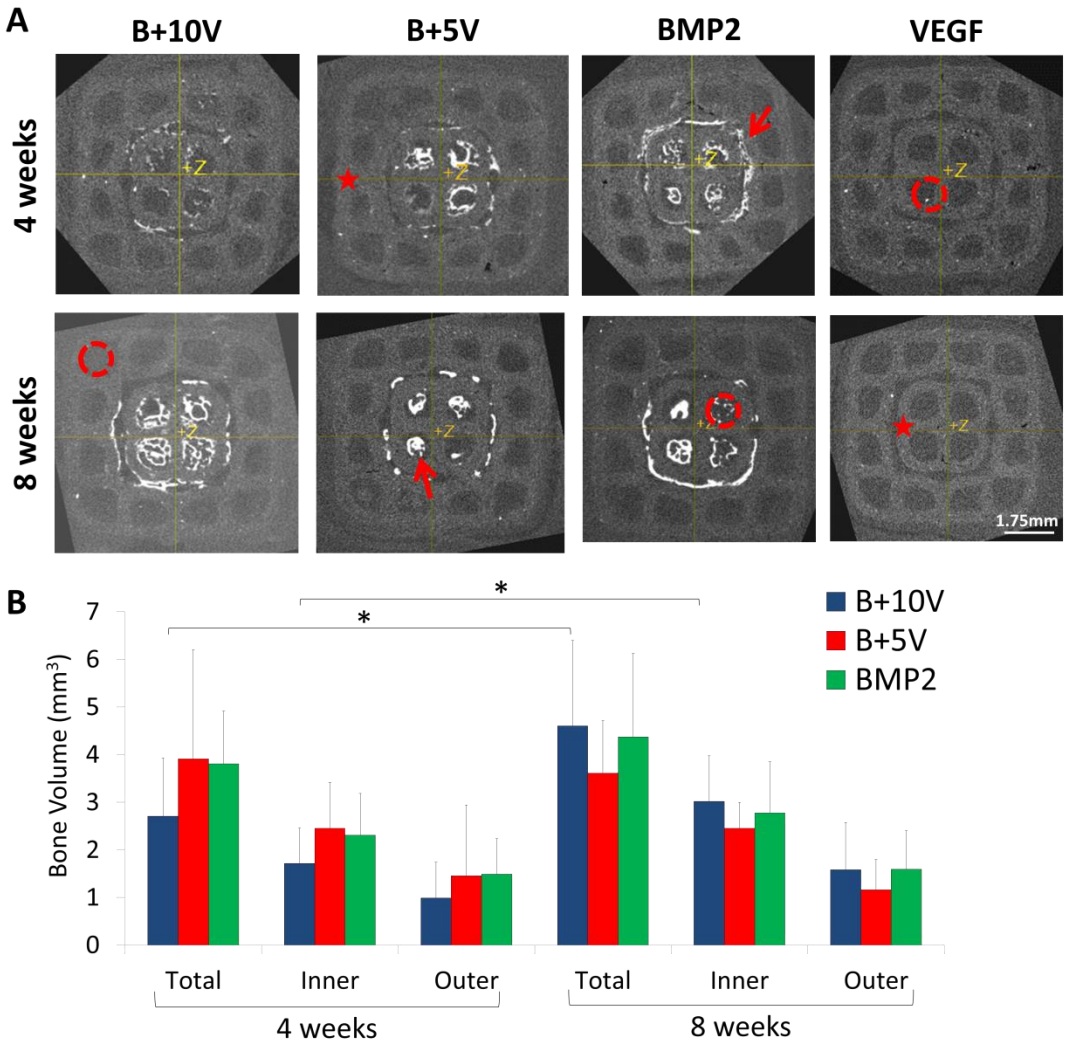

Figure 6.4: Modular Scaffold MicroCT Analysis
A) Scans taken of specimen explanted after 4 and 8 weeks implantation. Bright white areas indicate bone (red arrow), grey areas are the scaffold (red star) and darker grey areas indicate scaffold pores (red dashed line).
B) Bone volume was defined at a 1050HU threshold. The inner module ROI was 3.5mmx3.5mmx4.3mmH. Bone formed outside of that cubical ROI was defined as "outer" module bone volume. There was a significant increase in total and inner module regenerated bone volume from 4 to 8 weeks for the B+10V group but not for B+5V or BMP2 groups.
B+10V=BMP2+10µg/ml VEGF; B+5V = BMP2+5µg/ml VEGF (*p<0.05)

Bone Ingrowth

There was a significant increase from 4 to 8 weeks for the BV formed in the inner module pores for the B+10V group (p=0.011) but not for the other groups (Figure 6.5A). As seen in Figure 6.5B, for all groups there was significantly more bone ingrowth in the inner module than the outer module. There was a significant increase from 4 to 8 weeks for the B+10V group in the inner module (8.2±3.5 to 14.5±4.6%; p=0.011) and the total scaffold (1.86±0.8 to 3.2±1.2%; p=0.0021). BMP2 and B+5V groups did not show a significant increase in either the inner or outer modules. At each time point there was significantly more bone ingrowth in the experimental groups when compared to the VEGF group.

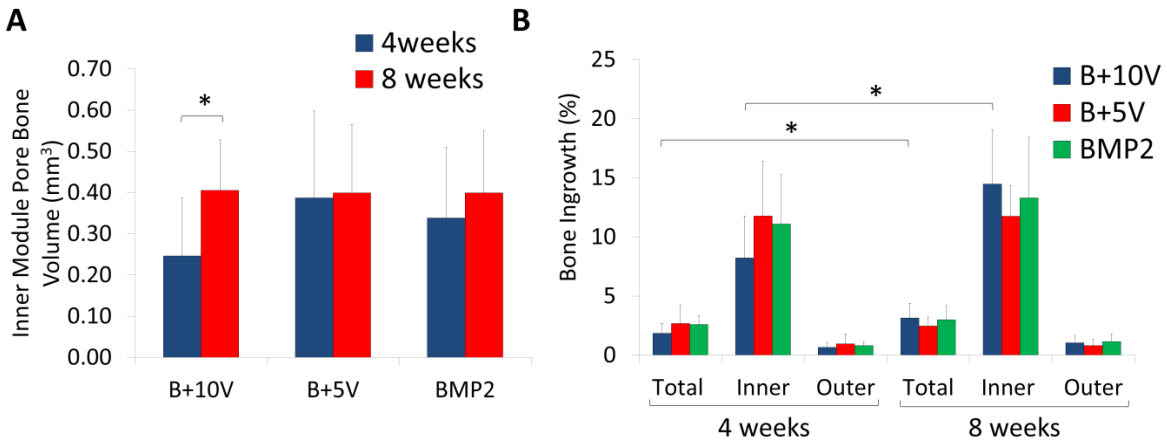

Figure 6.5: Bone Volume in Pores and Bone Ingrowth
A) There was a significant increase in bone formed in the center of the inner module vertical pores for B+10V. The ROI for each pore was 0.6750mmD, 4.3mmH.
B) Bone regenerated in each module was normalized by the available pore space to determine the % bone ingrowth. The B+10V group had a significant increase in total and inner module bone ingrowth from 4 to 8 weeks and no change was seen in the outer module.
B+10V=BMP2+10µg/ml VEGF; B+5V = BMP2+5µg/ml VEGF (*p<0.05)

TMD & TMC

As a reflection on the BV results, the TMC increased significantly for the B+10V group from 4 to 8 weeks (1.2±0.6 to 2.5±0.9mg HA). There was no increase for the B+5V and BMP2 groups. TMD increased significantly over time for all groups. B+10V and BMP2 increased from 460.6±35.9 to 554.5±29.9mg HA/cm^3 and from 478.4±23.9 to 553.2±33.7mg HA/cm^3, respectively (Figure 6.6). At 4 and 8 weeks there was no difference in TMD between BMP2, B+5V, and B+10V (p=0.54).

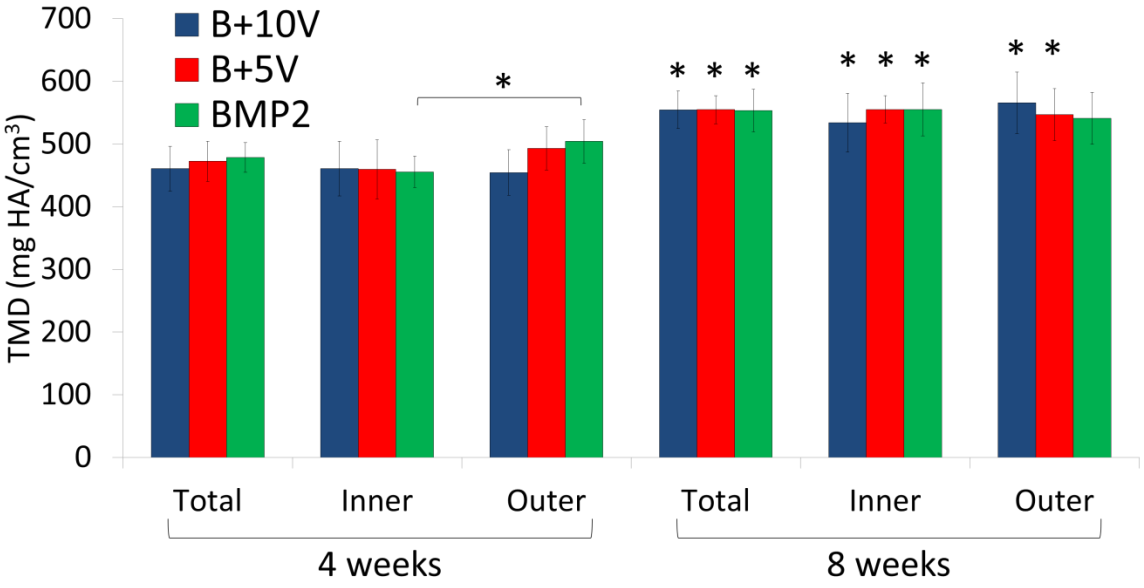

Figure 6.6: Tissue Mineral Density
Tissue mineral density was calculated for the total, inner module, and outer modules. All groups had a significant increase in TMD from 4 to 8 weeks except for the BMP2 group's outer module.
B+10V=BMP2+10µg/ml VEGF; B+5V = BMP2+5µg/ml VEGF (*p<0.05)

Histology

Histology staining shows healthy regenerated bone in all of the experimental groups. Blood vessels, osteoid, osteocytes, and cellular marrow are seen in the BMP2, B+5V, and B+10V groups. The VEGF only scaffolds were comprised mainly of fibrous tissue and blood vessels (Figure 6.7).

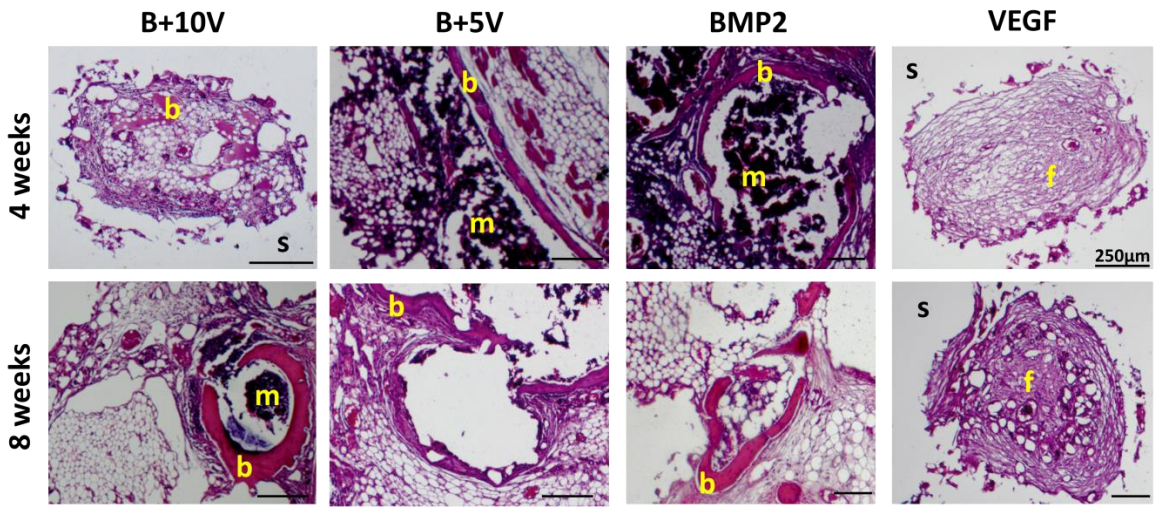

Figure 6.7: Histology: H&E Staining
BMP2, B+5V and B+10V groups showed osteoid, blood vessel, and fatty marrow formation at both time points.
b=bone, m=marrow, s=scaffold, f=fibrous tissue.
B+10V=BMP2+10µg/ml VEGF; B+5V = BMP2+5µg/ml VEGF

6.5 Discussion

Co-culture studies using endothelial cells and osteoblast-like cells have shown that the two cell types influence each other, suggesting that there is a coupling between osteogenesis and angiogenesis [26-28]. When determining the dual BMP2 and VEGF delivery dosages, one should consider that a high VEGF dose can inhibit osteogenesis and the ratio is important [29,30]. For this reason, we chose to investigate two VEGF doses. One VEGF dose was similar to the BMP2 (1:1), and the other was significantly less than the BMP2 dose (1:2). Previous dual delivery studies vary in study design, and there is a lack of knowledge as to the quality of ectopic bone regenerated if BMP2 and VEGF are co-delivered via adsorption from a modular PCL scaffold.

Previously in this laboratory, when adsorbed BMP2 was delivered from a PCL scaffold and VEGF was delivered from an internal collagen sponge, the BV significantly

increased from 4 to 8 weeks with the dual delivery group when compared to BMP2 group which did not increase [31]. Although those results were promising, the protein integration method is not easily translatable to the clinic because the BMP2 was adsorbed onto the PCL scaffold two days prior to implanting and complex machinery created the sponge. With that process, the construct would be fabricated outside of the OR and need to be sterilized which negatively impacts protein bioactivity. To create a simpler method of delivering both proteins, the modular PCL scaffold portions were exposed to their respective growth factors for 1 hour at room temperature and then assembled prior to implanting. Adsorption was chosen because it can be conducted in an OR environment with a short exposure time and does not require complex machinery. Furthermore, using a modular scaffold design to deliver VEGF and BMP2 has not been investigated to deliver two biologics to the best of our knowledge.

In this study, we used a modular PCL scaffold to deliver VEGF and BMP2 with the goal of further optimizing the pre-fabrication process and increasing the *in vivo* bone regeneration. 10µg/ml VEGF bound the same amount of protein on the outer module as the 65µg/ml BMP2 did on the inner module. 5µg/ml VEGF bound significantly less than the BMP2 and 10µg/ml VEGF groups resulting in two VEGF dosages. The BMP2 release trend was similar to the one found previously when the BMP2 was released from a different geometry PCL scaffold [16]. A limitation in this study is that the VEGF release profile could not be reliably and reproducibly determined due to VEGF's short half-life (about 90min) at 37^{o}C [32]. If the protein rapidly degraded, the assay would not accurately detect complete proteins releasing off of the surface. It is important to note that *in vitro* release kinetics are not an accurate representation of the release that would

occur *in vivo* due to neglecting physiological effects. Increased endothelial cell proliferation indicated that the VEGF adsorbed onto the PCL surface was bioactive.

In vivo bone analysis found the B+10V group significantly increased the total and inner module regenerated bone from 4 to 8 weeks when compared to B+5V, BMP2, and VEGF delivery. The increase in average bone regenerated from 4 to 8 weeks was 3.4 times higher for B+10V when compared to the BMP2 group. As a trend, at 4 weeks, B+10V had less bone than B+5V and BMP2; however, after 8 weeks it had more bone than the other two experimental groups. A possible explanation could be that VEGF initially hindered BMP2-induced bone regeneration, but then increased the bone regeneration rate so that the ultimate regenerated BV was higher than BMP2 alone. The migrating fibroblasts and mesenchymal stem cells could have interacted with the diffusing VEGF prior to interacting with the BMP2 which influenced them to differentiate into endothelial cells. These cells would have otherwise been influenced down an osteogenic lineage when exposed to BMP2. The increased vasculature could then have increased the bone regeneration rate because of increased nutrients and migrating cells.

With respect to bone formed in the center of the pores rather than the pore surface, B+10V had an increase in BV, whereas, the other groups did not change over time. This increased bone regeneration was reflected in the TMC results. For all conditions, the tissue mineral density was within the range of healthy native bone [12,33]. Bone ingrowth reflected the bone volume results because there was a significant increase in the inner module ingrowth over time for the B+10V group but not for B+5V or BMP2 alone groups. The inner module had the highest ingrowth for all of the experimental

groups when compared to the outer module because the BMP2 was adsorbed onto the inner module. All groups except for the VEGF group showed healthy bone formation with osteocytes embedded in osteoid and cellular marrow development.

This study's results reflect those found in a previous study conducted in this laboratory which delivered 65µg/ml adsorbed BMP2 from a PCL scaffold and 5µg VEGF from an internal collagen scaffold [31]. In both studies, the dual delivery group regenerated significantly more bone from 4 to 8 weeks, and the BMP2 group did not. Future studies should assess both an earlier time point to quantify neovascularization and a later time point to determine if bone volume with dual delivery eventually surpasses single growth factor delivery.

6.6 Conclusion

In this study we adsorbed VEGF and BMP2 in a clinically applicable setting onto a modular PCL scaffold and found that adsorbing similar VEGF and BMP2 dosages increases the total regenerated bone volume from 4 to 8 weeks in an ectopic site. Delivering multiple biologics is advancement to the process of pre-fabricating a bone flap, and the results of this study suggest that dual delivery could be a potential method to increase the regenerated bone volume.

Acknowledgements: This research was funded by the Tissue Engineering at Michigan trainee T-32 grant and NIH R21 DE 022439. We would like to thank Kevin Merchak and Jane Modes for assistance with data analysis and histology.

Author Disclosure Statement: Scott Hollister was a co-founder of Tissue Regeneration Systems (TRS), but is not long affiliated with TRS.

6.7 References

[1] Bhumiratana S, Vunjak-Novakovic G. Concise review: personalized human bone grafts for reconstructing head and face. Stem Cells Transl Med 2012 Jan;1(1):64-69.

[2] Warnke PH, Wiltfang J, Springer I, Acil Y, Bolte H, Kosmahl M, et al. Man as living bioreactor: fate of an exogenously prepared customized tissue-engineered mandible. Biomaterials 2006 Jun;27(17):3163-3167.

[3] Warnke PH, Springer IN, Wiltfang J, Acil Y, Eufinger H, Wehmoller M, et al. Growth and transplantation of a custom vascularised bone graft in a man. Lancet 2004 Aug 28-Sep 3;364(9436):766-770.

[4] Terheyden H, Knak C, Jepsen S, Palmie S, Rueger DR. Mandibular reconstruction with a prefabricated vascularized bone graft using recombinant human osteogenic protein-1: an experimental study in miniature pigs. Part I: Prefabrication. Int J Oral Maxillofac Surg 2001 Oct;30(5):373-379.

[5] Mesimaki K, Lindroos B, Tornwall J, Mauno J, Lindqvist C, Kontio R, et al. Novel maxillary reconstruction with ectopic bone formation by GMP adipose stem cells. Int J Oral Maxillofac Surg 2009 Mar;38(3):201-209.

[6] Alam MI, Asahina I, Seto I, Oda M, Enomoto S. Prefabrication of vascularized bone flap induced by recombinant human bone morphogenetic protein 2 (rhBMP-2). Int J Oral Maxillofac Surg 2003 Oct;32(5):508-514.

[7] Becker ST, Bolte H, Krapf O, Seitz H, Douglas T, Sivananthan S, et al. Endocultivation: 3D printed customized porous scaffolds for heterotopic bone induction. Oral Oncol 2009 Nov;45(11):e181-8.

[8] Terheyden H, Jepsen S, Rueger DR. Mandibular reconstruction in miniature pigs with prefabricated vascularized bone grafts using recombinant human osteogenic protein-1: a preliminary study. Int J Oral Maxillofac Surg 1999 Dec;28(6):461-463.

[9] Terheyden H, Menzel C, Wang H, Springer IN, Rueger DR, Acil Y. Prefabrication of vascularized bone grafts using recombinant human osteogenic protein-1--part 3: dosage of rhOP-1, the use of external and internal scaffolds. Int J Oral Maxillofac Surg 2004 Mar;33(2):164-172.

[10] Warnke PH, Springer IN, Acil Y, Julga G, Wiltfang J, Ludwig K, et al. The mechanical integrity of in vivo engineered heterotopic bone. Biomaterials 2006 Mar;27(7):1081-1087.

[11] Heliotis M, Lavery KM, Ripamonti U, Tsiridis E, di Silvio L. Transformation of a prefabricated hydroxyapatite/osteogenic protein-1 implant into a vascularised

pedicled bone flap in the human chest. Int J Oral Maxillofac Surg 2006 Mar;35(3):265-269.

[12] Williams JM, Adewunmi A, Schek RM, Flanagan CL, Krebsbach PH, Feinberg SE, et al. Bone tissue engineering using polycaprolactone scaffolds fabricated via selective laser sintering. Biomaterials 2005 Aug;26(23):4817-4827.

[13] Partee B, Hollister SJ, Das SS. Selective laser sintering process optimization for layered manufacturing of CAPA 6501 Polycaprolactone Bone Tissue Engineering Scaffolds. Journal of Manufacturing Science Engineering 2006;128:531.

[14] Fitzsimmons J. 510(k) Premarket Notification, Cover, Burr Hole, TRS CRANIAL BONE VOID FILLER. 2014; Available at: http://www.accessdata.fda.gov/scripts/cdrh/cfdocs/cfpmn/pmn.cfm?ID=K123633, 2014.

[15] Yeo A. 510(k) Premarket Notification, Methyl Methacrylate For Cranioplasty, OSTEOPORE PCL SCAFFOLD. 2014; Available at: http://www.accessdata.fda.gov/scripts/cdrh/cfdocs/cfpmn/pmn.cfm?ID=K051093, 2014.

[16] Patel JJ, Flanagan CL, Hollister S. Bone Morphogenetic Protein-2 Adsorption onto Poly-E-caprolactone Better Preserves Bioactivity in vitro and Produces More Bone in vivo than Conjugation under Clinically Relevant Loading Scenarios. Tissue Eng Part C Methods 2014 Oct 25.

[17] Huang YC, Kaigler D, Rice KG, Krebsbach PH, Mooney DJ. Combined angiogenic and osteogenic factor delivery enhances bone marrow stromal cell-driven bone regeneration. J Bone Miner Res 2005 May;20(5):848-857.

[18] Hankenson KD, Dishowitz M, Gray C, Schenker M. Angiogenesis in bone regeneration. Injury 2011 Jun;42(6):556-561.

[19] Yang YQ, Tan YY, Wong R, Wenden A, Zhang LK, Rabie AB. The role of vascular endothelial growth factor in ossification. Int J Oral Sci 2012 Jun;4(2):64-68.

[20] Kanczler JM, Ginty PJ, White L, Clarke NM, Howdle SM, Shakesheff KM, et al. The effect of the delivery of vascular endothelial growth factor and bone morphogenic protein-2 to osteoprogenitor cell populations on bone formation. Biomaterials 2010 Feb;31(6):1242-1250.

[21] Peng H, Usas A, Olshanski A, Ho AM, Gearhart B, Cooper GM, et al. VEGF improves, whereas sFlt1 inhibits, BMP2-induced bone formation and bone healing through modulation of angiogenesis. J Bone Miner Res 2005 Nov;20(11):2017-2027.

[22] Kakudo N, Kusumoto K, Wang YB, Iguchi Y, Ogawa Y. Immunolocalization of vascular endothelial growth factor on intramuscular ectopic osteoinduction by bone morphogenetic protein-2. Life Sci 2006 Oct 4;79(19):1847-1855.

[23] Geuze RE, Theyse LF, Kempen DH, Hazewinkel HA, Kraak HY, Oner FC, et al. A differential effect of bone morphogenetic protein-2 and vascular endothelial growth factor release timing on osteogenesis at ectopic and orthotopic sites in a large-animal model. Tissue Eng Part A 2012 Oct;18(19-20):2052-2062.

[24] Kempen DH, Lu L, Heijink A, Hefferan TE, Creemers LB, Maran A, et al. Effect of local sequential VEGF and BMP-2 delivery on ectopic and orthotopic bone regeneration. Biomaterials 2009 May;30(14):2816-2825.

[25] Patel ZS, Young S, Tabata Y, Jansen JA, Wong ME, Mikos AG. Dual delivery of an angiogenic and an osteogenic growth factor for bone regeneration in a critical size defect model. Bone 2008 Nov;43(5):931-940.

[26] Kaigler D, Krebsbach PH, West ER, Horger K, Huang YC, Mooney DJ. Endothelial cell modulation of bone marrow stromal cell osteogenic potential. FASEB J 2005 Apr;19(6):665-667.

[27] Wang DS, Miura M, Demura H, Sato K. Anabolic effects of 1,25-dihydroxyvitamin D3 on osteoblasts are enhanced by vascular endothelial growth factor produced by osteoblasts and by growth factors produced by endothelial cells. Endocrinology 1997 Jul;138(7):2953-2962.

[28] Peng H, Wright V, Usas A, Gearhart B, Shen HC, Cummins J, et al. Synergistic enhancement of bone formation and healing by stem cell-expressed VEGF and bone morphogenetic protein-4. J Clin Invest 2002 Sep;110(6):751-759.

[29] Shah NJ, Macdonald ML, Beben YM, Padera RF, Samuel RE, Hammond PT. Tunable dual growth factor delivery from polyelectrolyte multilayer films. Biomaterials 2011 Sep;32(26):6183-6193.

[30] Young S, Patel ZS, Kretlow JD, Murphy MB, Mountziaris PM, Baggett LS, et al. Dose effect of dual delivery of vascular endothelial growth factor and bone morphogenetic protein-2 on bone regeneration in a rat critical-size defect model. Tissue Eng Part A 2009 Sep;15(9):2347-2362.

[31] Patel JJ, Fan R, Miller S, Flanagan C, Edwards S, Hollister S. Dual BMP2 and VEGF Delivery from a Polycaprolactone/Collagen Sponge Construct to Increase Bone Growth in Ectopic Sites for Flap Prefabrication . Submitted 2014.

[32] Kleinheinz J, Jung S, Wermker K, Fischer C, Joos U. Release kinetics of VEGF165 from a collagen matrix and structural matrix changes in a circulation model. Head Face Med 2010 Jul 19;6:17-160X-6-17.

[33] Kontogiorgos E, Elsalanty ME, Zapata U, Zakhary I, Nagy WW, Dechow PC, et al. Three-dimensional evaluation of mandibular bone regenerated by bone transport distraction osteogenesis. Calcif Tissue Int 2011 Jul;89(1):43-52.

CHAPTER 7

DUAL DELIVERY OF BMP2 AND EPO FROM A NOVEL MODULAR POLYCAPROLACTONE SCAFFOLD TO INCREASE EARLY ECTOPIC BONE REGENERATION IN PREFABRICATED FLAPS

Jane Modes, Colleen Flanagan, Paul Krebsbach, Sean Edwards, and Scott Hollister assisted with the preparation of this chapter.

Submitted to Tissue Engineering Part C Nov, 2014

7.1 Abstract

A potential method to repair large craniofacial bone defects is to implant a scaffold with associated proteins into the latissimus dorsi, and then transplant it to the defect as a vascularized flap. Bone morphogenetic protein-2 (BMP2) delivered from polycaprolactone (PCL) produces bone when implanted subcutaneously. Erythropoietin (EPO) works synergistically with BMP2. In this study, adsorbed EPO and BMP2 are locally co-delivered from a modular PCL scaffold to increase ectopic bone growth. EPO (200IU/ml) and BMP2 (65µg/ml) were adsorbed onto the outer and inner portions of a modular scaffold, respectively. Protein binding and release studies were first quantified. Subsequently, EPO+BMP2 and BMP2 scaffolds were implanted subcutaneously in mice for 4 and 8 weeks. 8.6±1.4µg BMP2 (22%) and 140±29IU EPO (69.8%) bound to the scaffold and <1% and 83% was released in 7 days, respectively. Increased endothelial cell proliferation indicated EPO bioactivity. At 4 and 8 weeks, BMP2+EPO produced

more bone (5.1±1.1 and 5.5±1.6mm^3) than BMP2 (3.8±1.1 and 4.3±1.7mm^3). BMP2+EPO had more ingrowth (1.4±0.6%) in the outer module when compared to BMP2 (0.8±0.3%) at 4weeks. Dual delivery produced more dense cellular marrow while BMP2 had more fatty marrow. Dual delivery is a potential method to regenerate more bone for a pre-fabricated flap.

Keywords: BMP, Polycaprolactone, Protein adsorption, Bone tissue engineering

7.2 Introduction

The gold standard for treating a large craniofacial bone defect is an autograft usually taken from the fibula or iliac crest. This defect can be caused by trauma, tumor resection, or developmental abnormalities. Methods to tissue engineer a bone flap are under investigation to overcome the drawbacks associated with autografts including high donor site morbidity, increased risk of infection, and defect geometry mismatch. Tissue engineering a flap can be conducted *in vitro* or *in vivo*. *In vitro*, the scaffold with added cells would be place in an external bioreactor. However, regenerating a large bone volume *in vitro* is time consuming, and it is difficult to maintain an optimal nutrient perfusion of the scaffold [1]. As an alternative, we propose the process of pre-fabricating a bone flap *in vivo* which involves implanting a scaffold with associated biologics into the back muscle and then transplanting it to the defect site after a maturation period as a boney vascularized flap. Previous studies have created pre-fabricated flaps by utilizing a titanium cage, filling it with Bio-Oss blocks soaked in bone morphogenetic protein-7 (BMP-7) and cells, and implanting the construct inside of the patient's latissimus dorsi muscle [2-10]. After six weeks, the implant was transferred to the defect site but due to loading issues, the implant fractured and failed [2].

We are looking to advance this pre-fabrication process by integrating patient specific design, 3D printing, and multiple biologics delivery [11]. Poly-Ɛ-caprolactone (PCL) is a biocompatible and biodegradable polymer which can be 3D printed using a selective laser sintering (SLS) manufacturing technique to produce scaffolds of complex geometry based on the patient's CT scan [12]. SLS printing can reproducibly create scaffolds with designed porosity, mechanical properties, and permeability. Furthermore,

PCL leads to less inflammation and generates less acidic byproducts when compared to polylactic acid based co-polymers [13]. PCL is also currently utilized in 510(k) approved cranioplasty bone filling applications [14,15]. Previously in our laboratory we found BMP2 adsorbed onto a porous PCL scaffold in a clinically applicable setting (1 hour protein exposure at room temperature environment) regenerates bone when implanted subcutaneously in a murine model [16].

A flap needed for a large defect would need a large bone volume as well as a rich vascular network to supply nutrients to the growing bone, remove waste, and form a vascular pedicle that can be connected to a vessel at the defect site. Furthermore, for oncology patients awaiting adjuvant therapy, the speed at which bone is regenerated in the donor muscle site is essential. We hope to increase the regenerated bone volume at an earlier time point when compared to BMP2 delivery alone by delivering erythropoietin (EPO) along with the BMP2 in a clinically applicable manner.

EPO is a protein that stimulates erythropoiesis, acts as a cytokine for red blood cell precursors in the bone marrow, and has been shown to promote angiogenesis in a variety of tissues [17]. EPO indirectly impacts bone healing by influencing hematopoietic stem cells to produce BMP2 [18-20]. *In vitro*, EPO has shown to directly influence mesenchymal stem cells to differentiate into osteoblasts indicating that they must have EPO receptors [19,20]. EPO receptors are also expressed on endothelial cells, neurons, and trophoblast cells [19]. EPO has been used clinically to treat anemia and has some angiogenic properties [21-23].

EPO can be delivered systemically; however, drawbacks include serious side effects such as increased blood viscosity, hypertension and thromboembolic events

[21,24,25]. To avoid the drawbacks associated with systemic delivery, some studies have looked at local EPO delivery. Kobayashi et al delivered EPO using a gelatin hydrogel at the surface of a rabbit heart [26] and Chen et al delivered EPO using fibrin gel to increase neovascularization [27]. Interactions between EPO and BMP2 have been studied *in vitro* [19,20] and *in vivo* [28,29], and results have shown synergistic effects on bone formation. For example, BMP2 was delivered from a collagen scaffold implanted in a rat calvarial defect, and EPO was injected subcutaneously at the defect site every other day for 2 weeks [28]. At 6 weeks the dual delivery group produced a greater bone volume fraction when compared to BMP2 alone [28]**.**

Although these dual delivery results are promising, there is limited knowledge on the effects of locally delivering both BMP2 and EPO on ectopic bone regeneration for pre-fabricated flap applications. In addition, the use of 3D printed modular delivery of multiple growth factors has not been reported. In this study, we investigated the *in vitro* binding, release, and bioactivity of adsorbed BMP2 and EPO from a modular PCL scaffold and, furthermore, analyzed the regenerated ectopic bone volume and spatial distribution.

7.3 Materials & Method

PCL Scaffold Fabrication

Solid PCL discs (6mmD, 2mmH), and 44% porous inner (3.5mm sides, 4.3mmH, 106mm^{2}SA) and 79% porous outer (7mm sides, 4.3mmH, 357mm^{2}SA) PCL scaffolds were fabricated via SLS using a Formiga P100 (EOS, Inc., Novi, MI) (Figure 7.1). PCL powder (43-50kDa Polysciences, Warrington, PA) was mixed with 4 wt% hydroxyapatite (Plasma Biotal Limited, UK). After manufacturing, the scaffolds were air blasted,

sonicated in 70% ethanol (EtOH), sterilized in 0.22µm filtered 70% EtOH, and air-dried under sterile conditions.

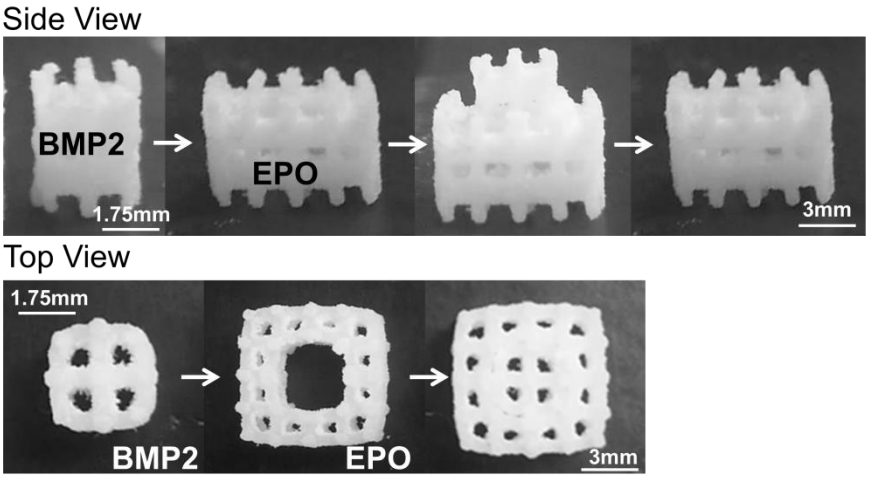

Figure 7.1: Modular Scaffold Assembly
BMP2 was adsorbed onto the inner scaffold module and EPO was adsorbed onto the outer scaffold module. The two scaffolds were then assembled

EPO Binding to PCL Scaffolds

100µg EPO (Creative Biomart, Shirley, NY) was reconstituted in 1ml sterile Dulbecco's phosphate buffered saline (DPBS) to result in 12,000 IU/ml (0.1mg/ml). The stock solution was further diluted to the desired concentrations in DPBS. The outer modular scaffolds were placed in an ultra low bind 24 well plate (Costar) and washed in DPBS to wet the surface. Scaffolds were then exposed to 1ml EPO solution at room temperature for 1 hour (n=3). 100 IU/ml per PCL disc was used for bioactivity studies to conserve materials and 200 IU/ml per scaffold was used for binding, release, and *in vivo* studies. Finally, scaffold modules were washed in DPBS to remove loosely bound protein. The washes and the remaining EPO solution following the exposure were collected to indirectly quantify EPO remaining in the solution utilizing a protein quantification kit (Fluoroprofile, Sigma). A standard curve was created from 2.5µg/ml to 0µg/ml (300

IU/ml to 0 IU/ml). A volume of working solution (Fluoroprofile reagent and buffer) was added to an equal volume of unknown EPO sample. Samples were read in triplicates with a fluorometric reader (520nm excitation, 620 emission).

$$EPO\ Bound\ (IU) = (EPO\ exposed\ to\ scaffold) - (EPO\ in\ remaining\ solution + EPO\ in\ washes)$$

BMP2 Binding and Quantification

BMP2 was adsorbed onto the inner scaffold modules as previously described [16]. Briefly, 1mg lyophilized BMP2 (BMP2-01H, Creative Biomart, Shirley, NY) was dissolved in 1ml 20mM acetic acid and it was then further diluted in BuPH (#28372, Pierce) buffer with 0.5M EDTA (pH 7.0) to 65µg/ml. A BMP2 ELISA (Peprotech), specific for *e.coli* derived BMP2, was used to quantify the protein content in the 65µg/ml BMP2 solution (average detected concentration was 28.12±4.6µg/ml), and the binding studies were normalized to this value. Briefly, the inner scaffold modules were washed in BuPH buffer (pH 7.2) followed by BuPH+0.5M EDTA buffer to wet the surface, exposed to 1ml of 65µg/ml BMP2 for 1 hour at 23^{o}C (n=3), and washed in water (di$H_2$0) prior to use. The washes and the BMP2 solution remaining after exposure were collected, 1% Bovine Serum Albumin (BSA) was added to result in 0.1% BSA content and samples were stored at -80^{o}C until ELISA analysis for BMP2 content.

$$BMP2\ Bound\ (\mu g) = (BMP2\ in\ original\ solution\ detected\ by\ ELISA) - (BMP2\ in\ remaining\ solution + BMP2\ in\ washes)$$

The ELISA was carried out according to the manufacturer's directions.

Release Kinetics

The outer scaffold modules with adsorbed EPO were manually assembled with the inner scaffold modules that had no BMP2 adsorbed (Figure 7.1). Constructs were submerged in 1ml DPBS and incubated at 37^{o}C, 95% humidity, 5% CO_2. The supernatant was collected and replenished at 1, 2, 3, 5, and 7 days after initial exposure. Samples were stored at -80^{o}C until FluroProfile assay analysis for protein content.

The inner scaffold modules with adsorbed BMP2 were assembled with an outer module that had no adsorbed EPO, submerged in 1ml DPBS, and incubated at 37^{o}C, 95% humidity, 5% CO_2. The supernatant was collected and replenished 1, 2, 3, 5, and 7 days after initial exposure. Supernatants with a final 0.1% BSA content were stored at -80^{o}C until BMP2 quantification with an ELISA.

Adsorbed EPO Bioactivity

Previous studies in the laboratory show that BMP2 adsorbed to PCL surface maintains bioactivity as seen by C2C12 cell Alkaline Phosphatase production [16]. In this study, endothelial cell proliferation was used to indicate EPO bioactivity as done in other studies [30-32]. A disc geometry with a flat surface was used for this assay due to a well defined surface area and a simple geometry. This assay's goal was to assess the protein's bioactivity and not the extent of bioactivity. Second passage human umbilical endothelial cells (HUVECs) were cultured in EGM-2 growth medium (Lonza CC-3162) for 4 days at 37^{o}C, 95% humidity, 5% CO_2. Cells were trypsinized using 0.05% Trypsin with EDTA (Gibco) and quantified with an automatic cell counter - MoxieZ (Orflo,Ketchum, ID).

1ml EGM-2 growth media was added to PCL discs exposed to 100 IU EPO (n=4) and $2.0x10^4$ HUVECs were seeded on each disc (11,765cells/cm^2). Cells seeded onto discs without EPO exposure and PCL discs without cells served as the negative control. After 72 hours static culture, the cell medium was replaced with 500µl fresh EGM-2 Medium and 100µl MTS solution (CellTiter96 Aqueous One Solution Promega) was added per well. Constructs were incubated with the MTS reagent at 37°C for 4 hours and triplicates for each condition were read at 490nm on a microplate reader.

Cells were also seeded at 0, $2x10^4$, $4x10^4$, $8x10^4$, $16x10^4$ cells/well in triplicate to create a standard curve (cell number vs. absorbance reading). After 1 hour, 100µl MTS solution was added to the in 500µl EGM medium in each well, and the absorbance was read at 490nm on a microplate reader.

In Vivo Bioactivity: Subcutaneous Implantation

BMP2 inner scaffold modules (adsorbed with 65µg/ml BMP2) were assembled with outer scaffold modules (adsorbed with 200 IU/ml EPO) for the dual delivery BMP2+EPO group. The negative control was outer modules with 200 IU/ml EPO adsorbed and no BMP2 adsorbed onto the inner modules (EPO group). The positive control was inner modules with 65µg/ml BMP2 adsorbed and no EPO adsorbed onto the outer modules (BMP2 group). Scaffolds from each group were implanted subcutaneously in 5-6 week old female C57BL/6N mice.

The mouse dorsal hair was shaved and an incision was made in the back. Two subcutaneous pockets were created, one on each side, and a scaffold was placed into each pocket. Scaffolds were randomly assigned a side to be implanted such that half of the samples from each group were implanted on both the right and left sides. The positive

control (the BMP2 group) was implanted in a parallel study such that a BMP2+EPO and BMP2 scaffold were not implanted in the same mouse. Mice were sacrificed at 4 and 8 weeks post-surgery to assess bone regeneration. The explanted specimens were placed in Z-Fix (Anatech, Battle Creek, MI) overnight, washed in diH_20 for 24 hours and stored in 70% EtOH until assays were performed. Table 7.1 describes the total sample numbers and the number of samples used for each specific analysis method. This study was conducted in compliance with the regulations set forth by the University Committee on Use and Care of Animals at the University of Michigan.

Group	µCT Scan		Histology		Total Samples	
	4wk	8wk	4wk	8wk	4wk	8wk
BMP2+EPO	9	8	3	2	9	8
BMP2	8	9	2	2	8	9
EPO	9	8	3	2	9	8

Table 7.1: Sample Numbers for *In Vivo* Analysis.
Number of samples used in explanted specimen analysis methods

Micro-Computed Tomography (MicroCT)

Fixed scaffolds were scanned in water with a high-resolution (16µm) microCT scanner (Scanco Medical, Wayne, PA), and the scans were calibrated to Hounsfield units (HU). Bone volume (BV) was defined at a 1050HU threshold using Microview software (Parallax Innovations, Ilderton, ON). Tissue mineral density (TMD) was determined using exported grayscale data. The total scaffold region was represented as a cubical region of interest (ROI) defined as 7mm x 7mm x 4.3mm height. An ROI defining the inner scaffold module (3.5mmx 3mmx 4.3mmH) was used to determine bone formation within the module. Bone regenerated in the outside scaffold modules was calculated as the inner scaffold module BV subtracted from the total scaffold BV. The total, inner module, and outer module scaffold bone ingrowth was calculated as the BV divided by

the available pore volume in each region. Available pore volume was calculated from the porosity of each ring based on the microCT scan of an assembled modular scaffold (pre-implantation). To determine the amount of bone formed in the central region of the inner module pores instead of on the PCL surface, a 0.6750mmD, 4.3mmH cylinder ROI was created in all 4 vertical pores, and the total BV in inner module pores was calculated. TMD was calculated for the total, inner module, and outer module scaffolds.

Histology

Fixed scaffolds from each group were decalcified with RDO (Sigma), processed, and embedded in paraffin. Samples were then sectioned at 7µm thickness using a MICRON HM 325 (Thermo Scientific) and slides were incubated at 37^{o}C overnight to dry. Sections were stained with hematoxylin and eosin (H&E) to visualize cells, tissue matrix, blood vessels, and general tissue morphology. Sections were imaged with a 4x objective.

Statistical Analysis

Data are expressed as mean ± standard deviation of the mean. An analysis of variance (ANOVA) was used to determine statistical significance between groups. A p-value less than 0.05 ($\alpha<0.05$) was considered statistically significant on a 95% confidence interval.

7.4 Results

Protein Binding and Release Kinetics

After 1 hour protein exposure, 139.6 ± 28.6 IU EPO (69.8%) and 8.56 ± 1.4µg BMP2 (22%) bound to the outer and inner scaffold modules, respectively. After 7 days, 0.0311 ± 0.0053µg BMP2 (<1%) and 119.2 ± 29.4IU EPO was released (85%) from the PCL surface (Figures 7.2A & 7.2C). For both proteins, there was a relatively small burst release in the first two days of 45.8 ± 24 IU EPO (32.8%) and 0.017 ± 0.007µg BMP2

(0.2%) (Figures 7.2B & 7.2D). HUVECs seeded on EPO adsorbed PCL discs experienced increased cell proliferation ($2.4 \pm 0.3x10^4$ cells/disc) when compared to cells seeded on PCL discs without any protein exposure ($1.6\pm0.1x10^4$cells/disc) (Figure 7.3).

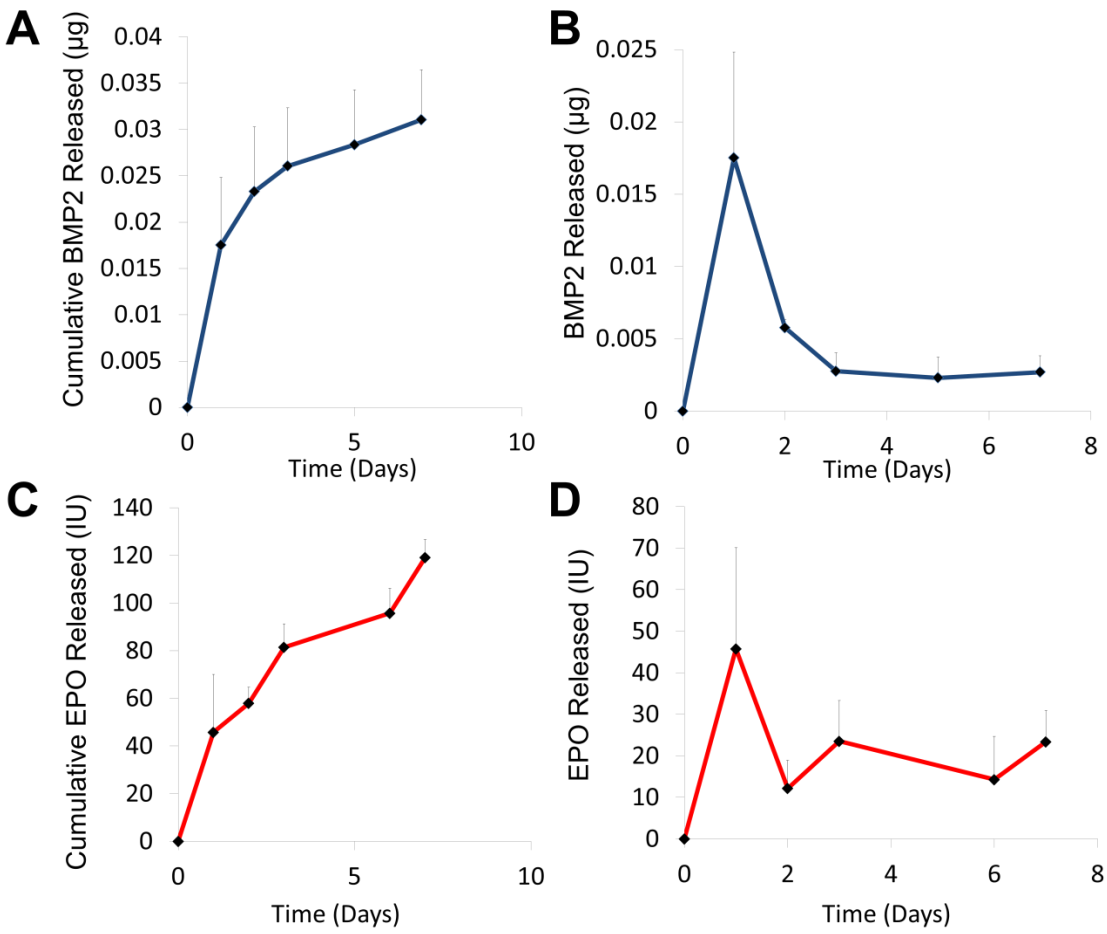

Figure 7.2: Protein Release Profiles
A) BMP2 cumulative release profile. After 7 days, 0.0311±0.0053µg BMP2 was released into 1xPBS at 37°C.
B) BMP2 release. A small burst release occurred in the first two days followed by sustained release.
C) EPO cumulative release profile. After 7 days, about 119.2±29.4IU of the 139.6±28.6IU bound was released.
D) EPO released over 7 days with a small burst release in the first two days. (n=3/group).

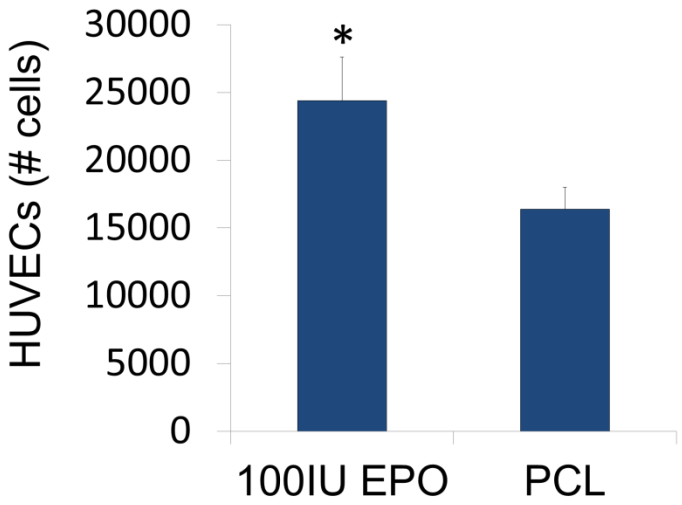

Figure 7.3: Adsorbed EPO Bioactivity
HUVEC cells seeded on PCL disc exposed to EPO showed increase levels of proliferation. n=4; *p<0.05.

MicroCT: Bone Volume

Visual analysis of the microCT scans show BMP2 only groups regenerated bone localized mainly on the inner module which had been adsorbed with the osteogenic factor (Figure 7.4A). The BMP2+EPO group regenerated bone not only in the inner module but also in the surrounding outer module. At both time points the dual delivery BMP2+EPO group produced more bone than the BMP2 group. The EPO group regenerated little to no visible bone. Microview software was utilized to quantify the bone volume observed in the microCT scans. At 4 weeks, the dual delivery group regenerated significantly more total bone ($5.1\pm1.1mm^3$) than the BMP2 group ($3.8\pm1.1mm^3$) ($p=0.019$) (Figure 7.4B). BMP2+EPO had more bone regenerated in the inner module, although it was not significantly more ($p=0.068$), and in the outer module ($p=0.276$). At 8 weeks, a similar trend was observed; however, there was no significant difference between dual and single GF delivery ($p=0.279$). Overall, BMP2+EPO regenerated more total, inner module, and

outer module bone volume than the BMP2 group. At both time points, the BMP2 and BMP2+EPO groups had significantly more bone volume than the EPO group (less than $0.2mm^3$).

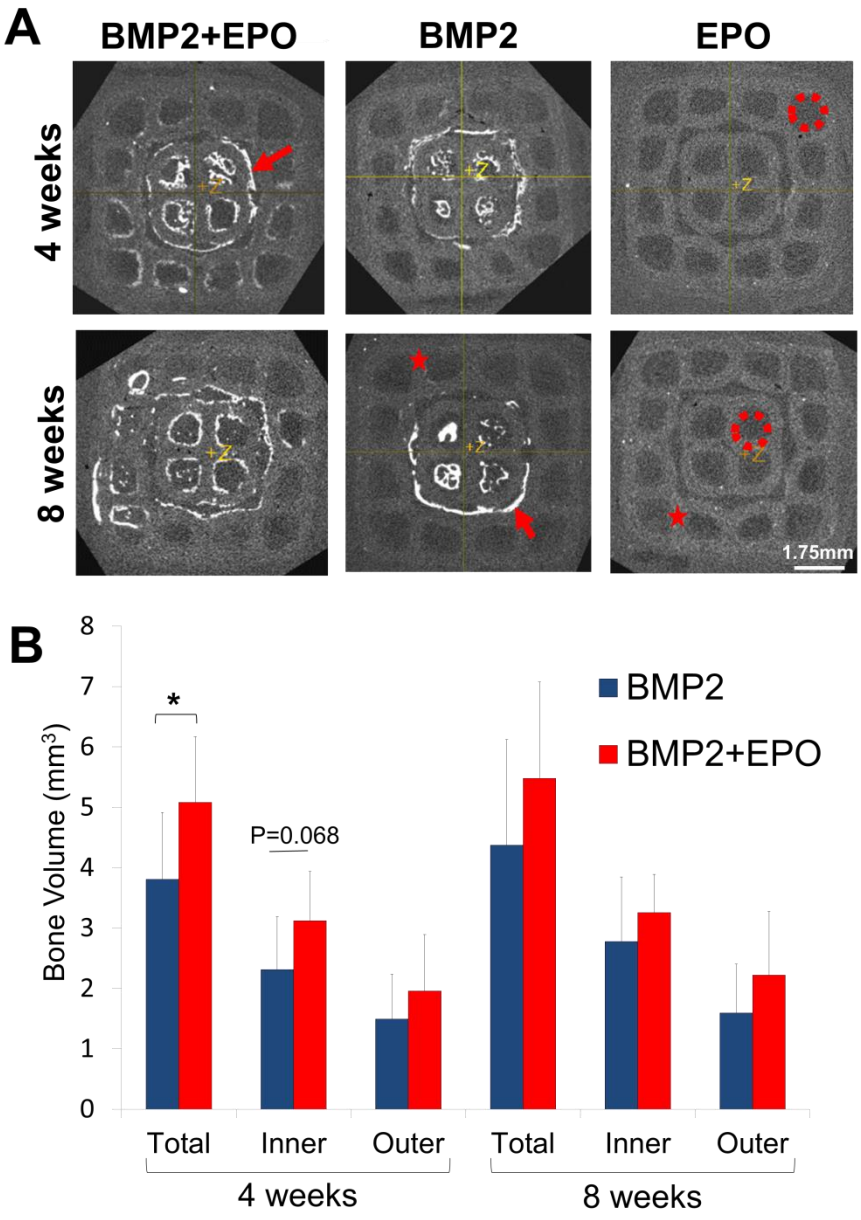

Figure 7.4: MicroCT Analysis of Regenerated Bone
A) Representative microCT images. The BMP2 group regenerated bone localized to the inner module and EPO+BMP2 regenerated bone in the outer module pores as well as in the inner module.
B) EPO+BMP2 resulted in significantly more total regenerated bone compared to the BMP2 group (*$p<0.05$).

Bone Ingrowth and TMD Analysis

Bone ingrowth analysis was not conducted for the EPO group because little to no regenerated bone volume was detected. At 4 and 8 weeks both of the BMP2+EPO and BMP2 groups had the same bone volume form in the inner module pores (Figure 7.5A). At 4 weeks BMP2+EPO had significantly more bone ingrowth in the outer module (1.44±0.6%) when compared to the BMP2 group (0.81±0.3%) (p=0.018) (Figure 7.5B). The increased bone ingrowth for dual delivery also occurred at 4 weeks in the inner module, however, the increase was not significant (p=0.067). With respect to the total scaffold, BMP2+EPO had significantly more ingrowth than BMP2 at 4 weeks (p=0.03). There were no significant differences in ingrowth between the two groups throughout the scaffold at 8 weeks (Figure 7.5B).

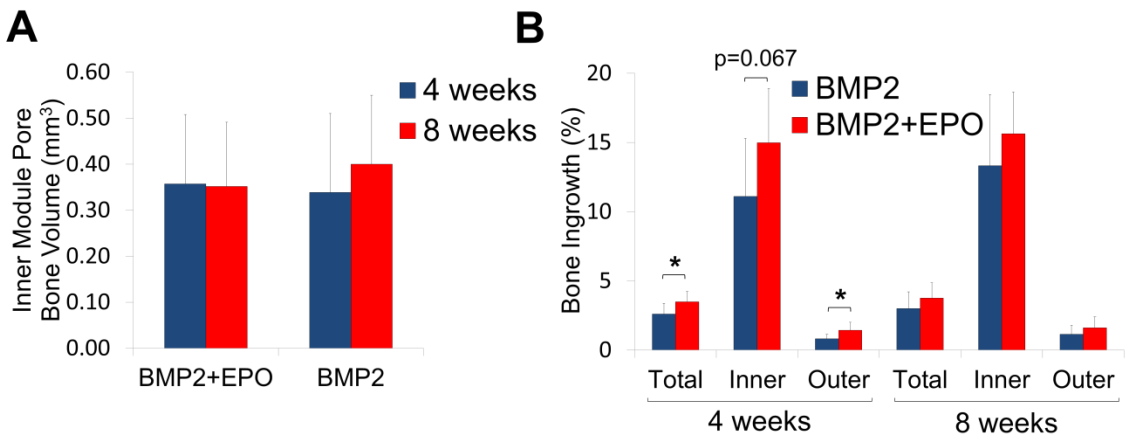

Figure 7.5: Pore Bone Growth and Scaffold Ingrowth
A) Bone volume formed inside of the inner module vertical pores was quantified at a 1050HU threshold. Pore ROIs used were 4.3mm height, 0.670mm diameter
B) Dual delivery had higher bone ingrowth in the total, inner module, and outer module at 4 weeks (*p<0.05).

TMD analysis showed that regenerated bone in the BMP2 group was significantly more mineralized than that of the BMP2+EPO group at 4 weeks (505.8±31.1 mg HA/cm^3 vs. 440.18±29.1 mg HA/cm^3; p=0.0001) and at 8 weeks (583.0±35.7mg HA/cm^3 vs.

501.7±40.6mg HA/cm^3; p=0.001). Further analysis of inner and outer scaffold module TMD at 4 weeks showed the BMP2 group had significantly more dense bone in the outer module when compared to the inner module (p=0.06). The BMP2+EPO group had no difference in TMD between the two scaffold modules. At 8 weeks, both BMP2 and BMP2+EPO groups had uniform TMD throughout the scaffold (Figure 7.6).

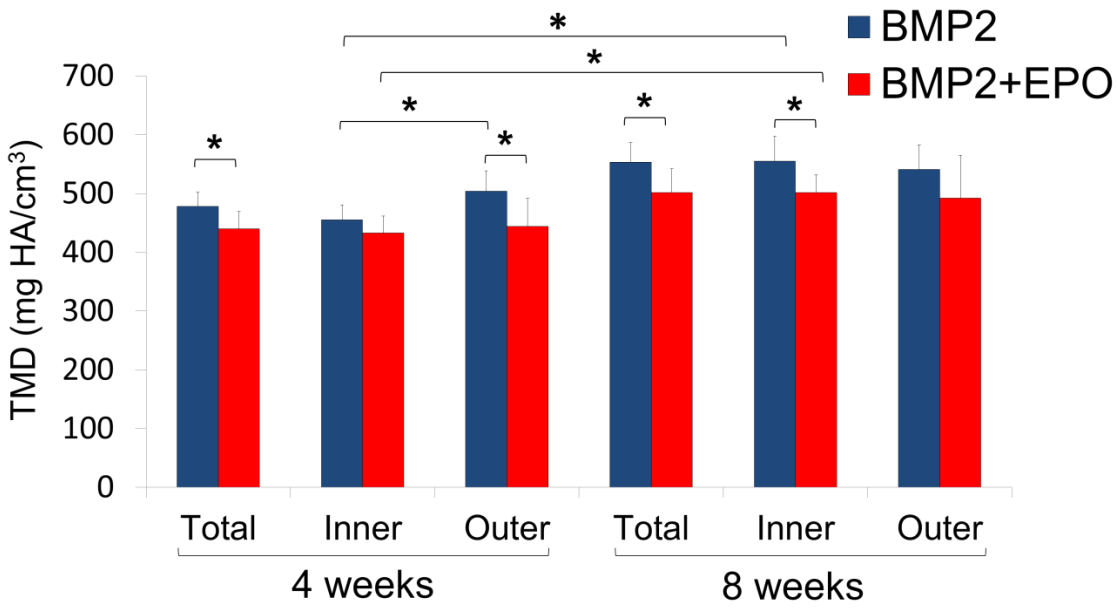

Figure 7.6: Tissue Mineral Density Analysis of Regenerated Bone
TMD of the total, inner module, and outer module was determined using Microview software. At 4 weeks the BMP2 group had more dense bone in the outer module and the dual delivery group had the same density bone throughout the scaffold *p<0.05.

Histology

Histology staining showed bone marrow, osteoid, blood vessels and osteocytes embedded in bone matrix for the BMP2+EPO and BMP2 groups. The dual delivery group had more dense cellular marrow and the BMP2 group seemed to have more fatty marrow. The EPO group was comprised mostly of fibrous tissue (Figure 7.7). For both

groups, osteocytes were embedded in the osteoid and osteoblasts were located at the periphery of forming bone.

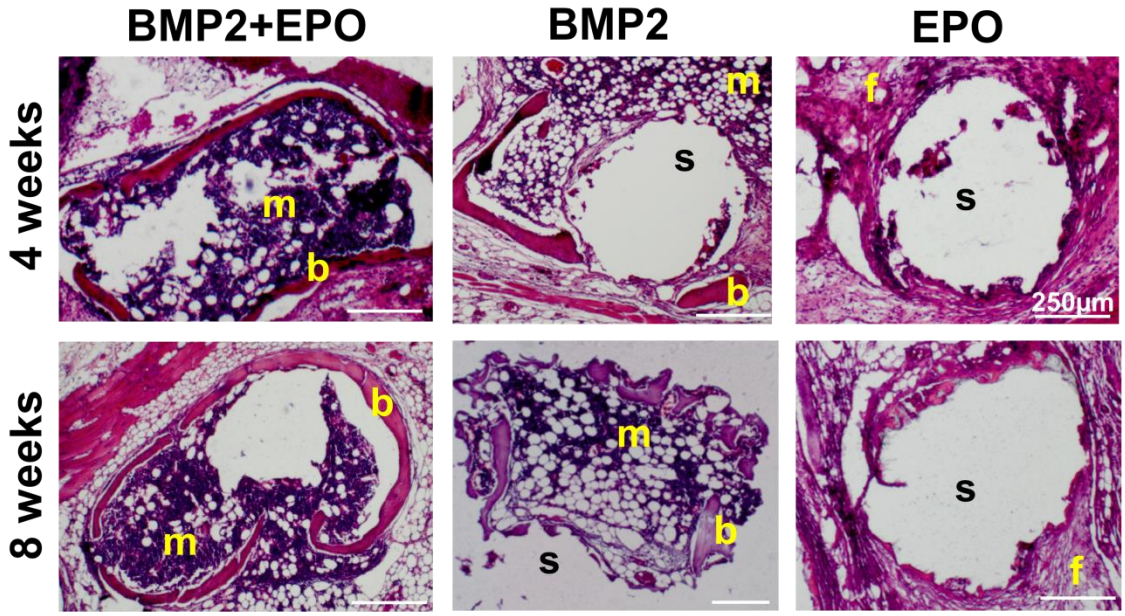

Figure 7.7: Histology: H&E Staining
BMP2+EPO and BMP2 groups showed osteoid, blood vessel, and marrow formation at both time points. The BMP2+EPO group had more dense cellular marrow and the BMP2 group had more fatty marrow. b=bone, m=marrow, s=scaffold, f=fibrous tissue.

7.5 Discussion

Medtronic's Infuse™ product has been FDA approved for BMP2 delivery from a collagen type 1 sponge for a variety of applications: spinal fusion, the treatment of open tibial fractures, sinus augmentation, and dental procedures [33]. Due to BMP2's short half-life, a 1.5mg/ml BMP2 dose was needed (greatly exceeding native concentrations of 18.8-22pg/mL) which resulted in a large burst release during the first 2-3 days causing adverse reactions in some patients [34]. Amgen's product EPOGEN® is also FDA approved and uses the EPO protein to increase red blood cell levels caused by chronic kidney disease in anemic patients. This administration avoids the need for red blood cell

transfusions [35,36]. Since these proteins are already FDA approved, the next step of dual delivery is feasible, although some regulatory hurdles would increase.

Although local BMP2 delivery from various scaffolds in a subcutaneous model has been widely studied for bone tissue engineering applications, there are very few investigations into local EPO delivery. EPO has been delivered via injectable hydrogels [37,38], gelatin [26] and fibrin gel [27] for angiogenesis studies; however, only one study of which we are aware has delivered EPO from a porogen-leached protein microbubble polyglycolic acid (PLGA) scaffold for the purpose of bone regeneration [29]. This delivery vehicle was used to investigate the effects of dual EPO and BMP2 delivery on bone regeneration in a calvarial defect model. There is limited to no knowledge of the binding and release of adsorbed EPO on PCL and, furthermore, the effect of dual EPO and BMP2 delivery on bone regenerated in an ectopic location for the application of pre-fabricated flaps is unknown.

In this study we used adsorption as the protein binding method to PCL due to the potential translational nature of this process. A short protein exposure time (<1hour) at room temperature prior to scaffold implantation is ideal for operating room environments. More complex processes that bind the protein outside of the OR will face increased regulatory hurdles such as sterilization, shelf life, maintained efficacy studies etc. Additionally, in this study a modular scaffold design is used which is a novel method to deliver multiple growth factors. The two components are simple to assemble while maintaining their geometric complexity due to SLS manufacturing.

One hour adsorption resulted in 139.6 ± 28.6 IU EPO (69.8%) and 8.56 ± 1.4µg BMP2 (22%) bound. After 7 days, less than 1% BMP2 was released. Even though this is

a small amount, it is shown to be therapeutically relevant in the *in vivo* study. Since an ELISA was used to detect the protein, the remaining BMP2 could have released off the surface but may have degraded which would go undetected by the assay. Another explanation is that it may not have released and required *in vivo* proteolytic activity to be released. As for EPO, 85% of the bound protein was released in the first week *in vitro*. HUVECs proliferated significantly more on PCL discs with adsorbed EPO indicating that the bound or released EPO was still bioactive. We have shown in previous studies that BMP2 released after adsorption onto PCL was still bioactive as seen with alkaline phosphatase activity [16].

In vivo, a modular scaffold that delivered EPO combined with BMP2 produced significantly more total bone at 4 weeks when compared to the BMP2 group. This increased early bone formation is important for pre-fabricated flap applications because the flap would mature faster for oncology patients awaiting adjuvant therapy. At 8 weeks, the dual delivery group still had more bone than the BMP2 alone group; however, the increase was not significantly different. Upon visual inspection, the BMP2 group regenerated bone localized to the inner module area where the BMP2 was adsorbed. The BMP2+EPO group regenerated bone in both the outer and inner modules indicating EPO's influence was not spatially constricted to the outer module. It may have had a synergistic effect on bone production in adjacent areas. Since EPO was released rather quickly, it could have diffused to interact with migrating cells. Bone formation was also controlled and limited within the scaffold boundary. Dual delivery produced more bone than the BMP2 group, but the amount of bone that grew in the inner module pores was the same; therefore, dual delivery may have grown more bone on the surface of the pores.

Bone ingrowth analysis found BMP2+EPO regenerated significantly more bone in the outer module available pore space at 4 weeks when compared to BMP2 alone. This increased bone growth seen with the dual delivery group could be explained by the synergistic effects between EPO and BMP2. EPO has shown to play a role in osteoclastogenesis and osteoclasts can recruit MSCs to the site of bone remodeling [28]. If EPO caused an initial increase in osteoclast numbers, this may have resulted in increased bone forming cells recruited to the construct. Interestingly, although dual delivery had more bone than the BMP2 group, the BMP2 group had a higher TMD when compared to BMP2+EPO at both time points. One potential explanation for this difference could be that the dual delivery bone was forming faster than BMP2 alone and the osteoblasts may not have been mineralizing the osteoid at the same rate. Despite the difference, dual delivery resulted in uniform TMD throughout the scaffold in the range of native bone; whereas, BMP2 had more dense bone in the outer module when compared to the inner module. With regard to developing a bone flap, having more bone with TMD in the normal range may be an advantage over less bone with higher mineral content overall. Gross tissue morphology analysis of explanted samples finds a more dense cellular marrow for the BMP2+EPO groups and a more fatty marrow for the BMP2 groups. This difference should be further investigated in future studies.

In this study we successfully detected adsorbed EPO and BMP2 binding and release kinetics from a novel modular PCL scaffold. Once adsorbed to the surface, these proteins maintain bioactivity. These two proteins are already FDA approved for several clinical indications, and the simple binding process can be conducted in a clinically applicable environment (1hour protein to scaffold exposure at ambient temperature).

Furthermore, delivering EPO along with the osteogenic protein BMP2 resulted in increased bone regeneration in comparison to single BMP2 or EPO delivery. Since the implant is acellular when implanted, circulating mesenchymal stem cells and fibroblasts could be interacting with the delivered growth factors and inducing bone formation. Future studies should investigate the effects of altering the BMP2 and EPO dose ratios, and more studies could be completed to elucidate the mechanisms of EPO and BMP2 synergy to further optimize the dual delivery protocol.

7.6 Conclusions

The speed at which bone forms in a pre-fabricated flap is crucial for oncology patients awaiting adjuvant therapy. In this study we have found that delivering EPO along with BMP2 could be a potential method to regenerate a greater bone volume at an earlier time point when compared to BMP2 alone delivery. Local dual delivery of EPO and BMP2 has not been investigated in depth, and delivering multiple biologics may advance the process of pre-fabricating flaps for skeletal reconstruction.

Acknowledgements: This research was funded by the Tissue Engineering at Michigan trainee T-32 grant, NIH R21 DE 022439, and NIH R01 AR 060892.

Author Disclosure Statement: Scott Hollister was a co-founder of Tissue Regeneration Systems (TRS), but is no longer is affiliated.

7.7 References

[1] Bhumiratana S, Vunjak-Novakovic G. Concise review: personalized human bone grafts for reconstructing head and face. Stem Cells Transl Med 2012 Jan;1(1):64-69.

[2] Warnke PH, Wiltfang J, Springer I, Acil Y, Bolte H, Kosmahl M, et al. Man as living bioreactor: fate of an exogenously prepared customized tissue-engineered mandible. Biomaterials 2006 Jun;27(17):3163-3167.

[3] Warnke PH, Springer IN, Wiltfang J, Acil Y, Eufinger H, Wehmoller M, et al. Growth and transplantation of a custom vascularised bone graft in a man. Lancet 2004 Aug 28-Sep 3;364(9436):766-770.

[4] Terheyden H, Knak C, Jepsen S, Palmie S, Rueger DR. Mandibular reconstruction with a prefabricated vascularized bone graft using recombinant human osteogenic protein-1: an experimental study in miniature pigs. Part I: Prefabrication. Int J Oral Maxillofac Surg 2001 Oct;30(5):373-379.

[5] Alam MI, Asahina I, Seto I, Oda M, Enomoto S. Prefabrication of vascularized bone flap induced by recombinant human bone morphogenetic protein 2 (rhBMP-2). Int J Oral Maxillofac Surg 2003 Oct;32(5):508-514.

[6] Becker ST, Bolte H, Krapf O, Seitz H, Douglas T, Sivananthan S, et al. Endocultivation: 3D printed customized porous scaffolds for heterotopic bone induction. Oral Oncol 2009 Nov;45(11):e181-8.

[7] Terheyden H, Jepsen S, Rueger DR. Mandibular reconstruction in miniature pigs with prefabricated vascularized bone grafts using recombinant human osteogenic protein-1: a preliminary study. Int J Oral Maxillofac Surg 1999 Dec;28(6):461-463.

[8] Terheyden H, Menzel C, Wang H, Springer IN, Rueger DR, Acil Y. Prefabrication of vascularized bone grafts using recombinant human osteogenic protein-1--part 3: dosage of rhOP-1, the use of external and internal scaffolds. Int J Oral Maxillofac Surg 2004 Mar;33(2):164-172.

[9] Warnke PH, Springer IN, Acil Y, Julga G, Wiltfang J, Ludwig K, et al. The mechanical integrity of in vivo engineered heterotopic bone. Biomaterials 2006 Mar;27(7):1081-1087.

[10] Heliotis M, Lavery KM, Ripamonti U, Tsiridis E, di Silvio L. Transformation of a prefabricated hydroxyapatite/osteogenic protein-1 implant into a vascularised pedicled bone flap in the human chest. Int J Oral Maxillofac Surg 2006 Mar;35(3):265-269.

[11] Hollister SJ, Murphy WL. Scaffold translation: barriers between concept and clinic. Tissue Eng Part B Rev 2011 Dec;17(6):459-474.

[12] Williams JM, Adewunmi A, Schek RM, Flanagan CL, Krebsbach PH, Feinberg SE, et al. Bone tissue engineering using polycaprolactone scaffolds fabricated via selective laser sintering. Biomaterials 2005 Aug;26(23):4817-4827.

[13] Wong DY, Hollister SJ, Krebsbach PH, Nosrat C. Poly(epsilon-caprolactone) and poly (L-lactic-co-glycolic acid) degradable polymer sponges attenuate astrocyte response and lesion growth in acute traumatic brain injury. Tissue Eng 2007 Oct;13(10):2515-2523.

[14] Fitzsimmons J. 510(k) Premarket Notification, Cover, Burr Hole, TRS CRANIAL BONE VOID FILLER. 2014; Available at: http://www.accessdata.fda.gov/scripts/cdrh/cfdocs/cfpmn/pmn.cfm?ID=K123633, 2014.

[15] Yeo A. 510(k) Premarket Notification, Methyl Methacrylate For Cranioplasty, OSTEOPORE PCL SCAFFOLD. 2014; Available at: http://www.accessdata.fda.gov/scripts/cdrh/cfdocs/cfpmn/pmn.cfm?ID=K051093, 2014.

[16] Patel JJ, Flanagan CL, Hollister S. Bone Morphogenetic Protein-2 Adsorption onto Poly-E-caprolactone Better Preserves Bioactivity in vitro and Produces More Bone in vivo than Conjugation under Clinically Relevant Loading Scenarios. Tissue Eng Part C Methods 2014 Oct 25.

[17] Holstein JH, Menger MD, Scheuer C, Meier C, Culemann U, Wirbel RJ, et al. Erythropoietin (EPO): EPO-receptor signaling improves early endochondral ossification and mechanical strength in fracture healing. Life Sci 2007 Feb 13;80(10):893-900.

[18] McGee SJ, Havens AM, Shiozawa Y, Jung Y, Taichman RS. Effects of erythropoietin on the bone microenvironment. Growth Factors 2012 Feb;30(1):22-28.

[19] Shiozawa Y, Jung Y, Ziegler AM, Pedersen EA, Wang J, Wang Z, et al. Erythropoietin couples hematopoiesis with bone formation. PLoS One 2010 May 27;5(5):e10853.

[20] Kim J, Jung Y, Sun H, Joseph J, Mishra A, Shiozawa Y, et al. Erythropoietin mediated bone formation is regulated by mTOR signaling. J Cell Biochem 2012 Jan;113(1):220-228.

[21] Bakhshi H, Rasouli MR, Parvizi J. Can local Erythropoietin administration enhance bone regeneration in osteonecrosis of femoral head? Med Hypotheses 2012 Aug;79(2):154-156.

[22] Haroon ZA, Amin K, Jiang X, Arcasoy MO. A novel role for erythropoietin during fibrin-induced wound-healing response. Am J Pathol 2003 Sep;163(3):993-1000.

[23] Ribatti D. Erythropoietin and tumor angiogenesis. Stem Cells Dev 2010 Jan;19(1):1-4.

[24] Saray A, Ozakpinar R, Koc C, Serel S, Sen Z, Can Z. Effect of chronic and short-term erythropoietin treatment on random flap survival in rats: an experimental study. Laryngoscope 2003 Jan;113(1):85-89.

[25] Maiese K, Chong ZZ, Shang YC. Raves and risks for erythropoietin. Cytokine Growth Factor Rev 2008 Apr;19(2):145-155.

[26] Kobayashi H, Minatoguchi S, Yasuda S, Bao N, Kawamura I, Iwasa M, et al. Post-infarct treatment with an erythropoietin-gelatin hydrogel drug delivery system for cardiac repair. Cardiovasc Res 2008 Sep 1;79(4):611-620.

[27] Chen F, Liu Q, Zhang ZD, Zhu XH. Co-delivery of G-CSF and EPO released from fibrin gel for therapeutic neovascularization in rat hindlimb ischemia model. Microcirculation 2013 Jul;20(5):416-424.

[28] Sun H, Jung Y, Shiozawa Y, Taichman RS, Krebsbach PH. Erythropoietin modulates the structure of bone morphogenetic protein 2-engineered cranial bone. Tissue Eng Part A 2012 Oct;18(19-20):2095-2105.

[29] Nair AM, Tsai YT, Shah KM, Shen J, Weng H, Zhou J, et al. The effect of erythropoietin on autologous stem cell-mediated bone regeneration. Biomaterials 2013 Oct;34(30):7364-7371.

[30] Haller H, Christel C, Dannenberg L, Thiele P, Lindschau C, Luft FC. Signal transduction of erythropoietin in endothelial cells. Kidney Int 1996 Aug;50(2):481-488.

[31] Anagnostou A, Lee ES, Kessimian N, Levinson R, Steiner M. Erythropoietin has a mitogenic and positive chemotactic effect on endothelial cells. Proc Natl Acad Sci U S A 1990 Aug;87(15):5978-5982.

[32] Desai A, Zhao Y, Lankford HA, Warren JS. Nitric oxide suppresses EPO-induced monocyte chemoattractant protein-1 in endothelial cells: implications for atherogenesis in chronic renal disease. Lab Invest 2006 Apr;86(4):369-379.

[33] Cahill KS, Chi JH, Day A, Claus EB. Prevalence, complications, and hospital charges associated with use of bone-morphogenetic proteins in spinal fusion procedures. JAMA 2009 Jul 1;302(1):58-66.

[34] Santo VE, Gomes ME, Mano JF, Reis RL. Controlled Release Strategies for Bone, Cartilage, and Osteochondral Engineering-Part I: Recapitulation of Native Tissue Healing and Variables for the Design of Delivery Systems. Tissue Eng Part B Rev 2013 Feb 19.

[35] Luksenburg H, Weir A, Wager R. Safety Concerns Associated with Aranesp (darbepoetin alfa) Amgen, Inc. and Procrit (epoetin alfa) Ortho Biotech, L.P., for the Treatment of Anemia
Associated with Cancer Chemotherapy. 2004; Available at: http://www.fda.gov/ohrms/dockets/ac/04/briefing/4037b2_04_fda-aranesp-procrit.htm.

[36] Amgen Initiates Voluntary Nationwide Recall of Certain Lots Of Epogen® And Procrit® (Epoetin Alfa). 2013; Available at: http://www.fda.gov/Safety/Recalls/ucm227202.htm.

[37] Wang T, Jiang XJ, Lin T, Ren S, Li XY, Zhang XZ, et al. The inhibition of postinfarct ventricle remodeling without polycythaemia following local sustained intramyocardial delivery of erythropoietin within a supramolecular hydrogel. Biomaterials 2009 Sep;30(25):4161-4167.

[38] Kang CE, Poon PC, Tator CH, Shoichet MS. A new paradigm for local and sustained release of therapeutic molecules to the injured spinal cord for neuroprotection and tissue repair. Tissue Eng Part A 2009 Mar;15(3):595-604.

CHAPTER 8

CONCLUSIONS AND FUTURE DIRECTIONS

8.1 Conclusions

Work presented in this dissertation represents significant contributions to the field of scaffold bone tissue engineering. There are multiple methods to deliver bone morphogenetic protein-2 (BMP2) from a biomaterial. Neither clinical applicability, nor the resulting bone regenerated *in vivo,* has been taken into consideration. The vascular endothelial growth factor (VEGF) and BMP2 dual delivery studies further optimized the regenerated bone volume by increasing the bone formation from 4 to 8 weeks. Finally, when compared to BMP2 delivery alone, the regenerated bone volume at 4 weeks was significantly increased when erythropoietin (EPO) was delivered with BMP2. By increasing the regenerated bone volume, a pre-fabricated flap can mature faster and be explanted to the defect site at an earlier time point. Future work with dual growth factor delivery should focus on adsorbing both proteins onto the entire scaffold to result in uniform bone distribution throughout the construct. Also, the protein dosages should be optimized to regenerate the most ectopic bone growth.

8.1.1 *Adsorbed BMP2 Produces More Bone than Conjugated BMP2*

There are multiple methods of binding BMP2 to biomaterial scaffolds requiring protein to scaffold exposure times ranging from 1-24 hours in environments ranging from

4^{o}C-37^{o}C [1-4]. Ideally, protein binding should be completed in less than one hour and at room temperature if it is conducted in a clinical setting. If the protein is incorporated onto the scaffold outside of the operating room (OR) room, regulatory hurdles increase significantly due to factors such as unknown sterilization effects on growth factor bioactivity and shelf life limitations. Adsorption and conjugation protocols have been superficially compared but have not been directly compared with such rigorously controlled scaffold geometry such as those printed using selective laser sintering technology [5,6]. Furthermore, studies have not compared *in vitro* binding and release studies and correlated them to *in vivo* bone regeneration. In our study, we found conjugation bound more protein than adsorption at a lower concentration and at room temperature. As the BMP2 concentration increased, the same amount of protein bound after 1 hour exposure at room temperature for both adsorption and conjugation. BMP2 was bioactive once adsorbed onto the poly-Ɛ-caprolactone (PCL) surface; however, conjugated BMP2 showed little to no signs of *in vitro* bioactivity. This inactivity may be because the chemical binding covered the protein's active site, the BMP2 was packed too tightly on the surface so cells could not access it, or physiological enzymes are needed to cleave the protein from the surface. It is important to note that preparing the PCL scaffold for conjugation required three days, whereas, adsorption required little advanced preparation. BMP2 adsorbed under a clinically relevant loading scenario made BMP2 available faster than conjugation (which had a sustained release).

When placed *in vivo*, the higher dose of adsorbed BMP2 (65µg/ml) regenerated the greatest bone volume that was also equally distributed throughout the scaffold pore space (bone ingrowth). Conjugation regenerated significantly less bone than the

adsorption groups. The elastic modulus was higher for the adsorption groups indicating superior mechanical properties when compared to conjugation, and the tissue mineral density (TMD) for both adsorption and conjugation groups were within the range of native bone. From the results of this study, we can conclude that the simpler adsorption method may be more optimal for use in the clinic because adsorbed BMP2 is bioactive *in vitro*, produces bone *in vivo*, increases the scaffold's elastic modulus, and produces healthy fatty bone marrow.

8.1.2 *Dual Delivery of BMP2 and VEGF from a PCL/Collagen Sponge Construct Increases the Bone Regenerated from 4 to 8 Weeks*

An irradiated large bone defect site is difficult to reconstruct and will not easily support a bone graft. An ideal bone flap would be composed of bone tissue as well as a rich vascular network to provide nutrients to and remove waste from the regenerating bone. Vessels also provide transportation for cells that are migrating to the implant site to assist with further remodeling. VEGF is a potent angiogenic growth factor that plays a role in bone healing [7-9]. A few studies delivered antibiotics and growth factors from collagen sponges and found a rapid release trend [10-15]. To imitate natural sequential expression of the two proteins, we combined the slower releasing BMP2 adsorbed PCL scaffold from AIM I with an internal collagen sponge to rapidly deliver VEGF. We found that BMP2 was bioactive after being subjected to the sponge fabrication conditions, and the VEGF released from the collagen sponge was also bioactive as indicated by increased human umbilical vein endothelial cell (HUVEC) proliferation.

In vivo, as a trend, initially at 4 weeks dual BMP2 and VEGF delivery regenerated less bone than BMP2 alone; however, at 8 weeks the dual delivery group had more bone

than BMP2 alone. Although the differences between the groups at each time point were not significant, there was a significant increase in bone volume from 4 to 8 weeks for the dual delivery group but not for the BMP2 alone group. Perhaps the released VEGF initially influenced migrating mesenchymal stem cells and fibroblasts to differentiate into endothelial cells rather than into osteoblasts resulting in less bone volume. However, after the vascular network was established, the bone formation may have rapidly increased due to increased migrating cells and nutrient transfer. To corroborate the bone volume results, the elastic modulus, TMD, and bone ingrowth also increased over time for the dual delivery group but did not change for the BMP2 alone group. In the future, a longer time point and larger sample number should be used to determine if dual delivery eventually regenerates significantly more bone than BMP2 alone. A limitation in this study was the inability to accurately measure the VEGF release profile. Without the release data, we could not be certain how much VEGF was delivered in comparison to the BMP2. This ratio is crucial to the bone volume formed [16]. Although the results from this study were promising, creating the collagen sponge required two days after the scaffold was coated with BMP2 which could negatively affect the protein's bioactivity.

8.1.3 *Dual Delivery of BMP2 and VEGF from a Modular PCL Scaffold Increases the Bone Regenerated from 4 to 8 Weeks*

As mentioned in Section 8.1.2, developing a rich vasculature is crucial to sustaining a large bone flap. Delivering potent angiogenic factor VEGF along with BMP2 is a possible method to increase bone regeneration. However, clinical constraints should be taken into account when designing the protein binding protocol to mitigate regulatory hurdles [7-9]. Considering AIM II results (Section 8.1.2), we developed a modular PCL

scaffold such that BMP2 and VEGF were adsorbed on the inner and outer modular scaffold components, respectively, and then assembled prior to implantation. This protocol is more applicable for use in the OR setting because the PCL components were exposed to the proteins for 1 hour at room temperature. The amount of 65µg/ml BMP2 that bound on the inner module was similar to the 10µg/ml VEGF that bound to the outer module. 5µg/ml VEGF bound significantly less than the two aforementioned groups, which created two protein dose ratios. With respect to VEGF, we were unable to calculate the release profile due to the protein's rapid degradation rate and short half-life. We found that adsorbed VEGF was bioactive due to increased HUVEC proliferation, and the *in vivo* bone regeneration trend followed the trend found with the PCL/collagen sponge construct (Section 8.1.2). The higher VEGF dose (10µg/ml) resulted in less bone than BMP2 alone (65µg/ml) group initially but then resulted in more than the BMP2 group at 8 weeks. The 10µg/ml VEGF dual delivery group had a significant increase in bone volume and ingrowth over time from 4 to 8 weeks, whereas, the 5µg/ml VEGF dual delivery and the BMP2 alone groups did not show an increase. Since we were unable to reliably determine the VEGF release profiles, we cannot confirm how much VEGF was released with the BMP2. As previously mentioned, it is important to note that the *in vitro* release profile may not correlate to the *in vivo* release due to neglecting physiological factors. A limitation in this study was that the mechanical testing machine parameters were not sensitive enough for this PCL geometry. Overall, delivering adsorbed VEGF (10µg/ml) along with BMP2 (65µg/ml) results in an increased bone regeneration rate from 4 to 8 weeks when compared to single BMP2 delivery.

8.1.4 *Local Dual Delivery of EPO and BMP2 from a Modular PCL Scaffold Increases Early Bone Regeneration in an Ectopic Location*

Clinicians will be hesitant to use as potent of an angiogenic factor as VEGF in an oncology patient because it could stimulate aberrant blood vessel production. EPO is a hematopoietic growth factor that has angiogenic properties, positively effects bone formation, and is Food and Drug Administration (FDA) approved [17-22]. Limited studies have investigated dual delivery of BMP2 and EPO [23,24], and local dual delivery from a scaffold has not yet been studied in an ectopic site to the best of our knowledge. In this study we found an average of 22% BMP2 bound to and <1% released from the inner module and 70% EPO bound to and 83% EPO released from the outer module (modular scaffold from Section 8.1.3). Once adsorbed, EPO bioactivity was indicated by increased HUVEC proliferation.

In vivo, BMP2 and EPO co-delivery regenerated significantly more bone and percent ingrowth than BMP2 alone at 4 weeks. At 8 weeks dual delivery was still greater, however, the difference was not significant. The increase in regenerated bone from 4 to 8 weeks was similar for both groups. Both groups had bone regenerating in the inner module where the BMP2 was adsorbed. Surprisingly, the dual delivery group had significantly more bone volume regenerating on the outer module when compared to BMP2 alone scaffolds. This indicates that the influence of EPO was not spatially constricted to the outer module, and it may have had a synergistic effect on bone production in adjacent areas. Since EPO was released rather quickly, it could have diffused to interact with migrating cells. Histology showed that the EPO and BMP2 dual delivery group had a more dense cellular marrow versus the more fatty marrow

associated with the BMP2 alone group. From these results, we can conclude that delivering EPO along with BMP2 from a modular scaffold significantly increases the regenerated ectopic bone at 4 weeks. The time in which the bone flap matures is crucial to oncology patients awaiting adjuvant therapy. In this study, the protein binding process is more clinically translatable since both of the proteins are FDA approved [15,21,22], although some hurdles may increase.

8.2 Future Work

8.2.1 *Utilize Other Conjugation BMP2 Binding Methods and BMP2 Detection Assays*

The sulfo-SMCC conjugation method was utilized in AIM I, and we believe an unfavorable reaction occurred because the cysteine group is located inside of the BMP2 protein structure and could be inaccessible to the sulfo-SMCC. We did not confirm where the sulfo-SMCC bound to the BMP2 protein chemically. In the future, fluorescence correlation spectroscopy should be utilized to assess protein binding to the PCL scaffold. Additionally, protein conformational changes should be analyzed with a Fourier transform infrared spectroscopy (FTIR) technique. These tests will give an insight into the protein binding site availability. Due to a very small amount of protein released *in vitro*, another protein detection method such as I^{125} radio-labeling should be conducted to confirm the release results. Heparin [5,25], 1-ethyl-3-(3-dimethylaminopropyl) carbodiimide (EDC) [26] and poly(ethylene-glycol) (PEG) [27] are a few of the other conjugation methods previously used to bind BMP2 to a surface. The bone regenerated after using one of these mentioned binding methods may be different than that found with sulfo-SMCC conjugation and should be investigated. FTIR can also be used in these studies to further understand the changes in protein morphology.

Along with altering the conjugation chemistry, future studies should investigate the point at which increasing the BMP2 solution concentration does not increase the regenerated bone volume *in vivo*. Once this threshold concentration is found, other growth factors (such as VEGF and EPO) can be co-delivered to further increase the regenerated bone volume.

8.3.2 *Assess Different Methods of Delivering VEGF from Inside of the BMP2 Scaffold*

It required two days to fabricate the collagen sponge inside of the PCL scaffold to deliver VEGF. A simpler method to deliver VEGF can be considered by mixing the VEGF solution into a fibrin gel and injecting it into the scaffold prior to implantation. The VEGF would diffuse out rather quickly in comparison to the adsorbed BMP2 - much like the VEGF released from the internal collagen sponge. Furthermore, for both AIMS II and III, we were unable to accurately detect the released protein. In the future, we should seek alternative methods to quantify the released VEGF such as radio-labeling or an enzyme-linked immunosorbent assay (ELISA). Future studies using the modular scaffold geometry should also use a more sensitive mechanical testing frame to calculate the specimen's elastic modulus. Nanoindentation is a sensitive alternative to the compression test frame to assess the local mechanical properties.

8.3.3 *Optimize Dual Delivery of BMP2 & VEGF and BMP2 & EPO*

In the modular PCL scaffold studies, the two proteins were individually adsorbed onto two scaffolds modules that were then manually assembled. With this design, the bone was generally localized to the inner module where the BMP2 was adsorbed. To increase the bone regenerated throughout the whole scaffold, a solution containing both VEGF and BMP2 or EPO and BMP2 should be created, and the entire PCL scaffold

should be submerged in this dual protein solution. This protocol would further simplify the dual delivery process while considering a clinical setting. Competitive binding must be considered if using this protocol. To understand the protein binding efficiencies, a constant BMP2 concentration can be used while gradually increasing the concentration of the second protein. Binding efficiencies will give insight as to how much of each protein is binding. The assay used to quantify protein binding would need to be specific to the protein; therefore, ELISA should be utilized rather than a generic protein assay. Binding between the protein and the PCL surface should be assessed using surface plasmon resonance or fluorescence correlation spectroscopy, and conformational changes should be determined with FTIR.

The contents of this dissertation advance the field of bone tissue engineering and the pre-fabrication process. We successfully regenerated bone on a designed PCL scaffold after implantation in an ectopic location and further optimized the regenerated bone volume by delivering multiple growth factors. There also exist a few limitations when translating this research into the clinic. An irradiated wound bed will be challenging to reconstruct considering it is not conducive to bone healing let alone to supporting the integration of a large bone graft. Increasing vascularity and the amount of bone in the scaffold will be crucial for applying this to oncology patients. Furthermore, the minimal regenerated bone volume needed to provide load bearing support and stimulate further bone remodeling once transplanted to the defect site is unknown. The studies in this dissertation have laid a foundation for pre-fabricated bone flaps using single and dual growth factor delivery from PCL scaffolds. Future studies should

investigate application in a large animal model that requires larger scaffold geometry to quantify the requirements for mechanical strength, bone volume, and vasculature.

8.3 References

[1] Apatite-Polymer Composite Particles for Controlled Delivery of BMP-2: *In Vitro* Release and Cellular Response. Proceedings of the Singapore-MIT Alliance Symposium; 2005.

[2] Park YJ, Kim KH, Lee JY, Ku Y, Lee SJ, Min BM, et al. Immobilization of bone morphogenetic protein-2 on a nanofibrous chitosan membrane for enhanced guided bone regeneration. Biotechnol Appl Biochem 2006 Jan;43(Pt 1):17-24.

[3] Zhao Y, Zhang J, Wang X, Chen B, Xiao Z, Shi C, et al. The osteogenic effect of bone morphogenetic protein-2 on the collagen scaffold conjugated with antibodies. J Control Release 2010 Jan 4;141(1):30-37.

[4] Autefage H, Briand-Mesange F, Cazalbou S, Drouet C, Fourmy D, Goncalves S, et al. Adsorption and release of BMP-2 on nanocrystalline apatite-coated and uncoated hydroxyapatite/beta-tricalcium phosphate porous ceramics. J Biomed Mater Res B Appl Biomater 2009 Nov;91(2):706-715.

[5] Jeon O, Song SJ, Kang SW, Putnam AJ, Kim BS. Enhancement of ectopic bone formation by bone morphogenetic protein-2 released from a heparin-conjugated poly(L-lactic-co-glycolic acid) scaffold. Biomaterials 2007 Jun;28(17):2763-2771.

[6] Zhang H, Migneco F, Lin CY, Hollister SJ. Chemically-conjugated bone morphogenetic protein-2 on three-dimensional polycaprolactone scaffolds stimulates osteogenic activity in bone marrow stromal cells. Tissue Eng Part A 2010 Nov;16(11):3441-3448.

[7] Huang YC, Kaigler D, Rice KG, Krebsbach PH, Mooney DJ. Combined angiogenic and osteogenic factor delivery enhances bone marrow stromal cell-driven bone regeneration. J Bone Miner Res 2005 May;20(5):848-857.

[8] Hankenson KD, Dishowitz M, Gray C, Schenker M. Angiogenesis in bone regeneration. Injury 2011 Jun;42(6):556-561.

[9] Yang YQ, Tan YY, Wong R, Wenden A, Zhang LK, Rabie AB. The role of vascular endothelial growth factor in ossification. Int J Oral Sci 2012 Jun;4(2):64-68.

[10] Wang AY, Leong S, Liang YC, Huang RC, Chen CS, Yu SM. Immobilization of growth factors on collagen scaffolds mediated by polyanionic collagen mimetic

peptides and its effect on endothelial cell morphogenesis. Biomacromolecules 2008 Oct;9(10):2929-2936.

[11] Uludag H, Gao T, Porter TJ, Friess W, Wozney JM. Delivery systems for BMPs: factors contributing to protein retention at an application site. J Bone Joint Surg Am 2001;83-A Suppl 1(Pt 2):S128-35.

[12] Seeherman H, Wozney JM. Delivery of bone morphogenetic proteins for orthopedic tissue regeneration. Cytokine Growth Factor Rev 2005 Jun;16(3):329-345.

[13] Mullen LM, Best SM, Brooks RA, Ghose S, Gwynne JH, Wardale J, et al. Binding and release characteristics of insulin-like growth factor-1 from a collagen-glycosaminoglycan scaffold. Tissue Eng Part C Methods 2010 Dec;16(6):1439-1448.

[14] Sorensen TS, Sorensen AI, Merser S. Rapid release of gentamicin from collagen sponge. In vitro comparison with plastic beads. Acta Orthop Scand 1990 Aug;61(4):353-356.

[15] Cahill KS, Chi JH, Day A, Claus EB. Prevalence, complications, and hospital charges associated with use of bone-morphogenetic proteins in spinal fusion procedures. JAMA 2009 Jul 1;302(1):58-66.

[16] Young S, Patel ZS, Kretlow JD, Murphy MB, Mountziaris PM, Baggett LS, et al. Dose effect of dual delivery of vascular endothelial growth factor and bone morphogenetic protein-2 on bone regeneration in a rat critical-size defect model. Tissue Eng Part A 2009 Sep;15(9):2347-2362.

[17] McGee SJ, Havens AM, Shiozawa Y, Jung Y, Taichman RS. Effects of erythropoietin on the bone microenvironment. Growth Factors 2012 Feb;30(1):22-28.

[18] Shiozawa Y, Jung Y, Ziegler AM, Pedersen EA, Wang J, Wang Z, et al. Erythropoietin couples hematopoiesis with bone formation. PLoS One 2010 May 27;5(5):e10853.

[19] Kim J, Jung Y, Sun H, Joseph J, Mishra A, Shiozawa Y, et al. Erythropoietin mediated bone formation is regulated by mTOR signaling. J Cell Biochem 2012 Jan;113(1):220-228.

[20] Holstein JH, Menger MD, Scheuer C, Meier C, Culemann U, Wirbel RJ, et al. Erythropoietin (EPO): EPO-receptor signaling improves early endochondral ossification and mechanical strength in fracture healing. Life Sci 2007 Feb 13;80(10):893-900.

[21] Luksenburg H, Weir A, Wager R. Safety Concerns Associated with Aranesp (darbepoetin alfa) Amgen, Inc. and Procrit (epoetin alfa) Ortho Biotech, L.P., for the Treatment of Anemia
Associated with Cancer Chemotherapy. 2004; Available at: http://www.fda.gov/ohrms/dockets/ac/04/briefing/4037b2_04_fda-aranesp-procrit.htm.

[22] Amgen Initiates Voluntary Nationwide Recall of Certain Lots Of Epogen® And Procrit® (Epoetin Alfa). 2013; Available at: http://www.fda.gov/Safety/Recalls/ucm227202.htm.

[23] Nair AM, Tsai YT, Shah KM, Shen J, Weng H, Zhou J, et al. The effect of erythropoietin on autologous stem cell-mediated bone regeneration. Biomaterials 2013 Oct;34(30):7364-7371.

[24] Sun H, Jung Y, Shiozawa Y, Taichman RS, Krebsbach PH. Erythropoietin modulates the structure of bone morphogenetic protein 2-engineered cranial bone. Tissue Eng Part A 2012 Oct;18(19-20):2095-2105.

[25] Kim TH, Oh SH, Na SY, Chun SY, Lee JH. Effect of biological/physical stimulation on guided bone regeneration through asymmetrically porous membrane. J Biomed Mater Res A 2012 Jun;100(6):1512-1520.

[26] Gharibjanian NA, Chua WC, Dhar S, Scholz T, Shibuya TY, Evans GR, et al. Release kinetics of polymer-bound bone morphogenetic protein-2 and its effects on the osteogenic expression of MC3T3-E1 osteoprecursor cells. Plast Reconstr Surg 2009 Apr;123(4):1169-1177.

[27] Liu HW, Chen CH, Tsai CL, Hsiue GH. Targeted delivery system for juxtacrine signaling growth factor based on rhBMP-2-mediated carrier-protein conjugation. Bone 2006 Oct;39(4):825-836.